

¹ Long-term shifts in Atlantic Cod and Yellowtail Flounder
² distributions on Georges Bank

³ David M. Keith^{1,2,4}, Jessica A. Sameoto², Freya M. Keyser², and Irene Andrushchenko³

⁴ ¹ Corresponding author - david.keith@dfo-mpo.gc.ca

⁵ ² Bedford Institute of Oceanography, Fisheries and Oceans Canada, Dartmouth, Nova Scotia

⁶ ³ St. Andrews Biological Station, Fisheries and Oceans Canada, St. Andrews, New Brunswick

⁷ ⁴ Dalhousie University, Halifax, Nova Scotia

⁸ **Abstract**

⁹ A significant challenge for fisheries management has been understanding the impacts of spatial and
¹⁰ temporal heterogeneity on population dynamics. Fisheries data are often spatial in nature and recent
¹¹ computational advances have resulted in new methodologies that better utilize this spatial information.
¹² We developed temporally variable species distribution models for Yellowtail Flounder (*Limanda ferruginea*)
¹³ and Atlantic Cod (*Gadus morhua*) on Georges Bank. These models identified seasonal and long-term
¹⁴ shifts in the distribution of both stocks with the average sea surface temperature (SST; average from
¹⁵ 1997-2008) and depth being significant predictors. Shifts in the distributions of these stocks were observed
¹⁶ at 3 or 5 year intervals with the core areas shifting northeast throughout the study period. For Atlantic
¹⁷ Cod, there was a decline in the size of the core area within the U.S. waters but minimal change was
¹⁸ observed in Canadian waters. In U.S. waters, the size of the Yellowtail Flounder core area started to
¹⁹ decline in the late 1970s but rebounded in the 1990s-2000s; minimal change was observed in Canadian
²⁰ waters. Simplified models using the random field for prediction performed similarly to models that
²¹ included environmental covariates. Incorporating this spatial information into science advice will facilitate
²² sustainable management of these stocks.

²³ **INTRODUCTION**

²⁴ The sustainable management of marine fisheries has been recognized as a critical challenge to address in the
²⁵ 21st century (CBD, 2018). Achieving sustainability goals requires an understanding of complex ecological,

26 socio-economic, and political factors and their interactions (Halpern *et al.*, 2013). For example, fisheries
27 management regions were often delineated as a result of political or geographic considerations rather than
28 biological or ecological rationale. As a result, defined management areas for a species often either encompass a
29 region in which environmental conditions and life-history traits are highly variable or only include a subset of
30 the population (Cadrin, 2020). Both of these scenarios are challenging for traditional assessment techniques
31 that assume closed populations along with homogeneous environments and life-history traits (Hilborn and
32 Walters, 1992).

33 Accounting for spatially and temporally variable processes has long been recognized as a challenge in fisheries
34 science (Ricker, 1944; Beverton and Holt, 1957; Hilborn and Walters, 1992). Many traditional fisheries
35 methods that are still operationalized today require assumptions about underlying spatial processes; these
36 assumptions generally result in models that treat stocks as spatially homogeneous entities (Beverton and Holt,
37 1957; Ricker, 1975; Hilborn and Walters, 1992). These simplifications were necessary because of computational
38 and statistical limitations and techniques, such as survey stratification, that were implemented to account for
39 spatial heterogeneity and reduce uncertainty in the indices feeding these models (Smith, 1996). Due in part
40 to the lack of spatial context provided by traditional stock assessments, indices were developed to quantify
41 changes in spatial patterns (e.g. Reuchlin-Hugenholz *et al.*, 2015). These indices are an additional source of
42 information for assessing stock health, and while they describe how distributions (e.g. abundance or biomass)
43 have changed over time they are unable to provide a detailed understanding of the spatial changes in these
44 distributions.

45 Species distribution models (SDMs) were one of the earliest modeling frameworks developed to better
46 understand how environmental factors influenced the distribution of a population (Grinnell, 1904; Box, 1981;
47 Booth *et al.*, 2014). These models combine environmental data and species' ecological information to map
48 the occurrence probability (OP; or some measure of abundance) of a species across some land(sea)-scape
49 (Box, 1981). In the marine realm, the influence of SDMs has increased rapidly in recent years; SDMs have
50 been used in the development of Marine Protected Areas (MPAs) and MPA networks, to better understand
51 the distribution of Species at Risk (SAR), and to predict the impact of climate change (Cheung *et al.*, 2008;
52 Robinson *et al.*, 2011; Sundblad *et al.*, 2011; Domisch *et al.*, 2019; McHenry *et al.*, 2019).

53 Historically, SDMs often did not explicitly consider temporal changes in the relationship between the
54 environment and the response of the species; these SDMs provided a snapshot in time based on available
55 data (Elith and Leathwick, 2009). However, more sophisticated SDM frameworks have been developed that
56 allow the underlying relationships to vary in time and space. This has led to dynamic models that better
57 utilize the latent spatio-temporal information contained in the data (Merow *et al.*, 2011; Thorson *et al.*,

58 2016; Martínez-Minaya *et al.*, 2018). These new spatio-temporal SDMs were made possible by a number of
59 recent statistical and computational advances such as the implementation of the Laplace approximation (LA),
60 Automatic Differentiation (AD), Stochastic Partial Differential Equations (SPDE), and Gaussian Markov
61 Random Fields (GMRFs) in commonly used programming languages (Kristensen *et al.*, 2016; Rue *et al.*,
62 2016; Thorson, 2019). The complex spatio-temporal analytical problems associated with these advanced
63 SDMs can now be solved in a fraction of the time required by traditional methods.

64 Georges Bank

65 Georges Bank (GB) is home to a wealth of natural resources and for centuries has had some of the most
66 productive fisheries in the world (Backus and Bourne, 1987). In the 1960s and 1970s numerous countries
67 conducted large unsustainable fisheries in the region, but with the introduction of Exclusive Economic Zones
68 (EEZ) in 1977, control of resource exploitation (e.g. fisheries) fell under the jurisdiction of the United States
69 (U.S.) and Canada (Halliday and Pinhorn, 1996; Anderson, 1997). The final demarcation of the Canadian
70 and U.S. territorial waters on GB was implemented with an International Court of Justice (ICJ) decision in
71 1984. Within three years both countries had independent groundfish surveys covering the entirety of GB at
72 different times of the year.

73 Historically, substantial groundfish fisheries occurred on GB, including Atlantic Cod (*Gadus morhua*) and
74 Yellowtail Flounder (*Limanda ferruginea*) (Anderson, 1997). As observed throughout the northwest Atlantic,
75 the biomass of Atlantic Cod on GB declined significantly in the early 1990s and there has been little evidence
76 for recovery of this stock since this collapse (Andrushchenko *et al.*, 2018). Between the 1970s and the 1990s,
77 the biomass of Yellowtail Flounder on GB was low, but evidence for a rapid recovery of this stock in the
78 early 2000s resulted in directed fisheries for several years. However, this recovery was short lived and the
79 biomass of this stock has been near historical lows for the last decade (Legault and McCurdy, 2018).

80 Here we use the R-INLA statistical framework (Lindgren and Rue, 2015; Rue *et al.*, 2016; Bakka *et al.*, 2018)
81 to develop spatio-temporal SDMs for two depleted groundfish stocks on GB (Atlantic Cod and Yellowtail
82 Flounder). Our objectives were to use data from three groundfish surveys in the region to: 1) develop
83 temporally variable SDMs and explore the influence of a suite of static environmental layers, 2) identify any
84 long-term shifts in the stock distributions, 3) identify any seasonal changes in the stock distributions using
85 available survey data, and 4) use the SDMs to quantify any shifts in core area within Canadian and U.S.
86 waters.

87 **Methods**

88 **Study area**

89 Georges Bank, located in the northwest Atlantic straddling the U.S.-Canada maritime border, is a 3-150 m
90 deep plateau that covers approximately 42,000 km² and is characterized by high primary productivity, and
91 historically high fish abundance (Townsend and Pettigrew, 1997). It is an eroding bank with no sediment
92 recharge and covered with coarse gravel and sand that provides habitat for many species (Valentine and
93 Lough, 1991). Since the establishment of the ICJ decision in 1984, the Canadian and U.S. portions of GB
94 have been largely managed separately by the two countries, though some collaborative management exists
95 (Figure 1).

96 **Data**

97 Survey data were obtained from the Fisheries and Oceans Canada (DFO) “*Winter*” Research Vessel (RV)
98 survey from 1987-2019 and the National Marine Fisheries Service (NMFS) “*Spring*” and “*Fall*” groundfish
99 surveys from 1972-2019. The *Winter* survey on GB typically occurs in February and early March, the *Spring*
100 survey typically occurs in April and May, while the *Fall* survey generally takes place between September
101 and November. For all surveys only tows deemed *successful* (Class 1 data) were used in this analysis. This
102 resulted in 2590 tows from the *Winter* survey, 2393 tows from the *Spring* survey, and 2506 tows from the
103 *Fall* survey.

104 **Environmental covariates**

105 A suite of 22 spatial environmental and oceanographic datasets were evaluated (Table 1). To eliminate
106 redundant variables, Variance Inflation Factors (VIFs) were calculated for all variables and any variables
107 with VIF scores > 3 were removed. This procedure was repeated until no variables remained with a VIF
108 score > 3 (Zuur *et al.*, 2010). A Principal Component Analysis (PCA) was undertaken using the data from
109 the associated station locations for each survey with variables excluded from the PCA if they showed no
110 evidence for correlation with other variables or if they had very non-linear correlation patterns (Table 1).
111 The top 4 PCA components, accounting for at least 80% of the variability in the data for a given survey,
112 were retained and included as covariates for the models in addition to the retained environmental covariates
113 (See Supplemental Figure S1).

₁₁₄ **Statistical Analysis**

₁₁₅ A Bayesian hierarchical methodology was implemented using the INLA approach available within the R
₁₁₆ Statistical Programming software R-INLA (Lindgren and Rue, 2015; Bakka *et al.*, 2018; R Core Team,
₁₁₇ 2020). In recent years, R-INLA has seen a rapid increase in use to model species distributions in both the
₁₁₈ terrestrial and marine realms (e.g. Cosandey-Godin *et al.*, 2015; Leach *et al.*, 2016; Boudreau *et al.*, 2017).
₁₁₉ This methodology solves SPDEs on a spatial triangulated mesh; the mesh is typically based on the available
₁₂₀ data (Rue *et al.*, 2016). The mesh used in this study included 6610 vertices and was extended beyond the
₁₂₁ boundaries of the data to avoid edge effects (Figure 2). Default priors were used for the analysis, except
₁₂₂ the range and standard deviation hyperparameters (Penalized Complexity (PC) priors) that were used to
₁₂₃ generate the random fields (Zuur *et al.*, 2017; Fuglstad *et al.*, 2019). The range PC prior had a median of 50
₁₂₄ km with a probability of 0.05 that the range was smaller than 50 km. The standard deviation of the PC prior
₁₂₅ had a median of 0.5 with a probability of 0.05 that the marginal standard deviation was larger than 0.5.

₁₂₆ Survey data up to 2016 were used for model development (*Winter* survey from 1987-2016, *Spring* and *Fall*
₁₂₇ surveys from 1972-2016), data from 2017-2019 were used only as a testing dataset. For all analyses, the
₁₂₈ response variable was the probability of the survey detecting the stock of interest (Occurrence Probability, OP_{it} ,
₁₂₉ where i is the individual observation at time t) and a *Bernoulli* GLM was utilized within R-INLA. Cells with
₁₃₀ an estimated OP ≥ 0.75 were considered the *core area*. An interactive dashboard (https://github.com/Dave-Keith/Paper_2_SDMS/tree/master/Dashboard) has been developed that can be used to explore the effect of
₁₃₁ defining different OPs as core area.
₁₃₂

$$OP_{it} \sim Bernoulli(\pi_{it})$$

$$E(OP_{it}) = \pi_{it} \quad \text{and} \quad var(OP_{it}) = \pi_{it} \times (1 - \pi_{it}) \quad (1)$$

$$\text{logit}(\pi_{it}) = \alpha + f(Cov_i) + u_{it}$$

$$u_{it} \sim GMRF(0, \Sigma)$$

133 Each variable retained after the VIF analysis, along with each of the 4 PCA components, was added to the
134 model individually. All continuous covariates were modelled using the INLA random walk '*rw2*' smoother,
135 which allows for non-linear relationships between the response and each covariate (Zuur *et al.*, 2017; Zuur
136 and Leno, 2018). The continuous covariates were centred at their mean value and scaled by their standard
137 deviation. Covariates that were highly skewed (e.g. depth) were log transformed before being standardized.
138 Due to low sample size of several of the levels the Sediment type (*Sed*; data obtained from McMullen *et al.*,
139 2014) these infrequent categories were amalgamated into one factor level that was represented by an *Other*
140 term, resulting in three levels for the Sediment covariate (*Other*, *Sand*, and *Gravel-Sand*). Across the three
141 surveys approximately 93% of the survey tows were on the *Sand* or *Gravel-Sand* bottoms and 7% were in the
142 amalgamated *Other* category.

143 Four spatial random field (u_{it}) models with differing temporal components were compared for each stock
144 and each survey, these were a) a static random field ($t = 1$), b) independent random fields every 10 years, c)
145 independent random fields every 5 years, and d) independent random fields every 3 years. The independent
146 random fields (options b through d) were set retroactively from the most recent year resulting in a shorter
147 duration random field at the beginning of the time series whenever the field time period was not a multiple of
148 the whole time series length (e.g. the 10 year random fields for the *Spring* models were 2007-2016, 1997-2006,
149 1987-1996, 1977-1986, and 1972-1976). Models with the same covariate structure but different random fields
150 were compared using WAIC, CPO, and DIC; the results for each of these metrics were similar and only the
151 WAIC results are discussed further. In all cases, the static random field was an inferior model when compared
152 to models with multiple random fields and the results discussed here are largely limited to the comparison of
153 the 10/5/3 year random fields. For brevity we refer to the results from each random field as an *era* (e.g. the
154 core area estimated when using the 2012-2016 random field is the core area during the 2012-2016 era).

155 Model Selection Overview

156 Models were tested using WAIC, CPO, and DIC; the results were similar for each of these diagnostics; only
157 WAIC is discussed further. The model selection results are available in the supplement and the complete
158 results can be found in the Model Output and Model Diagnostics sections of the interactive dashboard.
159 Stage 1 model selection for the different covariate models was undertaken using the static random field by
160 adding individual covariates. For this first analysis, covariates were identified if WAIC scores were more than
161 10 units smaller than the intercept model (e.g. SST for Atlantic Cod in the *Winter*; Figure S5) or were found
162 to be low relative to the suite of models tested in multiple seasons (e.g. Dep for Atlantic Cod in the *Spring*
163 and *Fall*; Figure S5). For Atlantic Cod, this analysis identified depth (*Dep*) and the average sea surface

temperature between 1997 and 2008 (*SST*) as having low WAIC scores in 2 of the 3 surveys (data obtained from Greenlaw *et al.*, 2010). For Yellowtail Flounder, Dep was identified as an informative covariate in all 3 surveys. In addition, Sed, and the average chlorophyll concentration between 1997 and 2008 (*Chl*) were retained based on their low WAIC scores in the *Fall* survey. Given the low number of informative covariates Dep, SST, and Chl were all retained for both species in Stage 2 of model selection. In Stage 2 of model selection, the variables were added pairwise (e.g. for Atlantic Cod, the models included *SST + Dep*, *Dep + Chl*, and *SST + Chl*) for both stocks and again compared using WAIC with the 10-year random fields. In Stage 3 of covariate model selection, models with 3 covariates were tested based on the Stage 2 results. For Atlantic Cod, a three term model that included additive terms for *SST*, *Dep*, and *Chl* was the most complex model tested. For Yellowtail Flounder, the most complex model included *SST*, *Dep*, and *Sed*. In Stage 3, additional covariates were retained if the WAIC for that model resulted in an improvement of the WAIC of more than 2, as compared to the lowest WAIC for the more parsimonious model.

Model selection on the temporal random fields was done while holding the environmental covariate terms the same. Initial model selection for the random fields (10 and 5-year fields) was done using the *Dep + SST* model for both species in all seasons given the general support for the *Dep + SST* model identified in Stage 2 of covariate model selection. For both species this indicated that the 10-year field was inferior to the more flexible 5-year random fields. For Atlantic Cod, the 3 and 5-year random fields were compared using the *Dep + SST* covariates (which was the covariate model with the lowest WAIC). For Yellowtail Flounder, the final step of the random field model selection used the *Dep + SST + Sed* model (which was the covariate model with the lowest WAIC) for the 3-year and 5-year random field comparison. The key model selection results are provided in the supplement and the full results can be found in the interactive dashboard. For Atlantic Cod the *final model* chosen included additive *Dep* and *SST* covariates and used a random field which changed every 5 years. For Yellowtail Flounder, the final model chosen included additive *Dep*, *SST*, and *Sed* covariates, the *Winter* and *Spring* models used a 3-year random field, while the *Fall* model used a 5-year random field.

Model Prediction

A predictive grid on GB was developed with cells having an area of approximately 9.1 km² (See Supplemental Figure S2). Each cell was intersected with average *SST*, *Dep*, and *Sed* fields (see Supplemental Figure S3 for the distribution of these environmental covariates) and the OP was estimated for each grid cell in each era for Atlantic Cod and Yellowtail Flounder in the *Winter*, *Spring*, and *Fall* using the final model for each stock and season respectively. The results using the predictive grid were used to calculate the size of the core area

195 (OP ≥ 0.75) for each era.
196 The predictive grid was also used to calculate the centre of gravity (COG) of the core area for each era. The
197 COG was calculated in the UTM coordinate system (EPSG Zone: 32619) using the easting (X) and northing
198 (Y) for each cell identified as core area (i) in each era (t) and weighted by the OP at each of these locations.

$$x_t^{cog} = \frac{\sum_{i=1}^n (X_{i,t} \times OP_{i,t})}{\sum_{i=1}^n OP_{i,t}} \quad (2)$$

$$y_t^{cog} = \frac{\sum_{i=1}^n (Y_{i,t} \times OP_{i,t})}{\sum_{i=1}^n OP_{i,t}} \quad (3)$$

199 The standard deviation around the mean COG in the X and Y direction was calculated as:

$$\sigma_{cog,t}^x = \sqrt{\frac{\sum_{i=1}^n OP_{i,t}}{[(\sum_{i=1}^n OP_{i,t})^2 - \sum_{i=1}^n OP_{i,t}^2] \times \sum_{i=1}^n (OP_{i,t} \times (X_{i,t} - x_t^{cog})^2)}} \quad (4)$$

$$\sigma_{cog,t}^y = \sqrt{\frac{\sum_{i=1}^n OP_{i,t}}{[(\sum_{i=1}^n OP_{i,t})^2 - \sum_{i=1}^n OP_{i,t}^2] \times \sum_{i=1}^n (OP_{i,t} \times (Y_{i,t} - y_t^{cog})^2)}} \quad (5)$$

200 To quantify the ability of these models to predict the location of the stocks in future years, data from the
201 2017-2019 surveys were used as a testing dataset to predict the OP in 2017, 2018, and 2019. In addition
202 to the final model, an *Intercept Model* which used only the temporally varying random field for prediction
203 (i.e. the model excluded all environmental covariates) was compared to the predictions from the final models.
204 Both the model residual and the 2017-2019 predictive error were calculated for each year using Root Mean
205 Squared Error (RMSE), Mean Average Error (MAE), and the standard deviation (SD). Given the similarity
206 of the results only the RMSE is presented (full results are available in the interactive dashboard).

207 Model Validation

208 Five fold cross validation was used to compare the out-of-sample predictive performance for a subset of the
209 5-year random field models: intercept only, SST (Atlantic Cod), Dep (Yellowtail Flounder), and Dep + SST.

210 The Atlantic Cod model validation was performed using the *Winter* survey data, the Yellowtail Flounder
211 validation used the *Spring* survey data. The data were randomly divided into 5 subsets and trained using 4
212 of the subsets; the 5th dataset was treated as a testing dataset to determine how well the model was able to
213 predict out-of-sample data. Model performance was measured by comparing the model residuals from the
214 training data to the prediction error from the testing data. The metrics used for this comparison were RMSE,
215 MAE, and SD. Given the similarity of the results only the RMSE is presented (full results are available in
216 the interactive dashboard). A subset of models were chosen because of the computational demands of this
217 validation procedure.

218 RESULTS

219 Distributional Shifts

220 For both stocks, the core areas ($OP \geq 0.75$) shifted towards the north and east throughout the study period
221 (Figure 3). For Atlantic Cod, the shift in distribution of the core area occurred relatively rapidly in the 1990s
222 and the centre of gravity (COG) of the core area has remained relatively stable since this period (Figure
223 3). In the 1970s and 1980s, core area was observed across the bank, however since the mid-1990s there was
224 a clear shift in distribution with core area concentrated in the north-east portion of the bank, mainly in
225 Canadian waters (see Supplemental Figures S9 -S11). In addition, in the *Fall*, Atlantic Cod was distributed
226 even further to the northeast along the edge of the study area. The size of the core area followed a similar
227 temporal pattern, with a rapid decline in the core area for Atlantic Cod occurring in the 1990s in the *Winter*
228 and *Spring* (Figure 4). The decline in the size of the core area was observed approximately a decade earlier in
229 the *Fall* and the size of the core area was always smaller in the *Fall* (Figure 4). The distribution of Atlantic
230 Cod along the edge of the bank during the *Fall* suggests that a substantial portion of this stock may have
231 been located on the slope where survey coverage was limited (Figure 1).

232 The Yellowtail Flounder shift in COG (Figure 3), was largely the result of a reduction in the core area in the
233 southwest portion of GB; the majority of core area was located in a central region of GB that straddles the
234 ICJ line dividing Canada and the U.S. (Supplemental Figures S12 -S14). The COG of Yellowtail Flounder
235 has slowly been shifting towards the northeast (Figure 4). The trends in the size of the core area during the
236 *Spring* and *Fall* have been very similar with rapid declines in the early 1980s followed by an increase in the
237 1990s and early 2000s (Figure 4). The size of the core area in the *Winter* has been in decline since a period
238 of increase in the 1990s (Figure 4).

239 For both stocks, the changes in the size of the core area were more pronounced in the U.S. than in Canadian

240 waters (Figure 5). In the U.S., the declines in the size of core area of Atlantic Cod occurred rapidly in the
241 early 1990s in the *Winter* and *Spring*. In the *Fall*, the loss of core area occurred approximately a decade
242 earlier, although the size of the core area in the U.S. during the *Fall* was always substantially lower than in
243 the *Winter* or *Spring*. In Canadian waters, there has been minimal change in the size of the core area for
244 Atlantic Cod in any of the seasons through time; the size of the core area in the *Fall* has tended to be lower
245 than observed in the *Winter* or *Spring* (Figure 5). For Yellowtail Flounder, the size of the core area in the
246 U.S. declined steadily throughout the 1970s and 1980s, this was followed by an increase in the 1990s and
247 early 2000s (Figure 5). Since the mid-2000s, the size of the core area in the U.S. appeared to stabilize. In
248 Canadian waters, the size of core area for Yellowtail Flounder throughout the 1970s and 1980s was relatively
249 low, slowly increased in the mid-1990s, and has been relatively stable since (Figure 5).

250 Environmental Covariates

251 The spatial fields for the three environmental variables retained by model selection are shown in Supplemental
252 Figure S3. The average SST between 1997 and 2008 had the largest effect on the OP of Atlantic Cod; they
253 were more likely to be found in regions of the bank with a lower SST (Figure 6). For all 3 surveys, the OP of
254 Atlantic Cod declined rapidly in regions of the bank where the SST was above approximately 10°C (Figure
255 6). Although depth was also retained in the final Atlantic Cod model, its effect on OP was substantially
256 smaller than the SST effect. During the *Winter* and *Spring*, the OP peaked between 70-82 m and declined
257 slowly in shallower and deeper waters (Figure 6). There was no clear relationship with depth in the Winter.
258 For Yellowtail Flounder, depth had the largest effect on OP, with Yellowtail Flounder most likely to be
259 observed between depths of 66-75 m in each of the 3 surveys and its effect on OP was highest during the
260 *Spring* (Figure 7). The average SST between 1997 and 2008 was also included in the final model, with
261 Yellowtail Flounder OP generally declining as SST increased. The effect of SST was least pronounced in the
262 *Fall*. The sediment type also had a significant influence on the OP for Yellowtail Flounder in the *Winter* and
263 *Fall*, with Sand and Gravel-Sand having higher OPs than the Other sediment category, this difference was
264 most notable during the *Winter* (Figure 7 and Supplemental Figure S7).

265 Model Hyperparameters

266 The decorrelation range for Atlantic Cod was above 100 km throughout the year and was generally higher
267 than that observed for Yellowtail Flounder (Figure 8). The range was highest for Atlantic Cod in the *Spring*
268 with an estimate of 218 (95% CI:131-346) km, while the range during the *Winter* spawning period was
269 the lowest at 154 (95% CI:99-227) km. In the *Fall*, the range declined from the *Spring*; this may indicate

270 spatial contraction or fish leaving the study domain (Figure 8). For Yellowtail Flounder, the lowest range was
271 estimated in the *Winter* at 86 (95% CI:63-109) km with the *Spring* and *Fall* range estimates being higher
272 and somewhat more variable than the *Winter* range estimate. The range estimates of Yellowtail Flounder
273 throughout the year were smaller and less variable than that observed for Atlantic Cod (Figure 8). The
274 uncertainty of these estimates precludes any statistical differences being observed between the seasons.

275 The standard deviation of the random field was lower for Atlantic Cod in the *Winter* and *Spring* than during
276 the *Fall* (Figure 9), this was indicative of the increased clustering of the stock and the relatively small effect
277 of the environmental covariates in the *Fall*. The standard deviation of the random field was highest for
278 Yellowtail Flounder in the *Winter* and the seasonal differences for Yellowtail Flounder were smaller than
279 those observed with Atlantic Cod (Figure 9). The standard deviation of the Yellowtail Flounder field was
280 higher than Atlantic Cod in the *Winter* and *Spring*, but lower in the *Fall* (Figure 9). The posteriors of other
281 hyperparameters for both stocks in the *Winter*, *Spring*, and *Fall* are provided in Supplemental Figures S35 -
282 S40.

283 Validation and Prediction

284 The five fold cross validation indicated that each of the models tested (intercept only, SST (Atlantic Cod),
285 Dep (Yellowtail Flounder), and Dep + SST) were able to predict the distribution for both stocks without an
286 increase in bias or a loss of accuracy (Figure 10). The mean error of the residuals for the validation training
287 set predictions were similar to the error from the predicted test data and while the mean error of the test
288 data was generally more variable, the estimates were centred on 0 and thus there was no evidence of bias in
289 these predictions (Figure 10). The RMSE from the test and training data showed similar patterns for both
290 stocks and most models, although for Yellowtail Flounder the RMSE for both the training and test data from
291 the intercept only model was slightly lower than either of the models with covariates. This indicates that the
292 inclusion of the environmental covariates may result in a small loss of out-of-sample prediction (Figure 10).

293 The error in the prediction of the distributions of each stock 1, 2, and 3 years into the future were well below
294 the RMSE associated with a model with no predictive ability (dashed line; Figure 11). The prediction for the
295 models without any environmental covariates were similar to the prediction from the models that included
296 both Dep and SST. For both stocks, the 2018 data consistently had the lowest prediction accuracy with the
297 models tending to predict individuals where none were observed. This was in agreement with observations
298 of the survey biomass indices being near historic lows for both stocks in 2018 (Andrushchenko *et al.*, 2018;
299 Legault and McCurdy, 2018). Generally, the predictive error from these models were near the high end of the
300 range of the annual model residual error, this indicates that these models were able to predict the spatial

301 OP patterns for both stocks up to 3 years into the future without a substantial loss of accuracy, even with
302 environmental covariates excluded from the models (Figure 11).

303 **DISCUSSION**

304 The SDMs developed here incorporated environmental, spatial, and multi-scale temporal information to
305 partition dynamic changes which occur both inter and intra-annually from static environmental relationships.
306 This framework provided a more complete understanding of the temporal shifts in the stocks' distributions
307 than simpler aggregation based indices that are often used in fisheries science [e.g. Reuchlin-Hugenholz *et al.*
308 (2015); see Supplemental Figure S4 showing the Gini index timeseries for Yellowtail Flounder and Atlantic
309 Cod on Georges Bank for each survey]. A general shift in the distributions of both stocks towards the east
310 and north was identified. For both stocks, this shift was in large part due to the loss of core area in the
311 southern and western portion of GB (primarily in U.S. waters). In addition, the analysis of surveys from
312 different times of the year provided a snapshot of the seasonal changes in the distributions of the stocks;
313 the Yellowtail Flounder distribution was relatively stable throughout the year, while Atlantic Cod moved
314 towards the northeastern slope of GB in the *Fall*. Finally, the models were able to predict the location of
315 Atlantic Cod and Yellowtail Flounder, without including environmental covariates, up to 3 years in the future
316 with only a modest loss of predictive ability. The SDMs developed here can be used to identify regions of
317 consistently high and low probability of occurrence, quantify changes in the size of a core area over time and
318 between seasons (surveys), quantify how rapidly distributional shifts occur, and provide short term forecasts
319 of the spatial distributions in future years.

320 The core area for Atlantic Cod collapsed rapidly in the early 1990s in unison with the collapse of Atlantic Cod
321 (and other groundfish) stocks throughout the Northwest Atlantic (Bundy *et al.*, 2009). Since this collapse,
322 the size of the core area has remained relatively consistent but there has been a shift to the northeast, which
323 was more pronounced in the *Fall*. The loss of core area from the warmer southern and western reaches of the
324 bank was the primary reason for the shift in the distribution of Atlantic Cod into Canadian waters. In more
325 recent years, the *Fall* distribution of Atlantic Cod was likely located on the northeastern slope of the bank
326 and outside of the core survey domains.

327 This northeastern shift of the stock over the course of this study suggests that the surveys may no longer
328 be sampling the entirety of Atlantic Cod throughout the course of the year (i.e. a higher proportion of the
329 stock may now be located outside of the survey domain in the *Fall* than in the past). The Atlantic Cod
330 stock assessment model for eastern GB Atlantic Cod used the survey indices from all three of the surveys

331 (Andrushchenko *et al.*, 2018). However, this assessment model suffered from such significant retrospective
332 patterns that the model was rejected in 2018; the results of this study are in agreement with the suggestion
333 that the observed shift in the distribution of Atlantic Cod outside of the survey domain was a contributing
334 factor to the model retrospective problems (Andrushchenko *et al.*, 2018, 2019). In addition, because the
335 management of this stock is shared between Canada and the U.S., the observed shift in the core distribution
336 to Canadian waters suggests that shared management policies, such as quota sharing agreements between the
337 two jurisdictions, may require regular review (e.g. TMGC, 2002).

338 Yellowtail Flounder were more likely to be found on sandy bottom types, in regions of the bank that
339 historically had lower temperatures, and at depths between 66-75 meters; this is consistent with the known
340 life history for this stock (Johnson *et al.*, 1999). In addition, there was a consistent elevated likelihood
341 of encountering Yellowtail Flounder in the region straddling the ICJ line that was not explained by the
342 environmental covariates. This suggests that this region has some unexplained ecological or environmental
343 significance to Yellowtail Flounder. The shift in the distribution of Yellowtail Flounder away from more
344 southern and western parts of GB combined with the declines in biomass of Yellowtail Flounder throughout
345 the U.S. supports the view that environmental change was a factor in the recent decline of Yellowtail Flounder
346 both on GB and throughout the region (NFSC, 2012; Pershing *et al.*, 2015; Legault and McCurdy, 2018;
347 NOAA, 2020). Given the loss of Yellowtail Flounder from the warmer portions of the bank observed in this
348 study, it is possible that the remaining core area straddling the ICJ line represents the most northern suitable
349 habitat on GB for this stock. If temperatures continue to increase, as projected with climate change, the
350 suitability of this habitat may decline, increasing the risk of extirpation of Yellowtail Flounder from GB
351 irrespective of any fisheries management action (Allyn *et al.*, 2020).

352 **Environmental Covariates and Random Fields**

353 Few of the static environmental covariates examined were related to the distribution of either stock. Only the
354 static SST layer, depth, and sediment type (Yellowtail Flounder only) had any consistent relationship to the
355 likelihood of encountering either stock throughout the duration of this study. The influence of the average
356 SST was somewhat surprising given this layer was derived from monthly SST composites from the Advanced
357 Very High Resolution Radiometer (AVHRR) satellite from 1997 to 2008 (Greenlaw *et al.*, 2010) and thus
358 represents an aggregate, static layer from only a subset of the time period covered by the groundfish survey
359 data. However, the importance of this SST layer may be due to its ability to capture general widespread
360 oceanographic features across the bank domain. Further, the observed variability of the effect between
361 seasons was likely a reflection of the connection between surface waters and the benthos given that the degree

362 of vertical mixing and stratification varies with season and spatially across the bank (Kavanaugh *et al.*,
363 2017). It is acknowledged that the interpretation of the static SST layer used in these analyses as a thermal
364 effect is likely somewhat unrealistic as it assumes that the relative temperature patterns and response of
365 the stocks to these patterns have remained static across more than four decades. To understand how the
366 thermal environment has influenced the stocks' distributions on GB, the development of more advanced
367 models that use either dynamic SST or modelled bottom temperature layers would be beneficial (Pershing *et*
368 *al.*, 2015; Greenan *et al.*, 2019). Further, changes in the distribution of a stock cannot be inferred from static
369 environmental layers like those used in this analysis, the random fields were the means by which the changes
370 in distribution could be tracked.

371 From a predictive standpoint, the random fields were often able to predict the OP without a substantial loss
372 of predictive ability when compared to the more complex models including the static environmental data
373 (e.g. Figure 10). This occurred because the random fields were flexible enough to capture the variability
374 inherent in the data in each era, while the environmental covariate relationships were constrained to be
375 invariant throughout the entire time series. Recent research suggests that using a static random field in
376 conjunction with a spatio-temporal random field may provide less biased and more accurate estimates than
377 models that rely solely on environmental covariates (Yin *et al.*, n.d.). The results of the current study
378 also suggest that when environmental data aren't available or are prohibitively expensive to collect, these
379 spatial models on their own can provide insight into the drivers of a stock's distribution. The information
380 from these spatio-temporal models could then be used as a first step to better understand the patterns and
381 processes driving change in the stock's distribution and subsequently help with the design of more efficient
382 data collection programs.

383 Finally, it should be noted that the observed shifts in the distributions could be due to environmental change
384 and/or direct anthropogenic factors [e.g. fishing; Boudreau *et al.* (2017)]. The shifts in the distributions
385 in the 1970s and 1980s may indeed have been related to either fishing or environmental factors given the
386 relatively high fishing effort during this period (Anderson, 1997; Andrushchenko *et al.*, 2018; Legault and
387 McCurdy, 2018). However, several lines of evidence suggest that fisheries are not inhibiting these stocks from
388 re-establishing themselves in the southern or western portions of GB in more recent years. The lack of a large
389 directed fishery for Atlantic Cod on GB since the early 1990s, along with the addition of two large closures in
390 U.S. waters (Murawski *et al.*, 2000) have not resulted in a shift in the distribution of this stock back into
391 southern or western portions of the bank. In addition, in the early 2000s there was a large increase in the
392 biomass of Yellowtail Flounder, which lead to a short-lived directed fishery, that was followed by a rapid
393 decline in the biomass of this stock (Legault and McCurdy, 2018). During this ephemeral Yellowtail Flounder

recovery, the size of the core area increased substantially on GB, but it remained centred on the ICJ line; there was no widespread re-establishment of this stock throughout southern and western regions where it was observed frequently in the 1970s. Finally, in recent years, bycatch of these two stocks in two lucrative scallop fisheries on GB has been in decline (O'Keefe *et al.*, 2014; Keith *et al.*, 2020), but this has not resulted in an expansion of the distribution of either stock. Given these patterns along with the regional trends observed for other stocks of these species (Bundy *et al.*, 2009; NFSC, 2012; Pershing *et al.*, 2015; NOAA, 2020), it seems likely the distributions of both stocks on GB in recent years were predominately influenced by environmental conditions.

Conclusion

Temporally variable SDMs provide insight into how the distributions of Yellowtail Flounder and Atlantic Cod have changed on GB. The only static environmental data which had a significant effect on the stocks distributions were the average SST (1997-2008), depth, and bottom type (Yellowtail Flounder only). The inter-annual shifts in the distributions indicate the increasing importance of Canadian waters for both stocks; these shifts are likely due to the long-term environmental shifts observed in the region. Given the habitat constraints faced by both stocks, further shifts in environmental conditions will likely put both stocks at increased risk of extirpation in the U.S. portion of Georges Bank and, eventually, all of GB irrespective of any fisheries management action. The shifts in species distribution identified in these spatio-temporal models can be used to improve science advice and lead to more informed fisheries management decisions.

ACKNOWLEDGEMENTS

Thanks to Christine Ward-Paige, Yanjun Wang, Dheeraj Busawon, Monica Finley, Phil Politis, and Nancy Shackell for help with data, questions, and the development and exploration of various parts of this project. Thanks to Tricia Pearo Drew, Jamie Raper, and Brittany Wilson for general support and we thank Dan Ricard and Joanna Mills Flemming for their feedback on a previous version of this manuscript. This project was made possible by funding from Fisheries and Oceans Canada (DFO) Strategic Program for Ecosystem-based Research and Advice (SPERA).

419 **REFERENCES**

- 420 Allyn, A. J., Alexander, M. A., Franklin, B. S., Massiot-Granier, F., Pershing, A. J., Scott, J. D., and Mills,
421 K. E. 2020. Comparing and synthesizing quantitative distribution models and qualitative vulnerability
422 assessments to project marine species distributions under climate change. PLOS ONE, 15: e0231595.
423 Public Library of Science. <https://journals.plos.org/plosone/article?id=10.1371/journal.pone.0231595>
424 (Accessed 1 September 2020).
- 425 Anderson, E. D. 1997. The history of fisheries management and scientific advice – the ICNAF/NAFO history
426 from the end of World War II to the present. J. Northw. Atl. Fish. Sci.
- 427 Andrushchenko, I., Legault, C. M., Martin, R., Brooks, E. N., and Wang, Y. 2018. Assessment of Eastern
428 Georges Bank Atlantic Cod for 2018. TRAC Ref. Doc. 2018/01.
- 429 Andrushchenko, I., Legault, C. M., and Barrett, M. A. 2019. Alternative Methodologies for Providing Interim
430 Catch Advice for Eastern Georges Bank Cod. TRAC Ref. Doc. 2019/XX.
- 431 Backus, R. H., and Bourne, D. W. 1987. Georges Bank. MIT, Cambridge, Mass. 593 pp.
- 432 Bakka, H., Rue, H., Fuglstad, G.-A., Riebler, A., Bolin, D., Krainski, E., Simpson, D., *et al.* 2018. Spatial
433 modelling with R-INLA: A review. <https://arxiv.org/abs/1802.06350v2> (Accessed 22 September 2020).
- 434 Beverton, R., and Holt, S. 1957. On the dynamics of exploited Fish Populations. UK Ministry of Agriculture,
435 Fisheries and Food.
- 436 Booth, T. H., Nix, H. A., Busby, J. R., and Hutchinson, M. F. 2014. Bioclim: The first species distribution
437 modelling package, its early applications and relevance to most current MaxEnt studies. Diversity and
438 Distributions, 20: 1–9. <http://onlinelibrary.wiley.com/doi/abs/10.1111/ddi.12144> (Accessed 22 September
439 2020).
- 440 Boudreau, S. A., Shackell, N. L., Carson, S., and Heyer, C. E. den. 2017. Connectivity, persistence, and loss
441 of high abundance areas of a recovering marine fish population in the Northwest Atlantic Ocean. Ecology
442 and Evolution, 7: 9739–9749. <http://onlinelibrary.wiley.com/doi/abs/10.1002/ece3.3495> (Accessed 6 May
443 2020).
- 444 Box, E. O. 1981. Predicting Physiognomic Vegetation Types with Climate Variables. Vegetatio, 45: 127–139.
445 Springer. <http://www.jstor.org/stable/20037033>.
- 446 Bundy, A., Heymans, J. J., Morissette, L., and Savenkoff, C. 2009. Seals, cod and forage fish: A comparative
447 exploration of variations in the theme of stock collapse and ecosystem change in four Northwest Atlantic

- 448 ecosystems. *Progress in Oceanography*, 81: 188–206. <http://www.sciencedirect.com/science/article/pii/S0079661109000305> (Accessed 1 September 2020).
- 449
- 450 Cadrin, S. X. 2020. Defining spatial structure for fishery stock assessment. *Fisheries Research*, 221: 105397.
451 <http://www.sciencedirect.com/science/article/pii/S0165783619302528> (Accessed 3 October 2019).
- 452 CBD. 2018, May 11. Aichi Biodiversity Targets. <https://www.cbd.int/sp/targets/> (Accessed 11 March 2020).
- 453 Cheung, W. W. L., Close, C., Lam, V., Watson, R., and Pauly, D. 2008. Application of macroecological
454 theory to predict effects of climate change on global fisheries potential. *Marine Ecology Progress Series*,
455 365: 187–197. <https://www.int-res.com/abstracts/meps/v365/p187-197/> (Accessed 22 September 2020).
- 456 Cosandey-Godin, A., Krainski, E. T., Worm, B., and Flemming, J. M. 2015. Applying Bayesian spatiotemporal
457 models to fisheries bycatch in the Canadian Arctic. *Canadian Journal of Fisheries and Aquatic Sciences*,
458 72: 186–197. <http://www.nrcresearchpress.com/doi/10.1139/cjfas-2014-0159> (Accessed 20 June 2019).
- 459 Domisch, S., Friedrichs, M., Hein, T., Borgwardt, F., Wetzig, A., Jähnig, S. C., and Langhans, S. D. 2019.
460 Spatially explicit species distribution models: A missed opportunity in conservation planning? *Diversity
461 and Distributions*, 25: 758–769. <http://onlinelibrary.wiley.com/doi/abs/10.1111/ddi.12891> (Accessed 22
462 September 2020).
- 463 Elith, J., and Leathwick, J. R. 2009. Species Distribution Models: Ecological Explanation and Prediction
464 Across Space and Time. *Annual Review of Ecology, Evolution, and Systematics*, 40: 677–697. <http://www.annualreviews.org/doi/10.1146/annurev.ecolsys.110308.120159> (Accessed 6 May 2020).
- 465
- 466 Fuglstad, G.-A., Simpson, D., Lindgren, F., and Rue, H. 2019. Constructing Priors that Penalize the
467 Complexity of Gaussian Random Fields. *Journal of the American Statistical Association*, 114: 445–452.
468 Taylor & Francis. <https://amstat.tandfonline.com/doi/full/10.1080/01621459.2017.1415907> (Accessed 22
469 September 2020).
- 470 Greenan, B. J. W., Shackell, N. L., Ferguson, K., Greyson, P., Cogswell, A., Brickman, D., Wang, Z., *et al.* 2019.
471 Climate Change Vulnerability of American Lobster Fishing Communities in Atlantic Canada. *Frontiers
472 in Marine Science*, 6. Frontiers. <https://www.frontiersin.org/articles/10.3389/fmars.2019.00579/full>
473 (Accessed 3 September 2020).
- 474 Greenlaw, M. E., Sameoto, J. A., Lawton, P., Wolff, N. H., Incze, L. S., Pitcher, C. R., Smith, S. J., *et al.*
475 2010. A geodatabase of historical and contemporary oceanographic datasets for investigating the role of
476 the physical environment in shaping patterns of seabed biodiversity in the Gulf of Maine. *Can. Tech.
477 Rep. Fish. Aquat. Sci.* 2895: iv + 35 p. <http://waves-vagues.dfo-mpo.gc.ca/Library/342505.pdf>.

- 478 Grinnell, J. 1904. The Origin and Distribution of the Chest-Nut-Backed Chickadee. *The Auk*, 21: 364–382.
- 479 American Ornithological Society. <http://www.jstor.org/stable/4070199>.
- 480 Halliday, R. G., and Pinhorn, A. T. 1996. North Atlantic Fishery Management Systems: A Comparison of
481 Management Methods and Resource Trends. *Journal of Northwest Atlantic Fishery Science*; Dartmouth,
482 20. Northwest Atlantic Fisheries Org, Dartmouth, Canada, Dartmouth. <http://search.proquest.com/docview/2377266062/abstract/B0E1653EF6254974PQ/1> (Accessed 22 September 2020).
- 484 Halpern, B. S., Klein, C. J., Brown, C. J., Beger, M., Grantham, H. S., Mangubhai, S., Ruckelshaus, M.,
485 *et al.* 2013. Achieving the triple bottom line in the face of inherent trade-offs among social equity,
486 economic return, and conservation. *Proceedings of the National Academy of Sciences*, 110: 6229–6234.
487 <https://www.pnas.org/content/110/15/6229> (Accessed 11 March 2020).
- 488 Hilborn, R., and Walters, C. J. 1992. Quantitative fisheries stock assessment: Choice, dynamics and
489 uncertainty. Chapman and Hall, New York.
- 490 Johnson, D. L., Morse, W. W., Berrien, P. L., and Vitaliano, J. J. 1999. Yellowtail Flounder, *Limanda*
491 *ferruginea*, Life History and Habitat Characteristics. NOAA Technical Memorandum, NMFS-NE-140.
- 492 Kavanaugh, M. T., Rheuban, J. E., Luis, K. M. A., and Doney, S. C. 2017. Thirty-Three Years of Ocean
493 Benthic Warming Along the U.S. Northeast Continental Shelf and Slope: Patterns, Drivers, and Ecological
494 Consequences. *Journal of Geophysical Research: Oceans*, 122: 9399–9414. <https://agupubs.onlinelibrary.wiley.com/doi/abs/10.1002/2017JC012953> (Accessed 9 October 2020).
- 496 Keith, D. M., Sameoto, J. A., Keyser, F. M., and Ward-Paige, C. A. 2020. Evaluating socio-economic and
497 conservation impacts of management: A case study of time-area closures on Georges Bank. *PLOS ONE*,
498 15: e0240322. Public Library of Science. <https://journals.plos.org/plosone/article?id=10.1371/journal.pone.0240322> (Accessed 15 October 2020).
- 500 Kristensen, K., Nielsen, A., Berg, C. W., Skaug, H., and Bell, B. M. 2016. TMB: Automatic Differentiation
501 and Laplace Approximation. *Journal of Statistical Software*, 70: 1–21. <https://www.jstatsoft.org/index.php/jss/article/view/v070i05> (Accessed 12 April 2020).
- 503 Leach, K., Montgomery, W. I., and Reid, N. 2016. Modelling the influence of biotic factors on species
504 distribution patterns. *Ecological Modelling*, 337: 96–106. <http://www.sciencedirect.com/science/article/pii/S0304380016302216> (Accessed 22 September 2020).
- 506 Legault, C. M., and McCurdy, Q. M. 2018. Stock Assessment of Georges Bank Yellowtail Flounder for 2018.
507 TRAC. Ref. Doc, 2018/03: 64.

- 508 Lindgren, F., and Rue, H. 2015. Bayesian Spatial Modelling with R-INLA. *Journal of Statistical Software*, 63:
509 1–25. <https://www.jstatsoft.org/index.php/jss/article/view/v063i19> (Accessed 22 September 2020).
- 510 Martínez-Minaya, J., Cameletti, M., Conesa, D., and Pennino, M. G. 2018. Species distribution modeling:
511 A statistical review with focus in spatio-temporal issues. *Stochastic Environmental Research and Risk
512 Assessment*, 32: 3227–3244. <https://doi.org/10.1007/s00477-018-1548-7> (Accessed 22 September 2020).
- 513 McHenry, J., Welch, H., Lester, S. E., and Saba, V. 2019. Projecting marine species range shifts from only
514 temperature can mask climate vulnerability. *Global Change Biology*, 0. <https://doi.org/10.1111/gcb.14828>
515 (Accessed 16 October 2019).
- 516 McMullen, K. Y., Paskevich, V. F., and Poppe, L. J. 2014. 2014, GIS data catalog, in Poppe, L.J., McMullen,
517 K.Y., Williams, S.J., And Paskevich, V.F., Eds., 2014, USGS east-coast sediment analysis: Procedures,
518 database, and GIS data (ver. 3.0, November 2014). U.S. Geological Survey Open-File Report 2005-1001.
519 <http://pubs.usgs.gov/of/2005/1001/>.
- 520 Merow, C., LaFleur, N., Silander Jr., J. A., Wilson, A. M., and Rubega, M. 2011. Developing Dynamic
521 Mechanistic Species Distribution Models: Predicting Bird-Mediated Spread of Invasive Plants across
522 Northeastern North America. *The American Naturalist*, 178: 30–43. The University of Chicago Press.
523 <http://www.journals.uchicago.edu/doi/full/10.1086/660295> (Accessed 22 September 2020).
- 524 Murawski, S. A., Brown, R., Lai, H.-L., Rago, P. J., and Hendrickson, L. 2000. Large-scale closed areas
525 as a fishery-management tool in temperate marine systems: The Georges Bank experience. *Bull. US
526 FIsh Comm*, 66: 775–798. <https://www.ingentaconnect.com/content/umrsmas/bullmar/2000/00000066/00000003/art00020> (Accessed 24 July 2019).
- 528 NFSC. 2012. 54th Northeast Regional Stock Assessment Workshop (54th SAW), assessment summary report.
529 Northeast Fisheries Science Center Reference Document 12-14. <https://repository.library.noaa.gov/view/noaa/4184> (Accessed 1 September 2020).
- 531 NOAA. 2020. NOAA Yellowtail Flounder Overview. NOAA Yellowtail Flounder Overview. <https://www.fisheries.noaa.gov/species/yellowtail-flounder#overview> (Accessed 1 September 2020).
- 533 O'Keefe, C. E., Cadrian, S. X., and Stokesbury, K. D. E. 2014. Evaluating effectiveness of time/area closures,
534 quotas/caps, and fleet communications to reduce fisheries bycatch. *ICES Journal of Marine Science*, 71:
535 1286–1297. <https://academic.oup.com/icesjms/article/71/5/1286/638196> (Accessed 19 June 2019).
- 536 Pershing, A. J., Alexander, M. A., Hernandez, C. M., Kerr, L. A., Bris, A. L., Mills, K. E., Nye, J. A.,
537 et al. 2015. Slow adaptation in the face of rapid warming leads to collapse of the Gulf of Maine

- 538 cod fishery. *Science*, 350: 809–812. American Association for the Advancement of Science. <https://science.sciencemag.org/content/350/6262/809> (Accessed 3 September 2020).
- 539
- 540 R Core Team. 2020. R: A language and environment for statistical computing. R Foundation for Statistical
541 Computing, Vienna, Austria. <https://www.R-project.org/>.
- 542 Reuchlin-Hugenholtz, E., Shackell, N. L., and Hutchings, J. A. 2015. The Potential for Spatial Distribution
543 Indices to Signal Thresholds in Marine Fish Biomass. *PLOS ONE*, 10: e0120500. Public Library of
544 Science. <https://journals.plos.org/plosone/article?id=10.1371/journal.pone.0120500> (Accessed 3 March
545 2021).
- 546 Ricker, W. E. 1944. Further Notes on Fishing Mortality and Effort. *Copeia*, 1944: 23–44. <http://www.jstor.org/stable/1438245>.
- 547
- 548 Ricker, W. E. 1975. Computation and Interpretation of Biological Statistics of Fish Populaions. *Bulletin of*
549 *the Fisheries Research Board of Canada*, 191. Environment Canada, Ottawa.
- 550 Robinson, L. M., Elith, J., Hobday, A. J., Pearson, R. G., Kendall, B. E., Possingham, H. P., and Richardson,
551 A. J. 2011. Pushing the limits in marine species distribution modelling: Lessons from the land present
552 challenges and opportunities. *Global Ecology and Biogeography*, 20: 789–802. <http://onlinelibrary.wiley.com/doi/abs/10.1111/j.1466-8238.2010.00636.x> (Accessed 22 September 2020).
- 553
- 554 Rue, H., Riebler, A., Sørbye, S. H., Illian, J. B., Simpson, D. P., and Lindgren, F. K. 2016. Bayesian
555 Computing with INLA: A Review. <https://arxiv.org/abs/1604.00860v2> (Accessed 22 September 2020).
- 556
- 557 Smith, S. J. 1996. Analysis of Data from Bottom Trawl Surveys. *NAFO Scientific Council Studies*: 25–53.
- 558
- 559 Sundblad, G., Bergström, U., and Sandström, A. 2011. Ecological coherence of marine protected area
560 networks: A spatial assessment using species distribution models. *Journal of Applied Ecology*, 48: 112–
120. <http://besjournals.onlinelibrary.wiley.com/doi/abs/10.1111/j.1365-2664.2010.01892.x> (Accessed 22
September 2020).
- 561
- 562 Thorson, J. T., Ianelli, J. N., Larsen, E. A., Ries, L., Scheuerell, M. D., Szuwalski, C., and Zipkin, E. F.
563 2016. Joint dynamic species distribution models: A tool for community ordination and spatio-temporal
564 monitoring. *Global Ecology and Biogeography*, 25: 1144–1158. <http://onlinelibrary.wiley.com/doi/abs/10.1111/geb.12464> (Accessed 22 September 2020).
- 565
- 566 Thorson, J. T. 2019. Guidance for decisions using the Vector Autoregressive Spatio-Temporal (VAST)
567 package in stock, ecosystem, habitat and climate assessments. *Fisheries Research*, 210: 143–161. <http://www.sciencedirect.com/science/article/pii/S0165783618302820> (Accessed 28 October 2019).

- 568 TMGC. 2002. Development of a Sharing Allocation Proposal for Transboundary Resources of Cod, Haddock
569 and Yellowtail Flounder on Georges Bank. Fisheries and Oceans Canada. Fisheries Management Regional
570 Report, 2002/01: 1–59. http://www.bio.gc.ca/info/intercol/tmgc-cogst/documents/FMR_2002_01.pdf.
- 571 Townsend, D. W., and Pettigrew, N. R. 1997. Nitrogen limitation of secondary production on Georges Bank.
572 Journal of Plankton Research, 19: 221–235. <https://academic.oup.com/plankt/article/19/2/221/1544306>
573 (Accessed 4 June 2019).
- 574 Valentine, P., and Lough, R. G. 1991. The Sea Floor Environment and the Fishery of Eastern Georges Bank -
575 The Influence of Geological and Oceanographic Environmental Factors on the Abundance and Distribution
576 of Fisheries Resources of the Northeast United States Continental Shelf. Open- File Rep: 91–439.
- 577 Yin, Y., Sameoto, J. A., Keith, D. M., and Mills Flemming, J. (n.d.). (In Review) A Spatiotemporal Model
578 of the Meat Weight - Shell Height Relationship for Sea Scallops in the Bay of Fundy.
- 579 Zuur, A. F., Ieno, E. N., and Elphick, C. S. 2010. A protocol for data exploration to avoid common statistical
580 problems: Data exploration. Methods in Ecology and Evolution, 1: 3–14. <http://doi.wiley.com/10.1111/j.2041-210X.2009.00001.x> (Accessed 12 September 2013).
- 582 Zuur, A. F., Leno, E. N., and Saveliev, A. A. 2017. Beginner's guide to spatial, temporal, and spatial-temporal
583 ecological data analysis with R-INLA /. Highland Statistics Ltd, Newburgh, United Kingdom. 362 pp.
- 584 Zuur, A. F., and Leno, E. N. 2018. Beginner's guide to spatial, temporal, and spatial-temporal ecological
585 data analysis with R-INLA /. Highland Statistics Ltd, Newburgh, United Kingdom. 362 pp.

586 **TABLES**

Table 1: Environmental variables used in the analysis. Variables in **bold** were retained after Variance Inflation Factor (VIF) analyses and were included in the linear models. Variables in *italics* were used for the Principal Component Analysis (PCA)

Data	Variable	Source	Resolution(m)	Units
USGS Yearly median Bottom Shear Stress <i>Stratification from 1996-2007</i>	Year.median <i>strat</i>	USGS(SFS – SMD) ³ CoML ¹	3500 2500	Pa none
Seasonal Range of SST <i>Average SST</i>	sst.rg <i>sst.avg</i>	CoML ¹	972	°C
Benthic Silicate	<i>sil</i>	CoML ¹	6000	µM
Sediment Grain size (CONMAP)	Sed	USGS(CONMAP) ²	-	none
Sand	<i>sand</i>	CoML ¹	6000	%
<i>Seasonal Range of Benthic Salinity 1996-2007</i>	<i>sal.rg</i>	CoML ¹	6000	psu
<i>Benthic Salinity 1996-2007</i>	<i>sal.avg</i>	CoML ¹	6000	psu
<i>Benthic Phosphate 1996-2007</i>	<i>phos.avg</i>	CoML ¹	6000	µM
<i>Benthic Nitrate 1996-2007</i>	<i>nit.avg</i>	CoML ¹	40000	µM
<i>Mud</i>	<i>Mud</i>	CoML ¹	6000	%
Average K490	k490.avg	CoML ¹	8000	none
<i>USGS Median of Bottom Shear Stress</i>	<i>gmaine</i>	USGS(SFS – SMD) ³	3500	Pa
Benthic Complexity	<i>complexity</i>	CoML ¹	397	°
Slope	<i>slope</i>	CoML ¹	397	°
<i>Depth</i>	<i>Dep</i>	CoML ¹	397	m
<i>Aspect</i>	<i>comlaspect</i>	CoML ¹	397	°
Seasonal Range of Sea Surface Chlorophyll	<i>chl.rg</i>	CoML ¹	1119	mg × m ⁻³
<i>Average Sea Surface Chlorophyll</i>	<i>Chl</i>	CoML ¹	855	mg × m ⁻³
Benthic Current Stress with Wind and Tidal Influences	botstr.wt	CoML ¹	952	N × m ⁻²
Benthic Current Stress with only tidal influence	botstr.t	CoML ¹	3800	N × m ⁻²

¹ CoML obtained from <http://waves-vagues.dfo-mpo.gc.ca/Library/342505.pdf>

² USGS(CONMAP) obtained from <https://woodshole.er.usgs.gov/openfile/of2005-1001/htmldocs/datacatalog.htm>

³ USGS(SFS-SMD) obtained from <https://woodshole.er.usgs.gov/project-pages/mobility/gmaine.html>

587 **FIGURES**

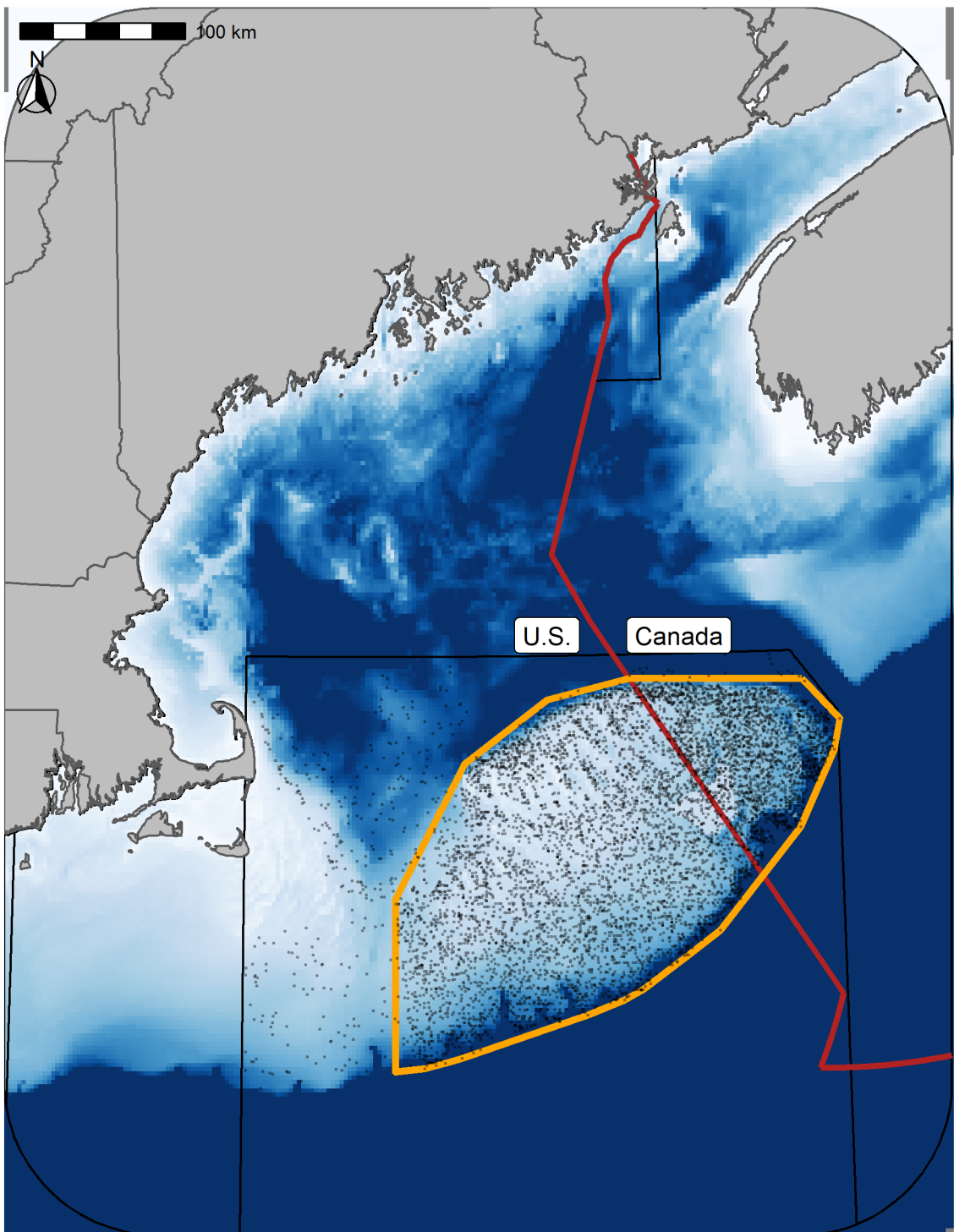


Figure 1: Georges Bank (GB) study area. Points represent the sample locations for each of the three surveys and the orange outline represents the core region of GB included in these analyses ($42,000 \text{ km}^2$). The red line delineates the Canadian exclusive economic zone (EEZ).

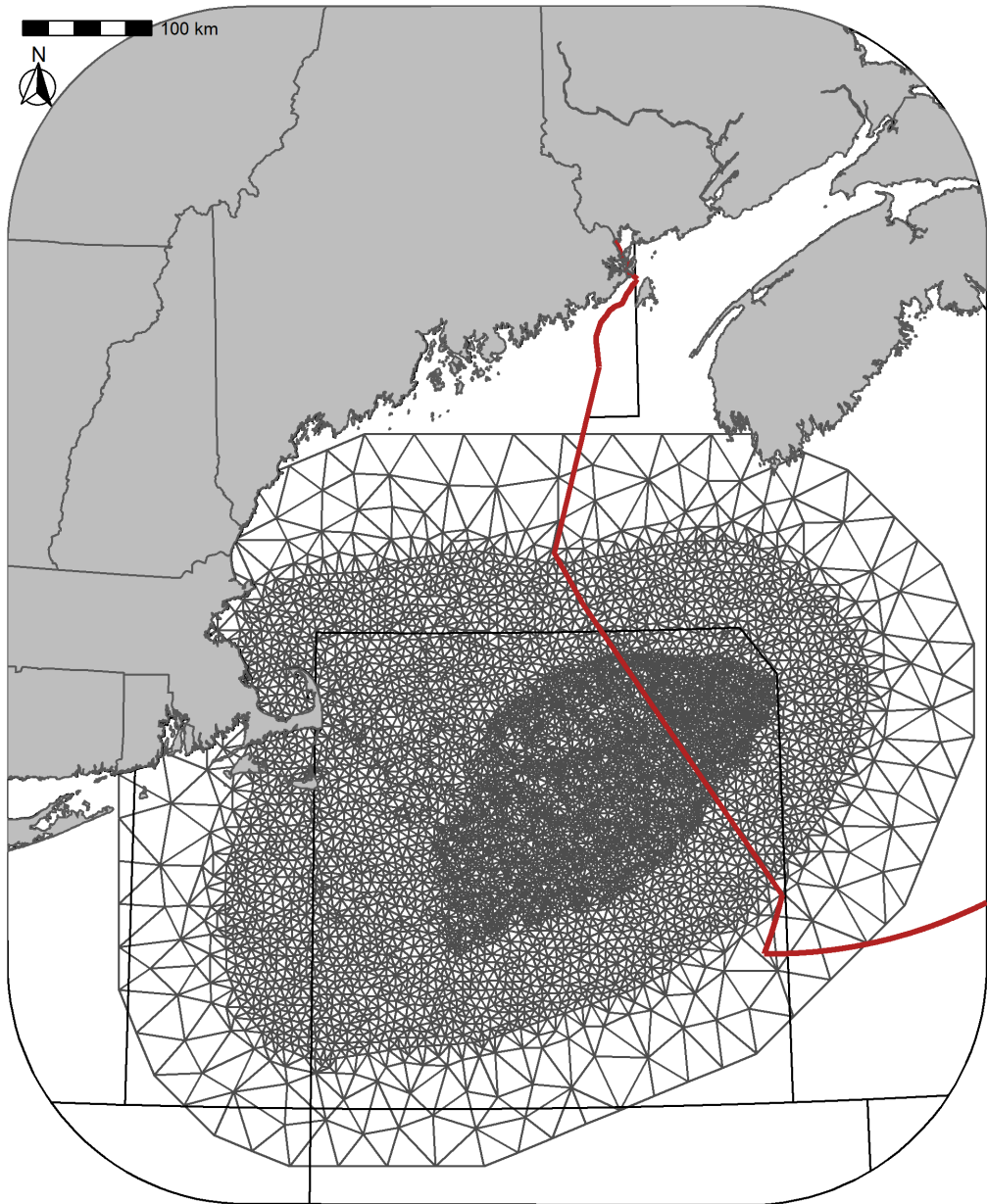


Figure 2: Delaunay triangular mesh used for the analyses. The mesh contains 6610 vertices. The red line delineates the Canadian exclusive economic zone (EEZ).

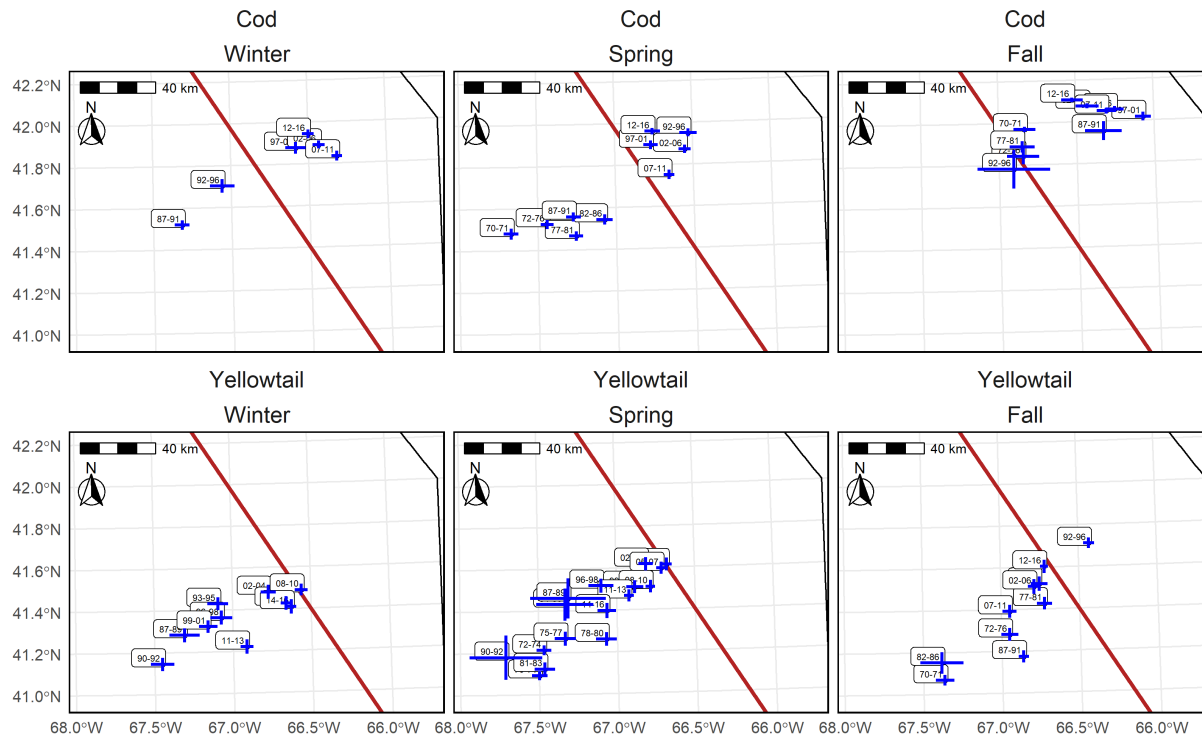


Figure 3: Center of Gravity (COG) for the core area ($OP \geq 0.75$) of Atlantic Cod (top panel) and Yellowtail Flounder (bottom panels) in the Winter (left), Spring (center), and Fall (right) using the final models. Blue lines indicate ± 3 standard deviation units from the mean COG. Labels indicate the years associated with each era and the red line is border between the U.S. and Canada.

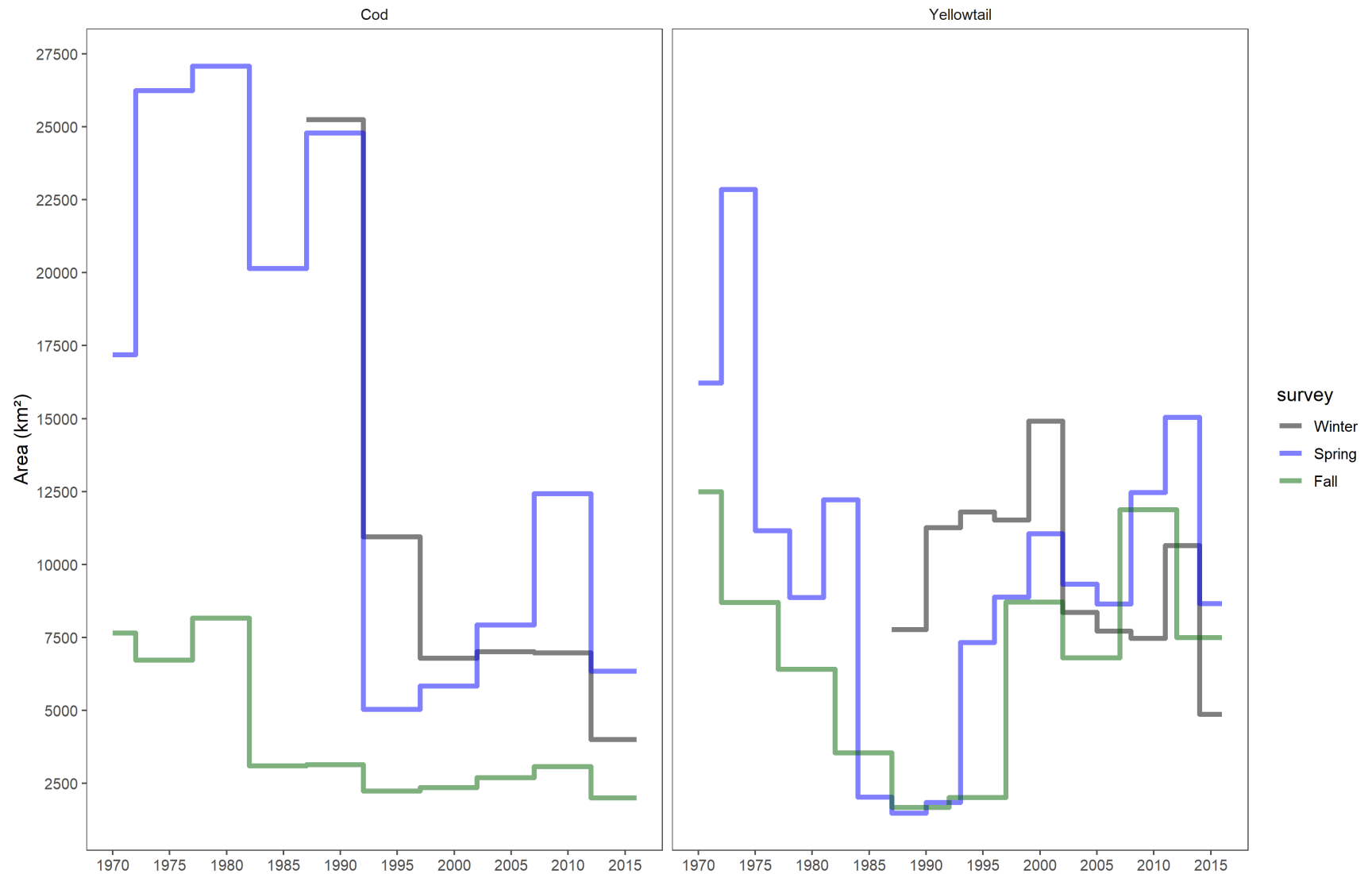


Figure 4: Time series of the size of the core area ($OP \geq 0.75$) on GB for each of the three seasons using the final models. The Atlantic Cod time series is on the left and the Yellowtail Flounder on the right. The black line represents the Winter trend, the blue line is the Spring trend, and the green line is the Fall trend.

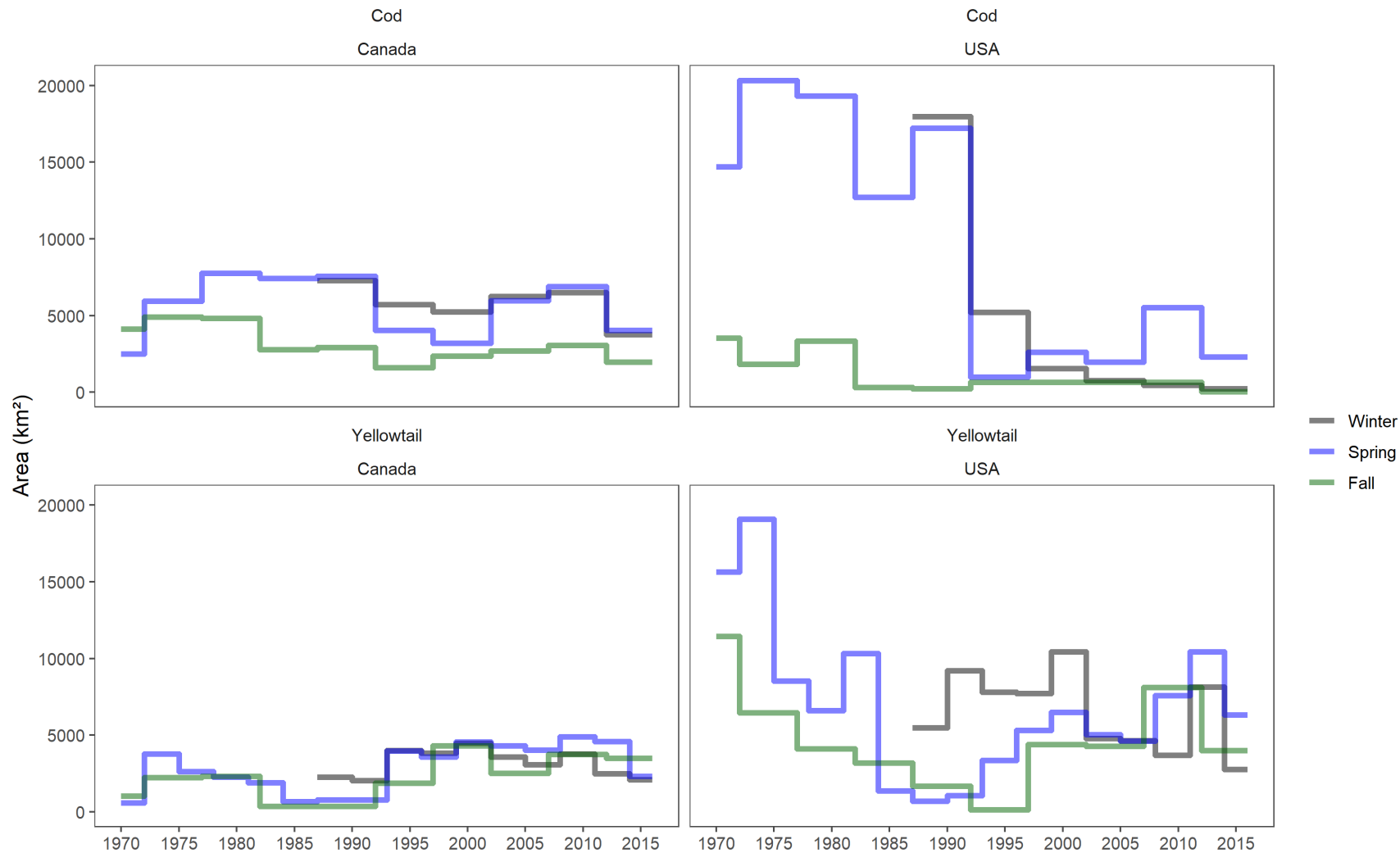


Figure 5: Time series of the size of the core area ($OP \geq 0.75$) on for each of the three seasons in Canada and the U.S.. The Atlantic Cod time series is in the top row and Yellowtail Flounder in the bottom row, Canada is on the left and U.S. is on the right. The black line represents the Winter trend, the blue line is the Spring trend, and the green line is the Fall trend.

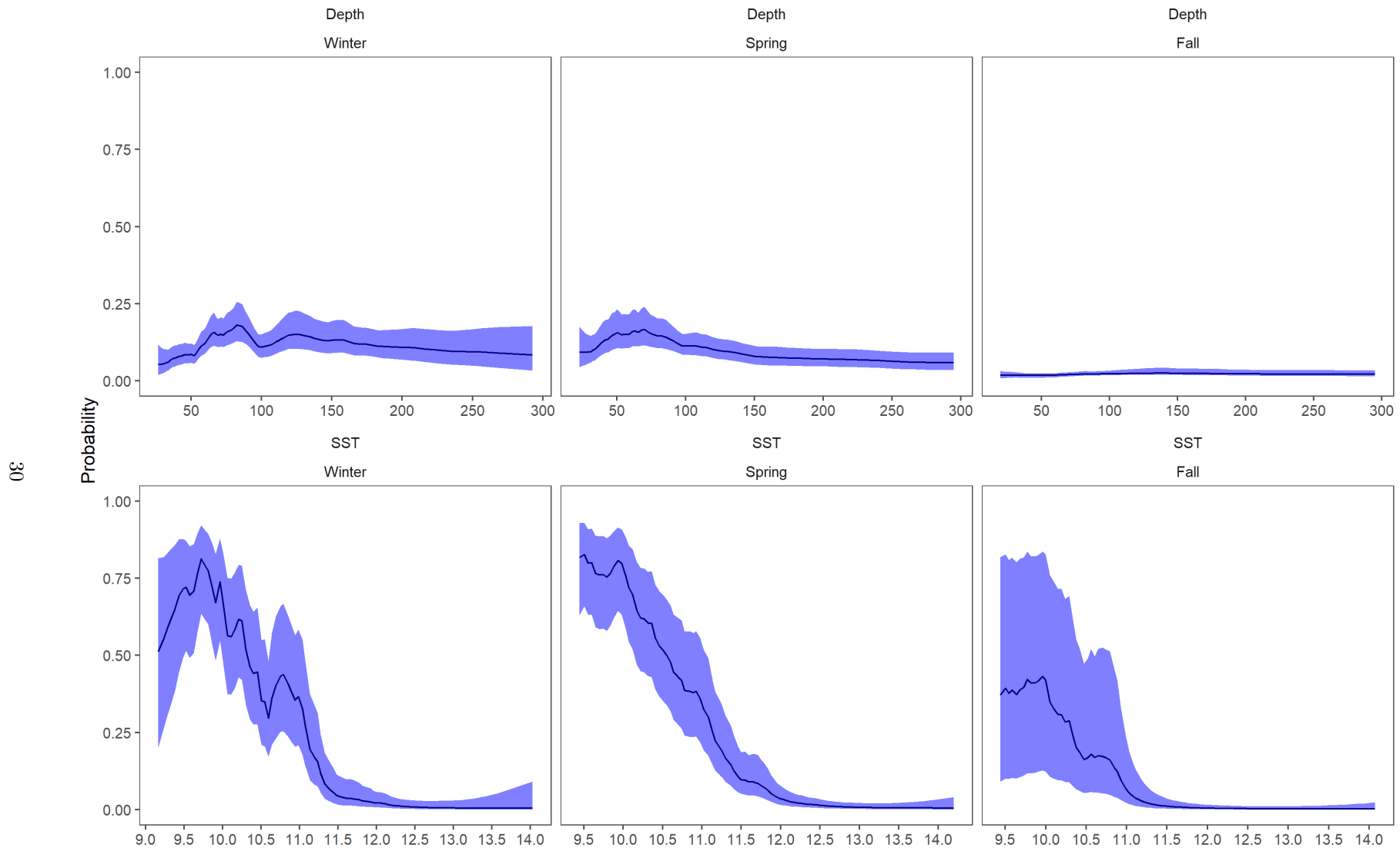


Figure 6: Environmental covariate effects for Atlantic Cod for each season, top row is the Dep covariate effect, bottom row is the SST effect. Results have been transformed to the probability scale and the blue shaded region represents the 95% credible interval.

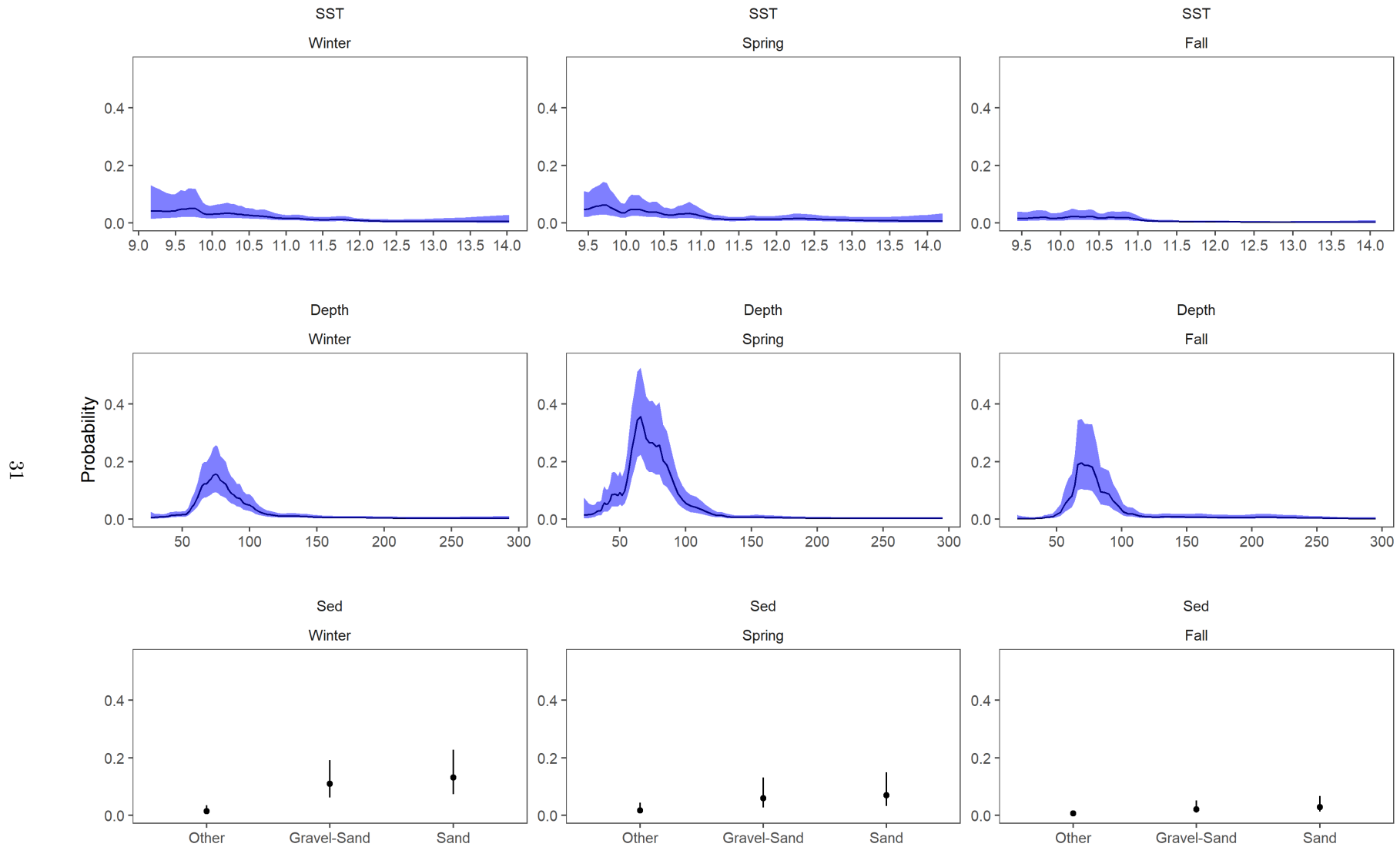


Figure 7: Environmental covariate effects for Yellowtail Flounder for each season, the top row is the Dep covariate effect, middle row is the SST effect, and the bottom row is the Sed effect. Results have been transformed to the probability scale, and the blue shaded region and the error bars represent the 95% credible intervals. The Winter and Spring results use a 3 year random field while the Fall results are for the 5 year random field model.

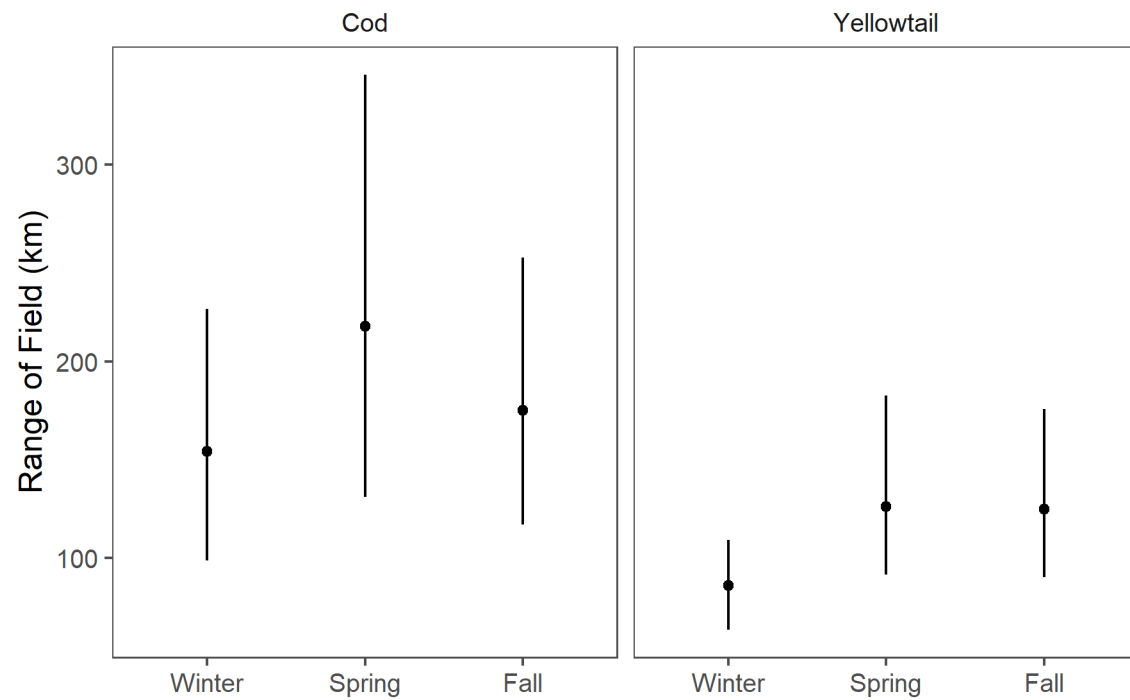


Figure 8: Decorrelation range estimate with 95% credible intervals for each season.

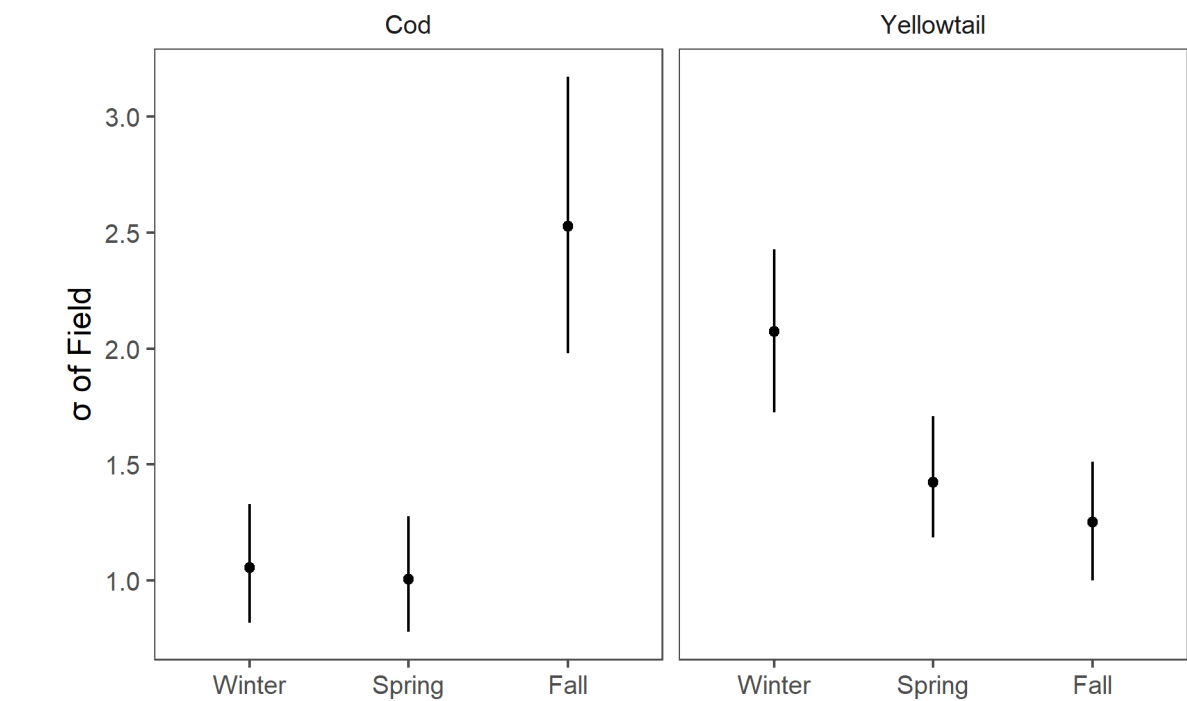


Figure 9: Standard Deviation of the field with 95% credible intervals for each season.

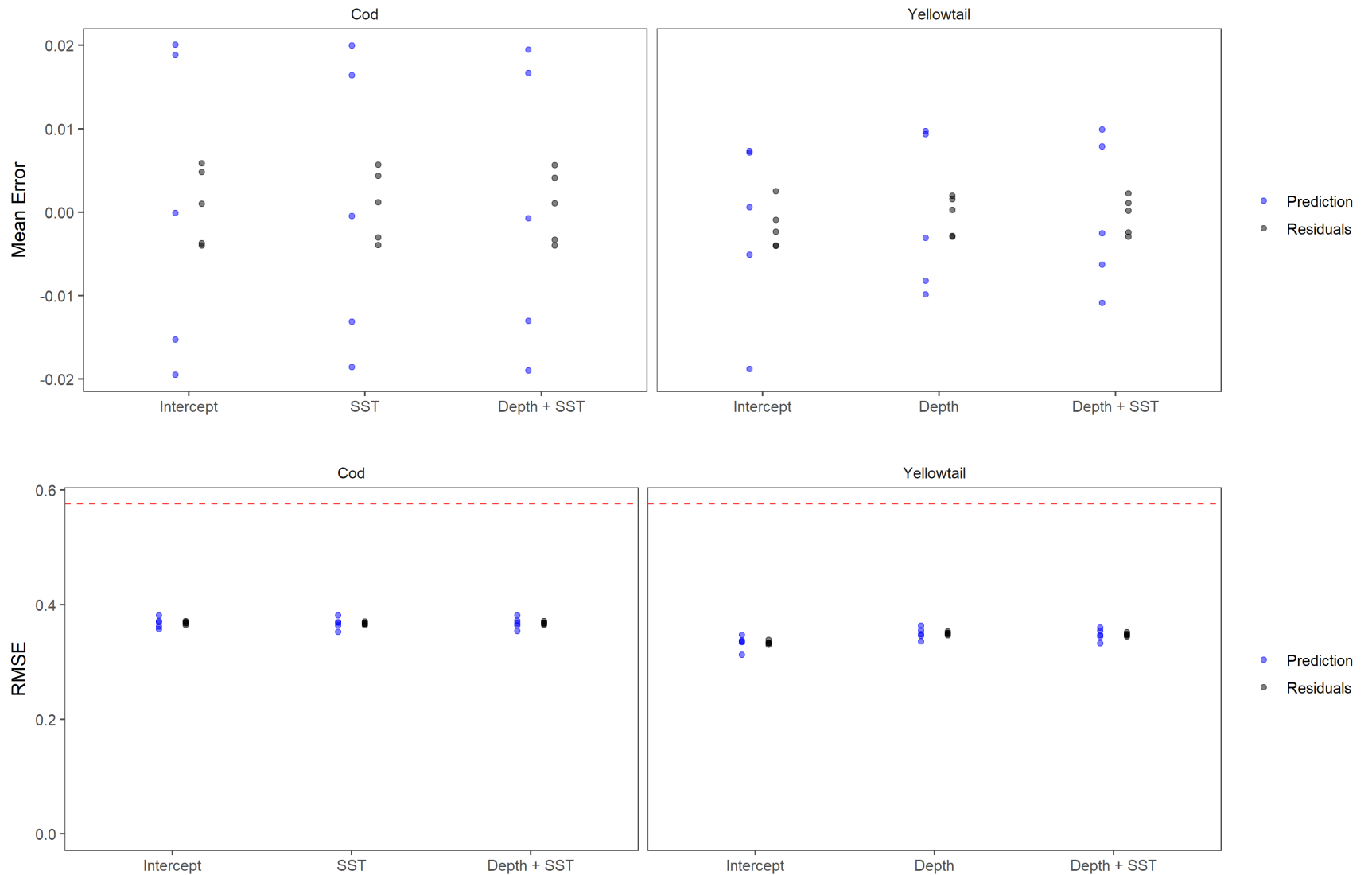


Figure 10: Results of five fold cross validation analyses. Top panels represents the mean error for each of the three covariate models tested for Atlantic Cod (using Winter data) and Yellowtail Flounder (using Spring data). Blue points represent the prediction error from the testing dataset, while the black points are the residuals from the training dataset. The bottom panels are the RMSE for these models. The red dashed line represents the RMSE for randomly generated data and represents the RMSE for a model with no predictive ability. All models use the 5 year random field due to computational constraints.

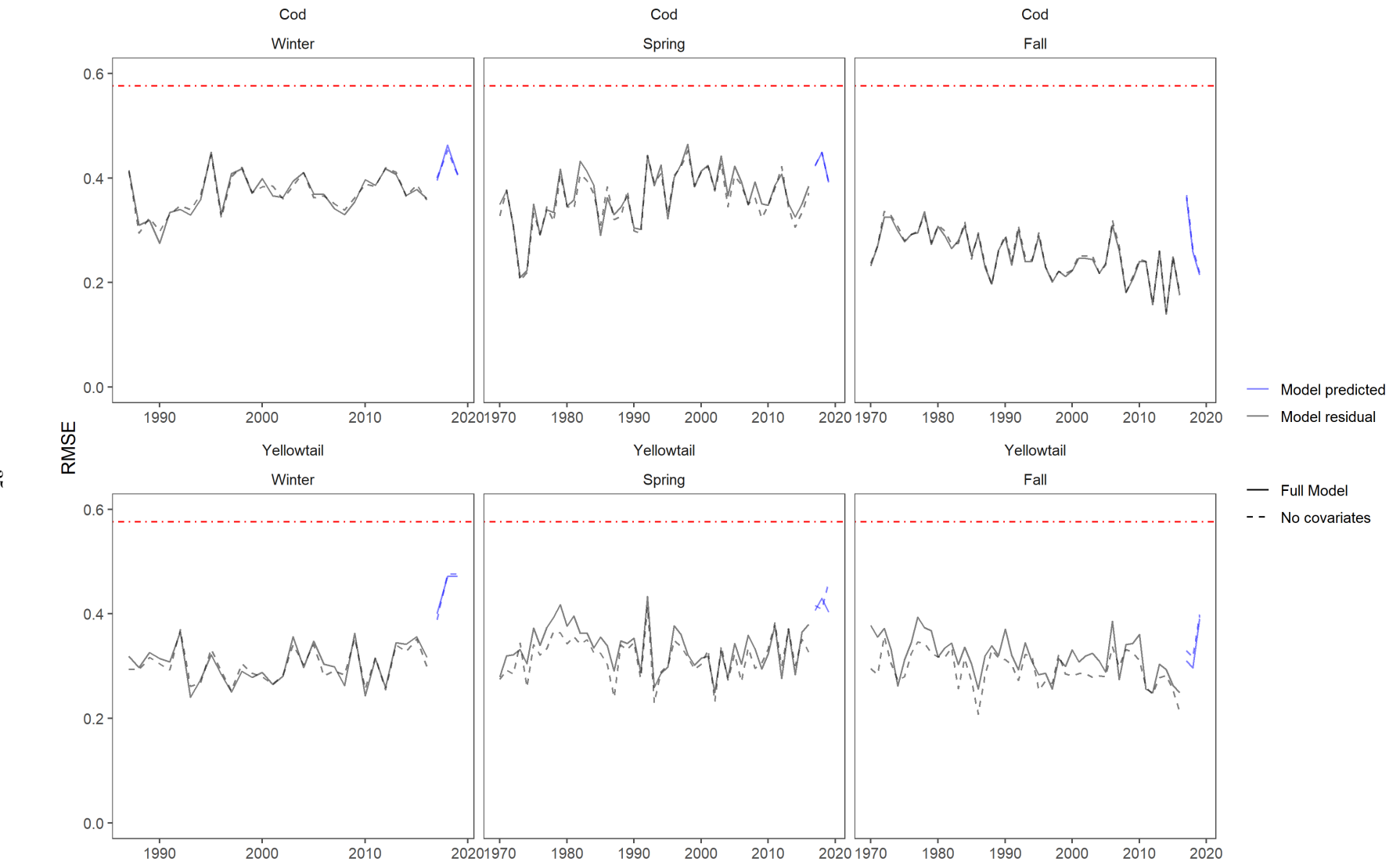


Figure 11: The residual RMSE for the model is shown in black, while the blue lines represent the prediction RMSE for data in years 2017, 2018, and 2019. The models compared were a model with no covariates (intercept + random field) represented by the dashed line and a model which includes the additive SST and Dep covariates along with the random field represented by the solid line. Atlantic Cod results are in the top row and use a 5 year random field. Yellowtail Flounder results are in the bottom row and use a 3 year random field for the Winter and Spring and the 5 year random field for the Fall. The red dot-dash line represents the RMSE for randomly generated data and represents the RMSE for a model with no predictive ability.

588 **SUPPLEMENT 1**

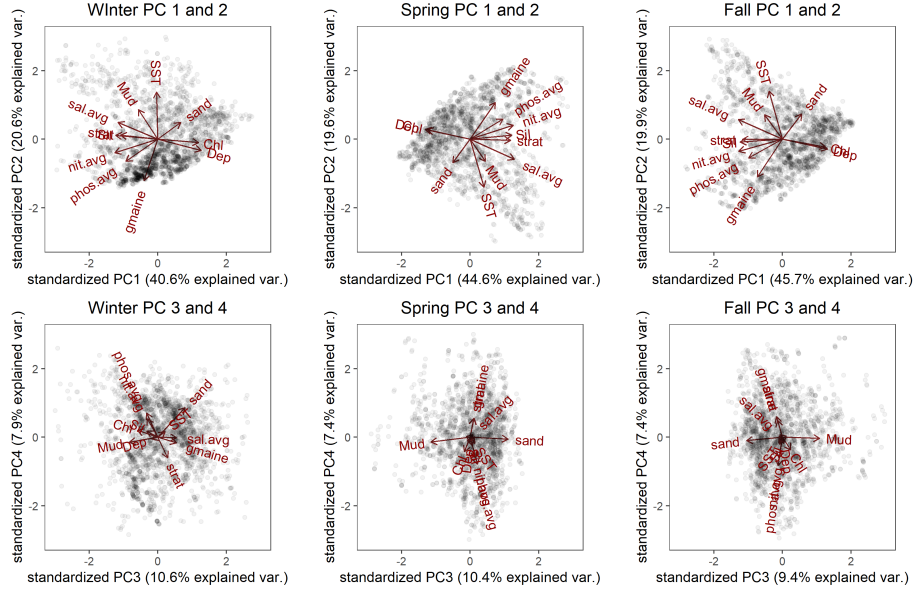


Figure S1: Principal Component Analysis (PCA) results for the Winter, Spring, and Fall seasons using the retained environmental data and the 4 retained Principal Components (PCs). The results for PC 1 and 2 for each season are on the top and the PC 3 and 4 results are on the bottom. Left column are the results for Winter, middle column for Spring, and right column is for the Fall. The percentage of the variance explained by each PC is provided on the axes labels. Points represent the score for each survey observation. The loadings for each covariate in the analysis are shown by the length of their respective lines. PC scores greater than ± 3 units not shown.

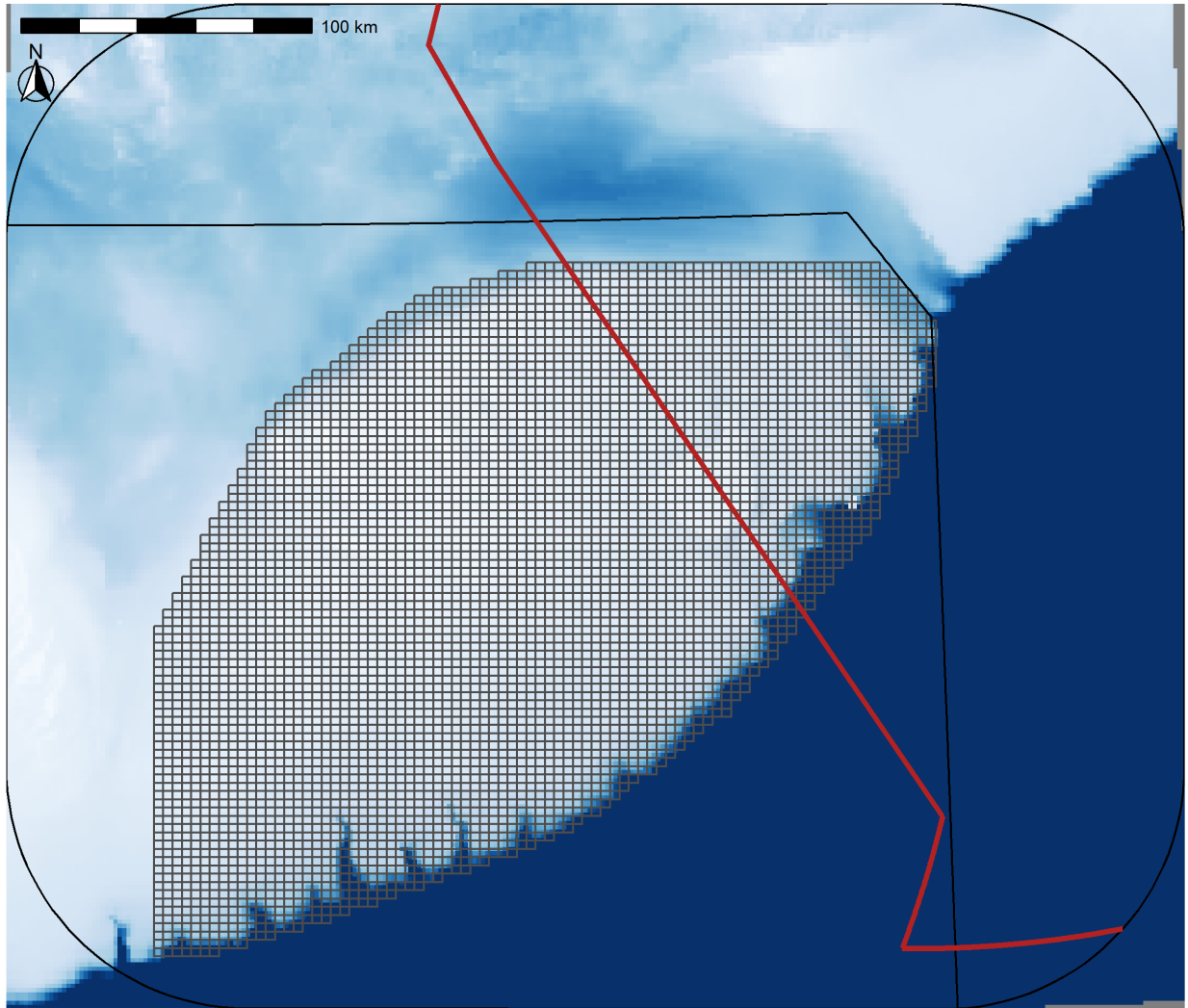


Figure S2: Prediction grid used for prediction of occurrence probability (OP).

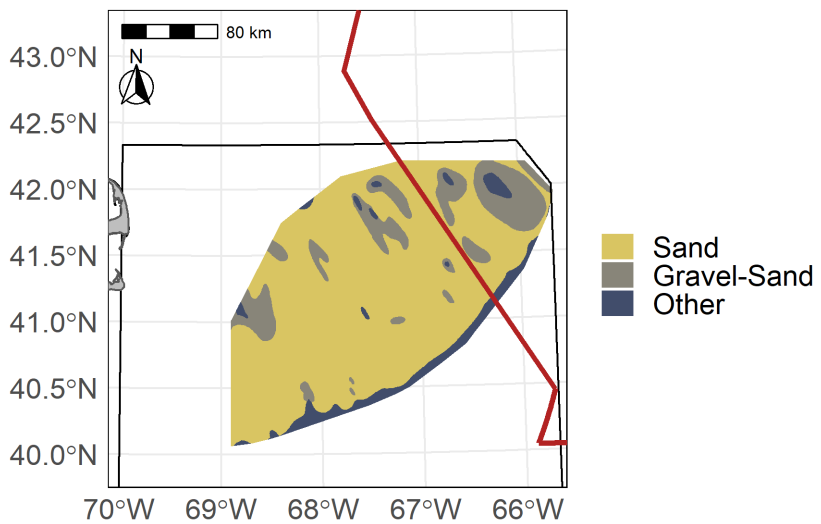
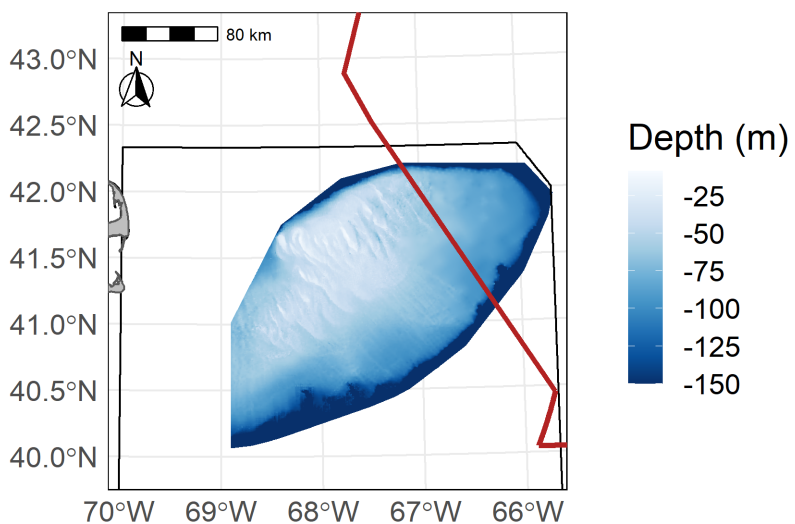
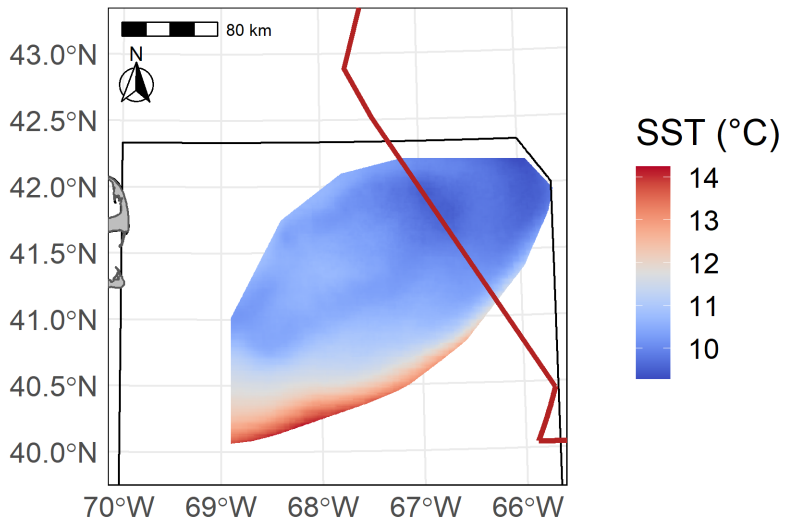


Figure S3: Georges Bank (GB) Average Sea Surface Temperature from 1997-2008 (SST in °C) in the top panel, bathymetry (depth in meters) in the center panel, and sediment type in the bottom panel.

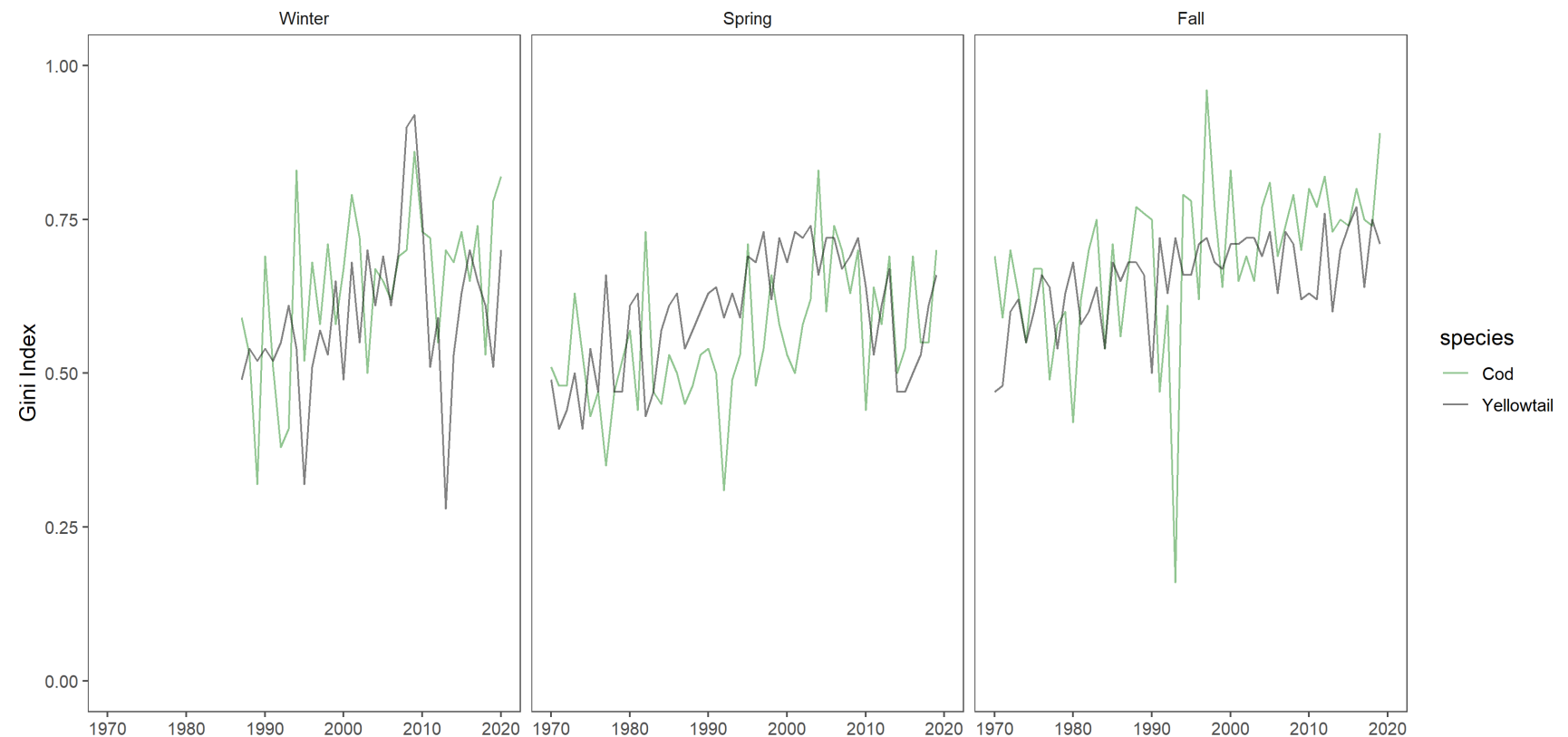


Figure S4: Gini Index

589 **Model Selection**

590 Stage 1 of model selection resulted in a significant reduction in the number of covariates. For Atlantic Cod,
591 sea surface temperature (SST) was identified as a significant covariate in the *Winter* and *Spring*, in addition
592 Dep and stratification were also significant predictors in the *Spring*. In the *Fall* no covariates had a WAIC
593 that were a significant improvement from the intercept only model (Figure S5). Further model selection
594 indicated that an additive Dep + SST model was the *final model* in all 3 seasons for Atlantic Cod (Figures
595 S6 and S7). When exploring the effect of temporal variability on the random fields, the models using the
596 5-year random field had the lowest WAIC in all seasons (Figure S8).

597 For Yellowtail Flounder, stage 1 of model selection indicated that the inclusion of Dep significantly improved
598 the models in all 3 seasons (surveys), while Sediment type (Sed) and chlorophyll concentration (Chl) in the
599 *Fall* had a similar impact on the model WAIC as Dep. As a result SST, Dep, Chl, and Sed were used to
600 explore the development of more complex covariate models. For Yellowtail Flounder the best models in stage
601 2 of model selection included 2 covariates with a combination of Dep, SST, and Sed (Figure S6). Further
602 model selection indicated that the *final model* for Yellowtail Flounder in all 3 seasons was an additive model
603 including Dep, SST, and Sed (Figure S7). When exploring the effect of temporal variability on the random
604 fields, the 3-year field had the lowest WAIC in the *Winter* and *Spring*, while the 5-year field had the lowest
605 WAIC in the *Fall* (Figure S8). Additional model selection results are available in the Model Output and
606 Model Diagnostics sections of the interactive dashboard.

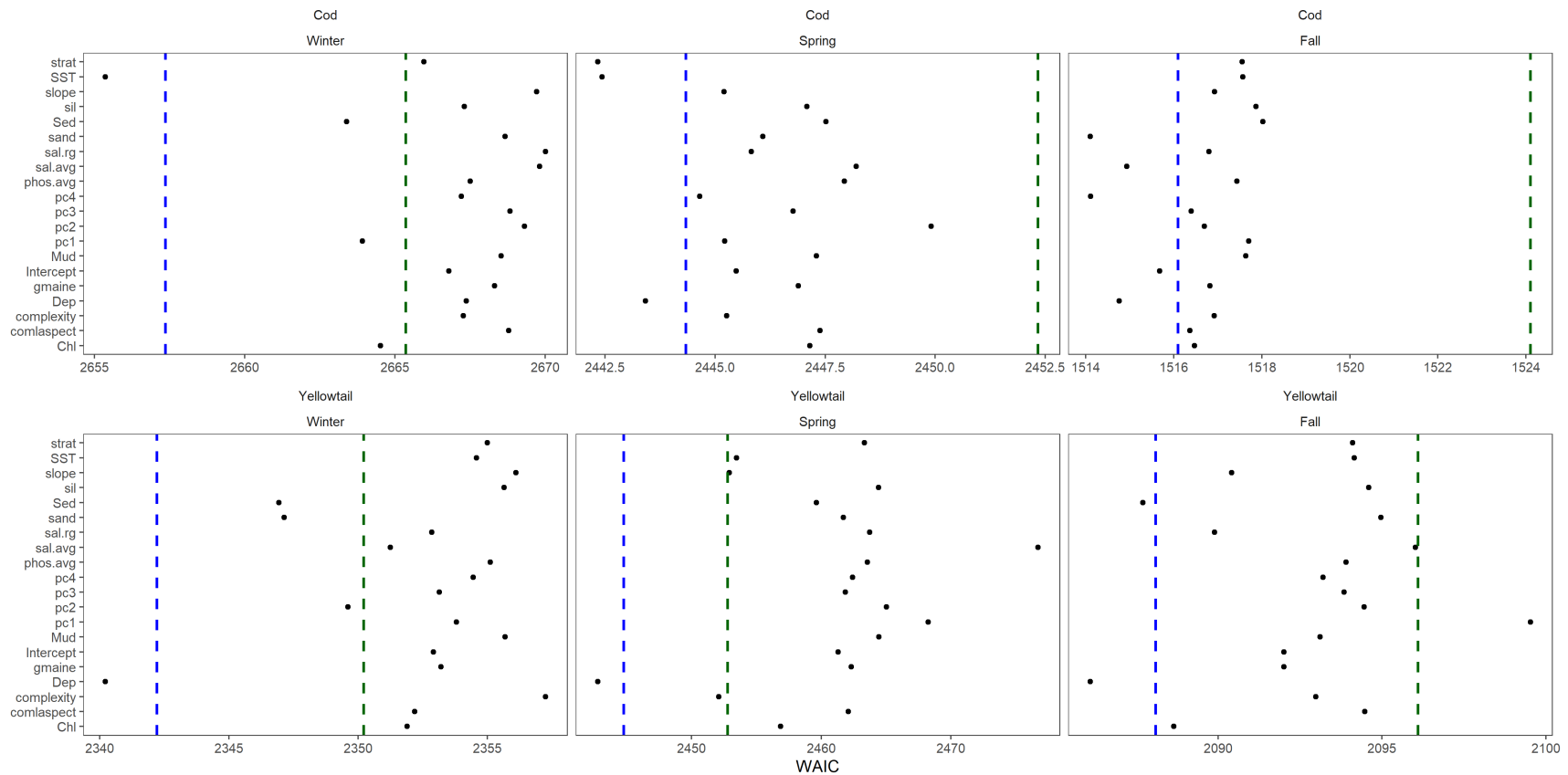


Figure S5: Initial stage of forward model selection using each of the environmental covariates individually. This model selection was done using a static random field. Blue dashed line is 2 WAIC units larger than the model with the lowest WAIC, the green dashed line is 10 WAIC units larger than the model with the lowest WAIC. The full description of the environmental variables can be found in Table 1.

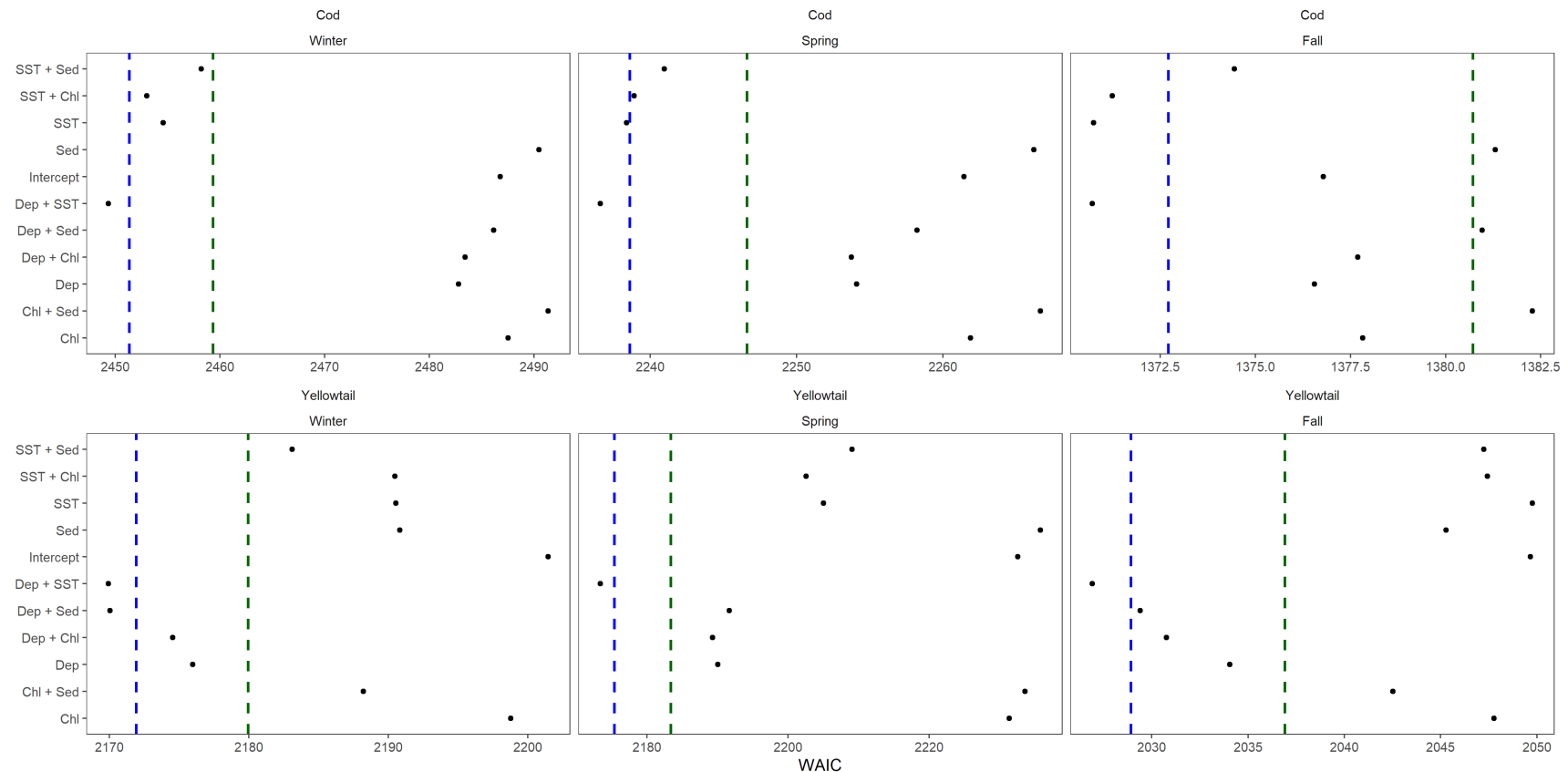


Figure S6: Stage 2 of model selection including additive models with 2 covariates based on the covariates identified in the initial model selection stage. These models were compared using the 10-year random field models. Blue dashed line is 2 WAIC units larger than the model with the lowest WAIC, the green dashed line is 10 WAIC units larger than the model with the lowest WAIC. The full description of the environmental variables can be found in Table 1.

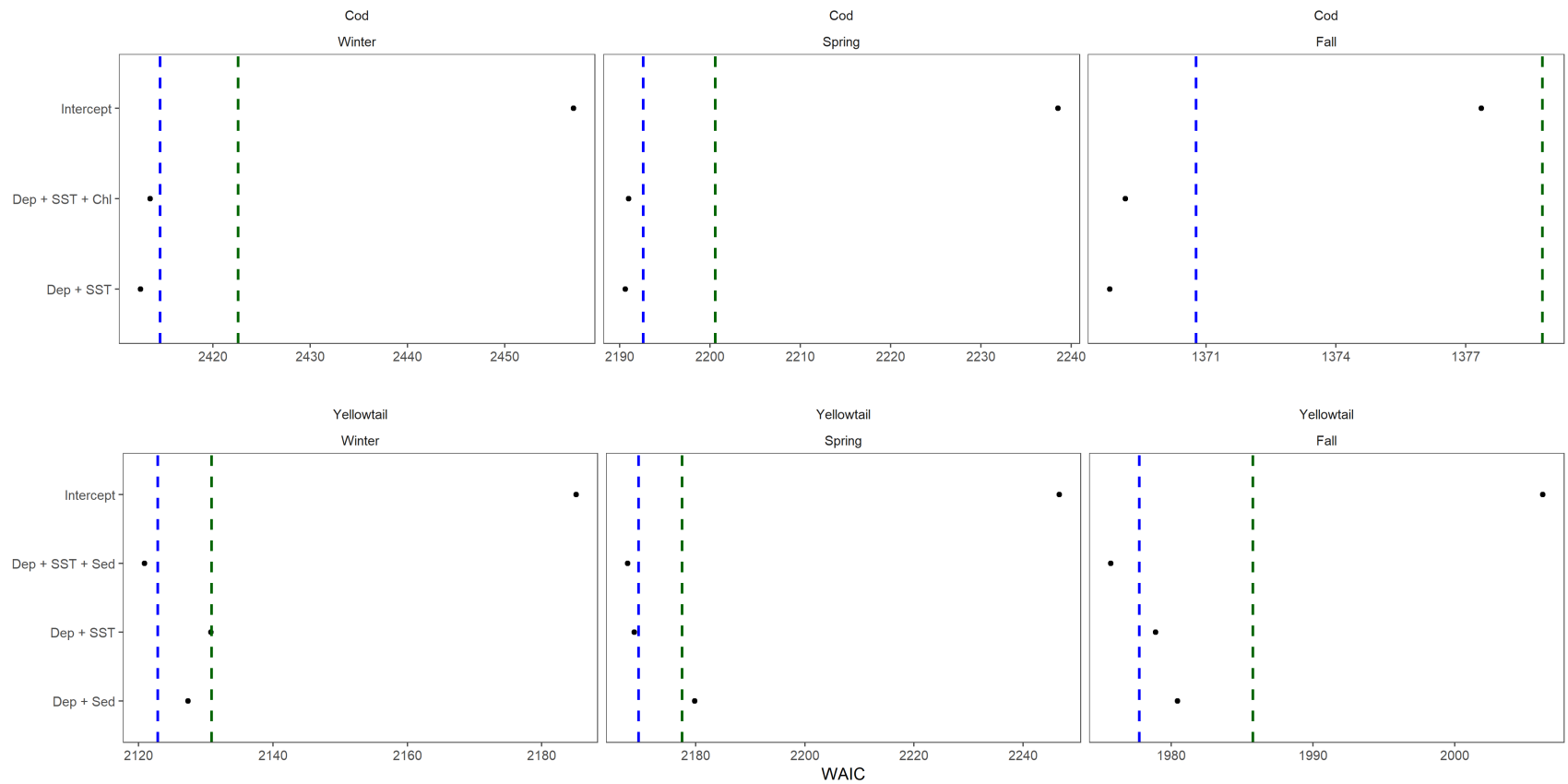


Figure S7: Final stage of covariate model selection which includes model with up to 3 covariate terms based on models selected at stage 2. Blue dashed line is 2 WAIC units larger than the model with the lowest WAIC, the green dashed line is 10 WAIC units larger than the model with the lowest WAIC. The full description of the environmental variables can be found in Table 1.

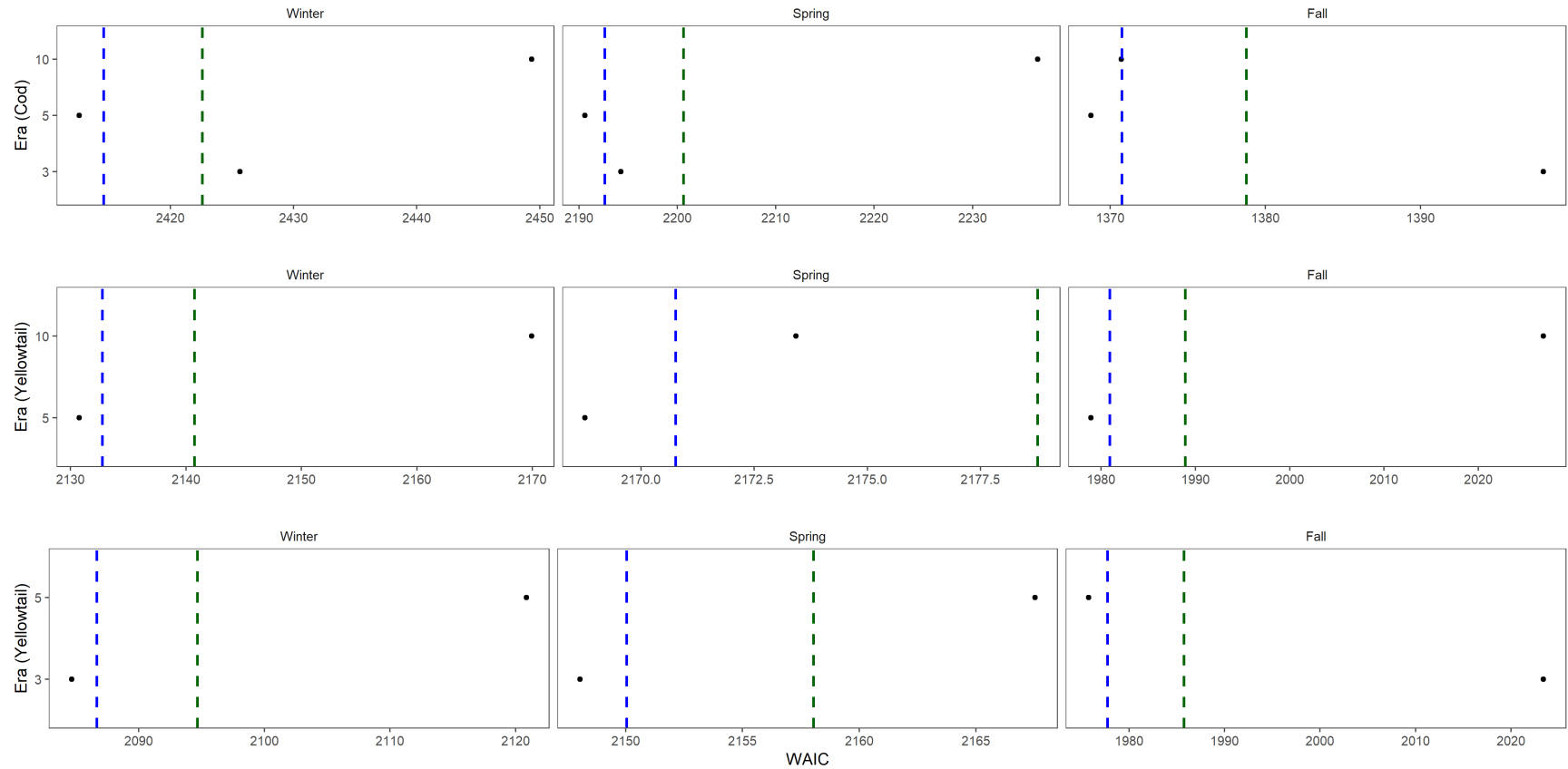


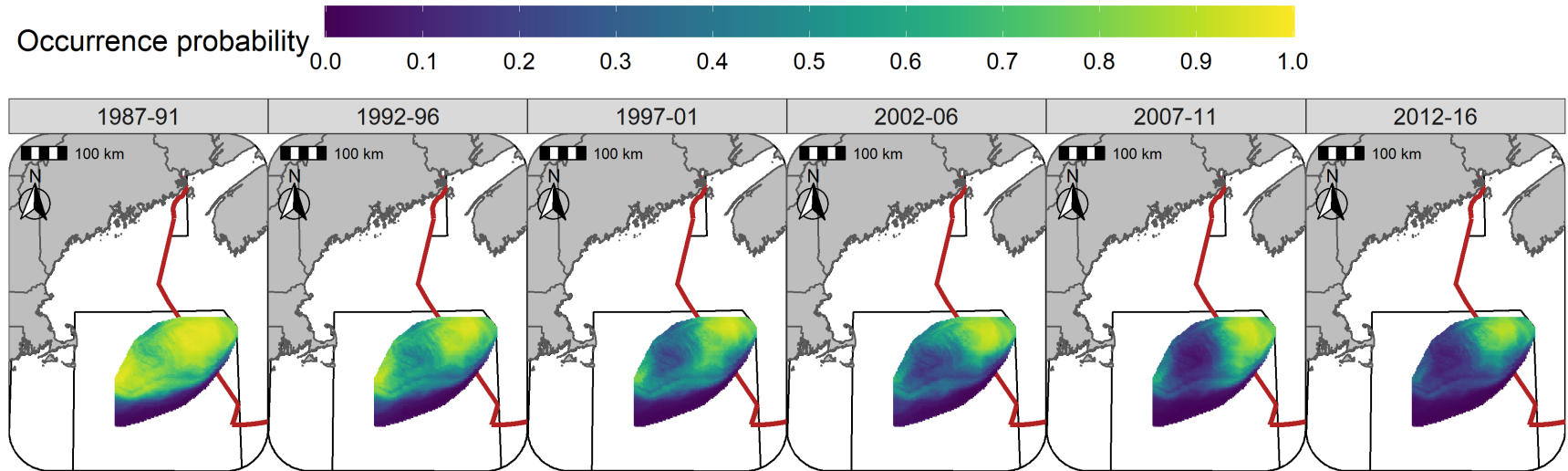
Figure S8: Model selection comparing the random fields models. For cod the model used is Dep + SST for all of the random fields. For Yellowtail the 5 and 10 year random fields were compared using the Dep + SST model, while the 5 and 3 fields were compared using the slightly preferred Dep + SST + Sed model. Blue dashed line is 2 WAIC units larger than the model with the lowest WAIC, the green dashed line is 10 WAIC units larger than the model with the lowest WAIC.

607 Predicted Occurrence Probability

608 The modeled OP for Atlantic Cod in the *Winter* and *Spring* was elevated on all but the most southern
609 portion of GB in the 1970s and 1980s, in the early 1990s there was an abrupt decline in the OP throughout
610 much of the U.S. portion of GB, while OP remained elevated in Canadian waters and in the area straddling
611 the ICJ line (Figures S9 - S10). In the *Fall* the core areas were isolated in northern of GB. An area on the
612 northwest of GB had some core area until the early 1980s but the OP in this area declined steadily after this
613 time and has had a low OP in the *Fall* for over 20 years, the highest OP areas remaining during the *Fall* are
614 along the northern edge of the bank and mostly in Canadian waters (Figure S11).

615 The modeled OP patterns for Yellowtail Flounder on GB are similar in the *Winter*, *Spring*, and *Fall* with
616 core area consistently observed in the region straddling the ICJ line in each season and throughout the study
617 period (Figures S12 - S14). A second region along the western border of the bank also has an elevated OP
618 and appears to be connected via a narrow band of varying width to the core area straddling the ICJ line.
619 The core area of Yellowtail Flounder declined in the late 1980s and early 1990s and was relatively stable until
620 2016 (Figure S14).

621 The standard deviation (SD) of the Atlantic Cod prediction field in the *Winter* and *Spring* tended to be
622 elevated in the central portion of the bank, and lowest in the south and along the edges of the prediction
623 domain. In the *Fall* the Atlantic Cod prediction field SD was lowest in the south, with the low SD area
624 expanding to central regions later in the study period (Figures S15 - S17). For Yellowtail Flounder, the SD
625 was consistently low in the part of the region with a core area that straddled the ICJ line in the *Winter*,
626 *Spring*, and *Fall* (Figures S18 - S20). Areas surrounding this region displayed an increase in the SD, while
627 a region in the north and along the southern flank of GB had relatively low SDs; these regions also had
628 relatively low OPs (Figures S12 - S14 and S18 - S20).



47

Figure S9: Predicted occurrence probability for Atlantic Cod in each era during the Winter (RV survey) using the SST + Dep model and 5-year random field.

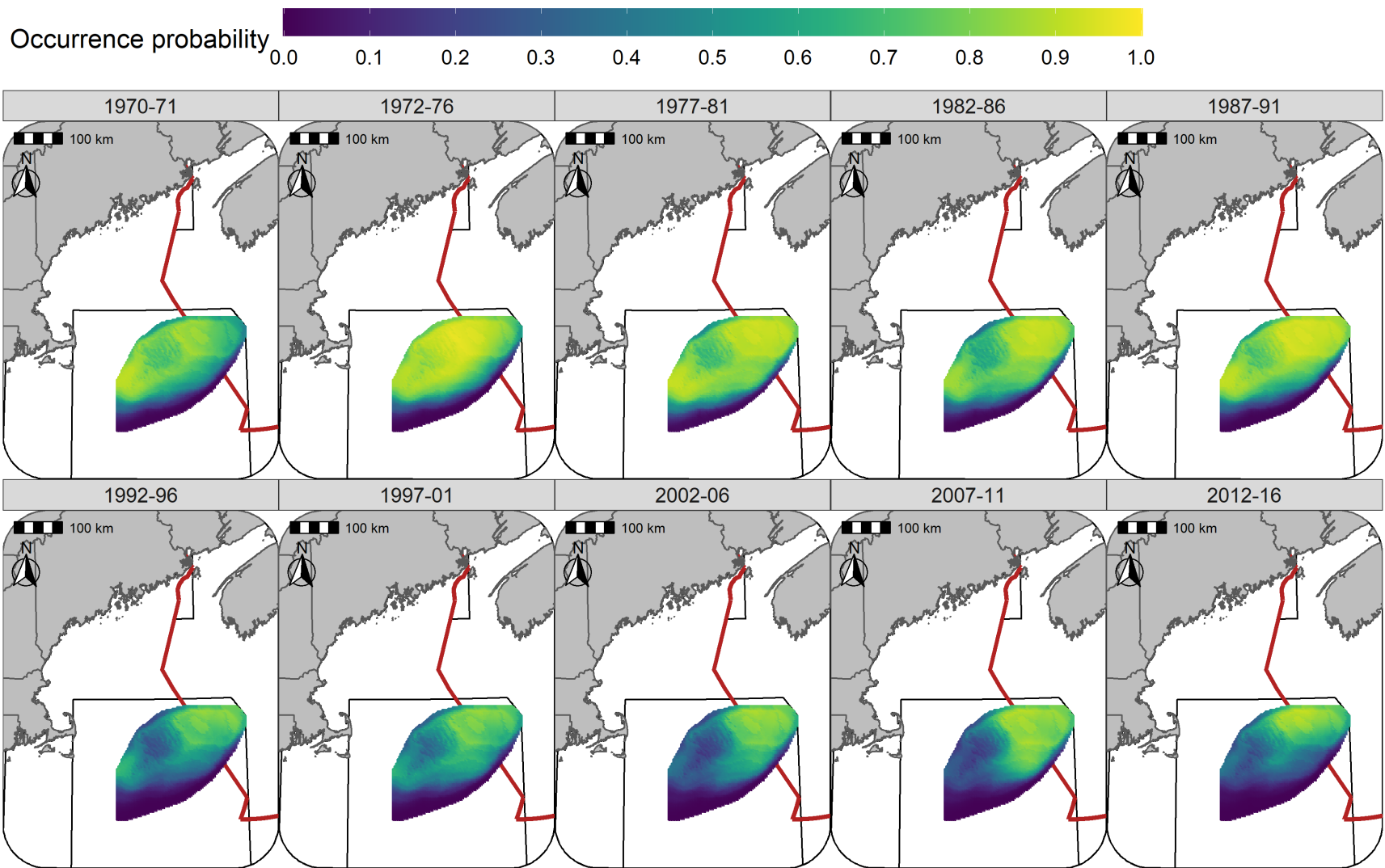


Figure S10: Predicted occurrence probability for Atlantic Cod in each era during the Spring (NMFS-spring survey) using the SST + Dep model and 5-year random field.

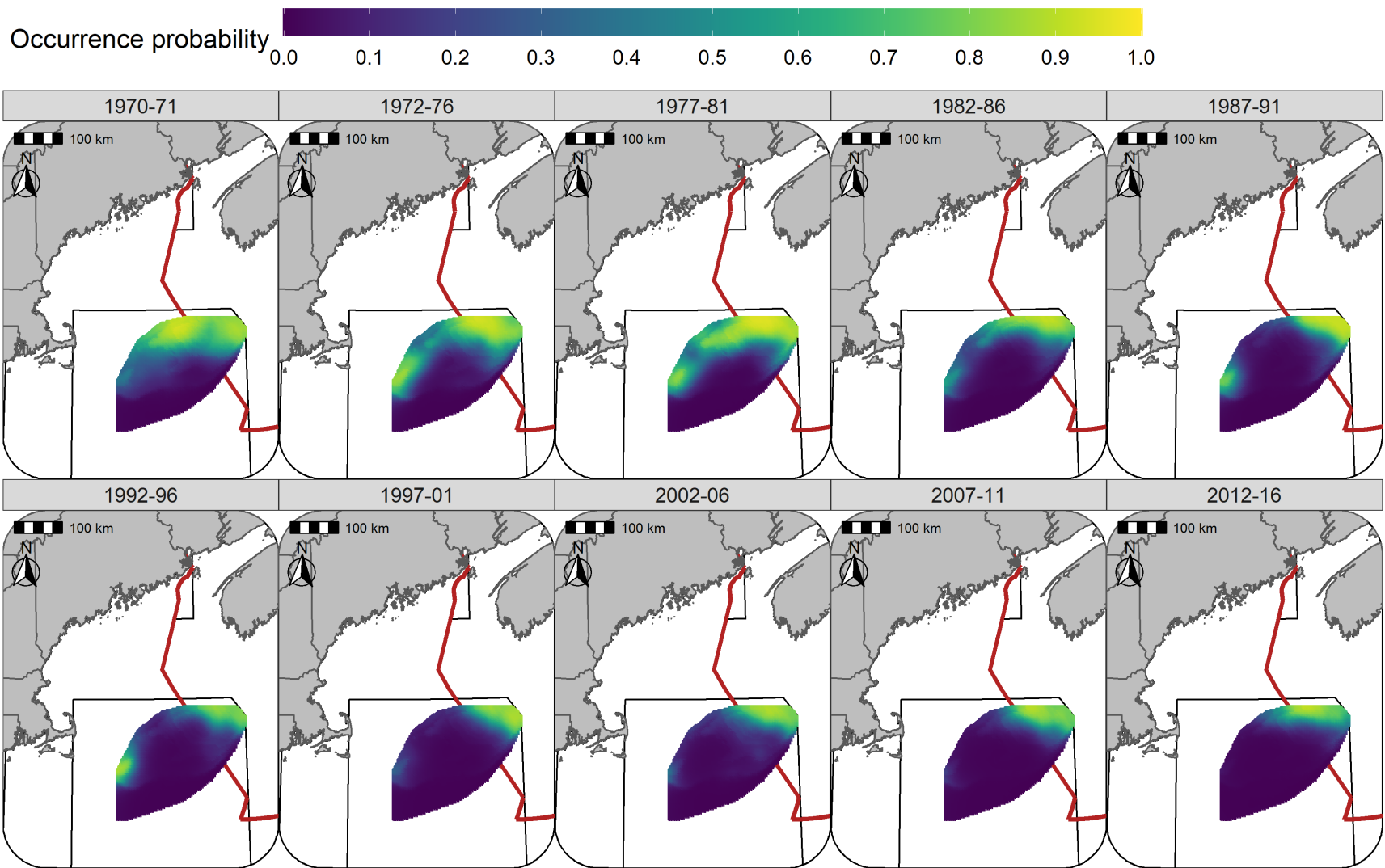


Figure S11: Predicted occurrence probability for Atlantic Cod in each era during the Fall (NMFS-fall survey) using the SST + Dep model and 5-year random field.

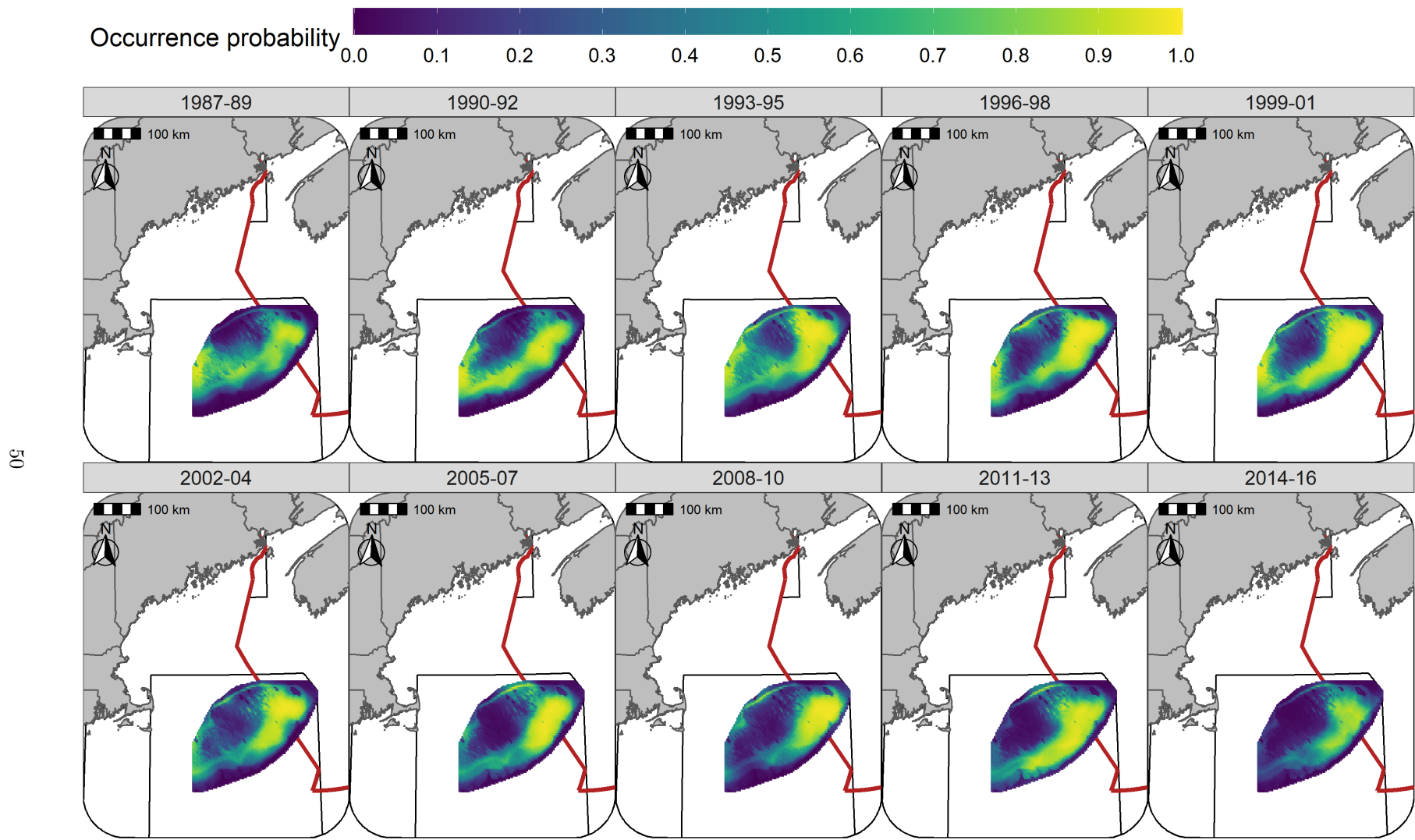


Figure S12: Predicted occurrence probability for Yellowtail Flounder in each era during the Winter (RV survey) using the SST + Dep + Sed model and 3-year random field.

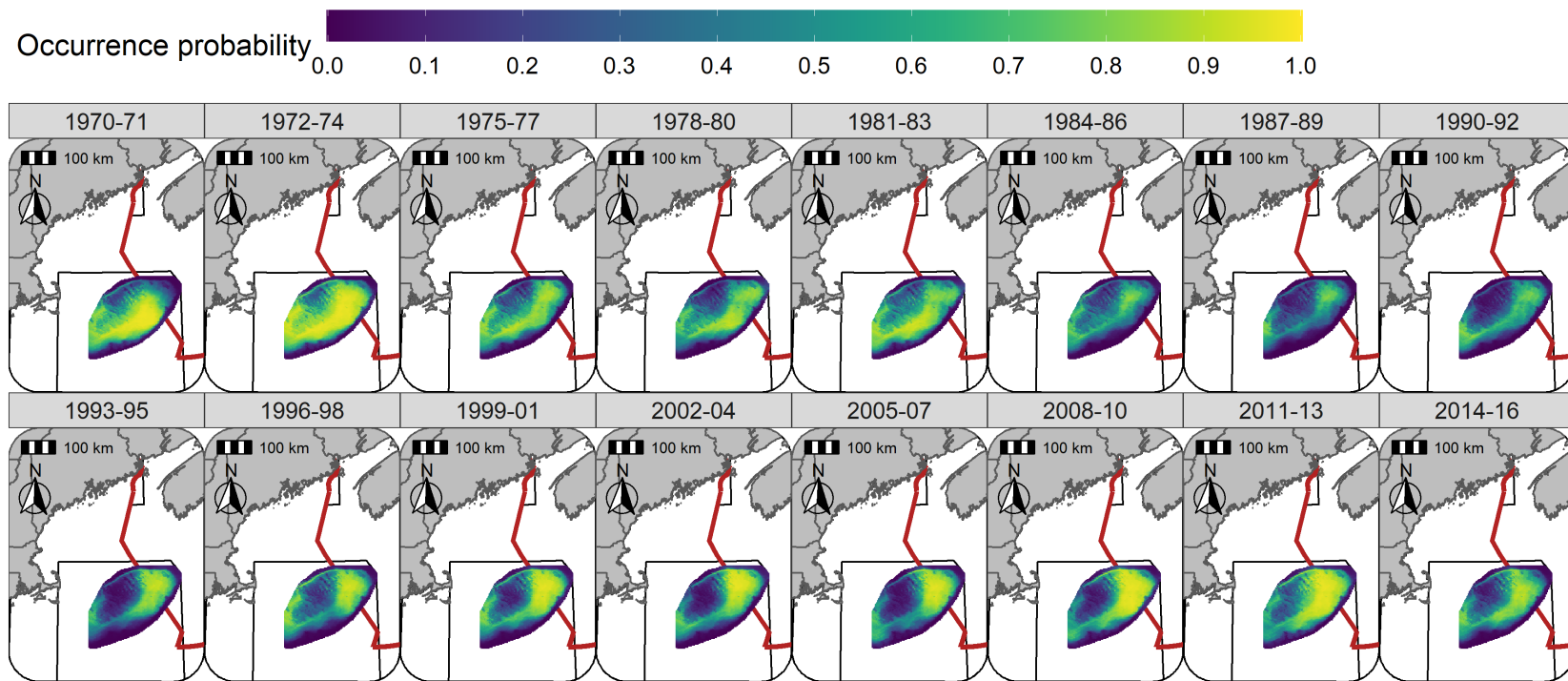


Figure S13: Predicted occurrence probability for Yellowtail Flounder in each era during the Spring (NMFS-spring survey) using the SST + Dep + Sed model and 3-year random field.

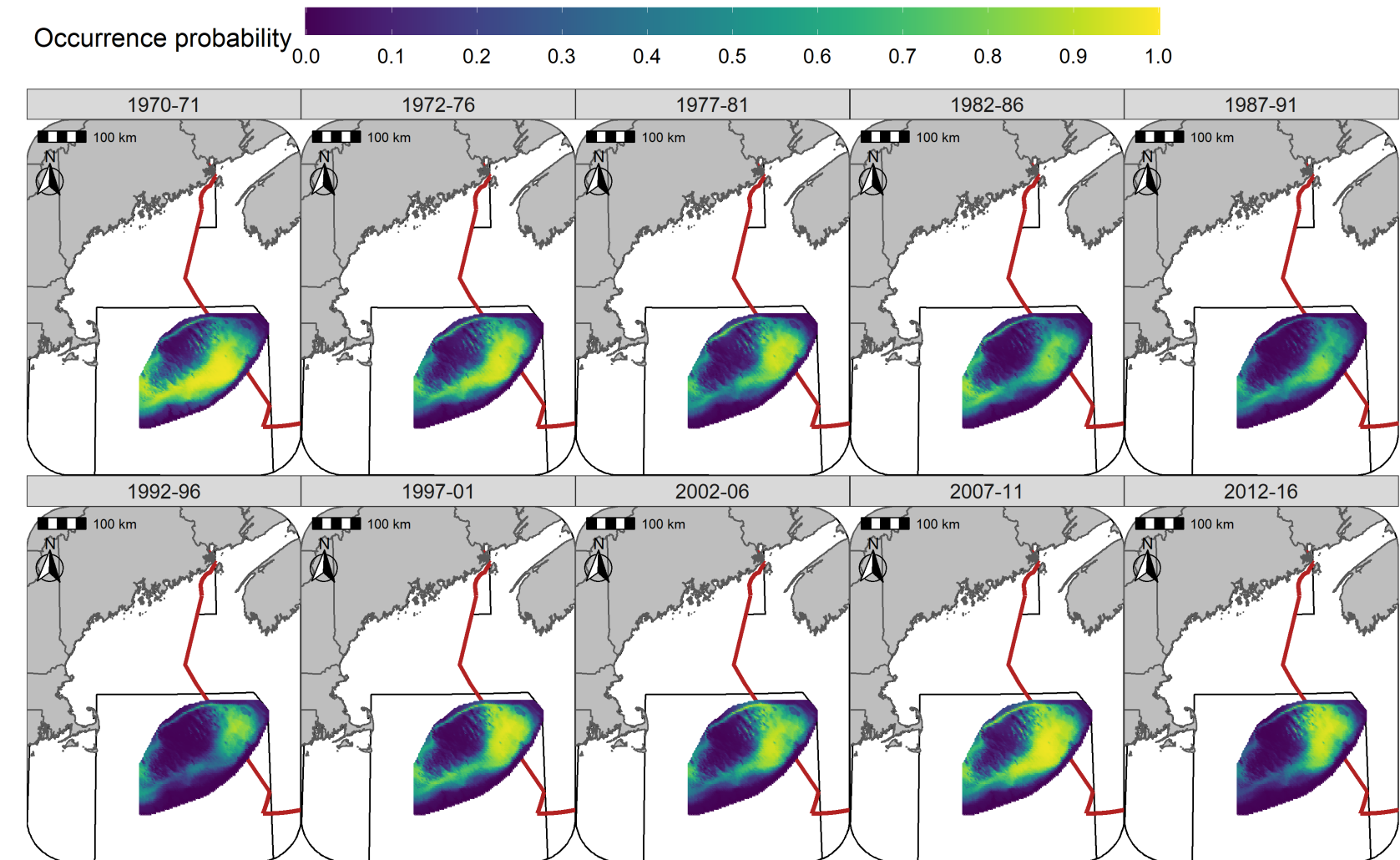


Figure S14: Predicted occurrence probability for Yellowtail Flounder in each era during the Fall (NMFS-fall survey) using the SST + Dep + Sed model and 5-year random field.

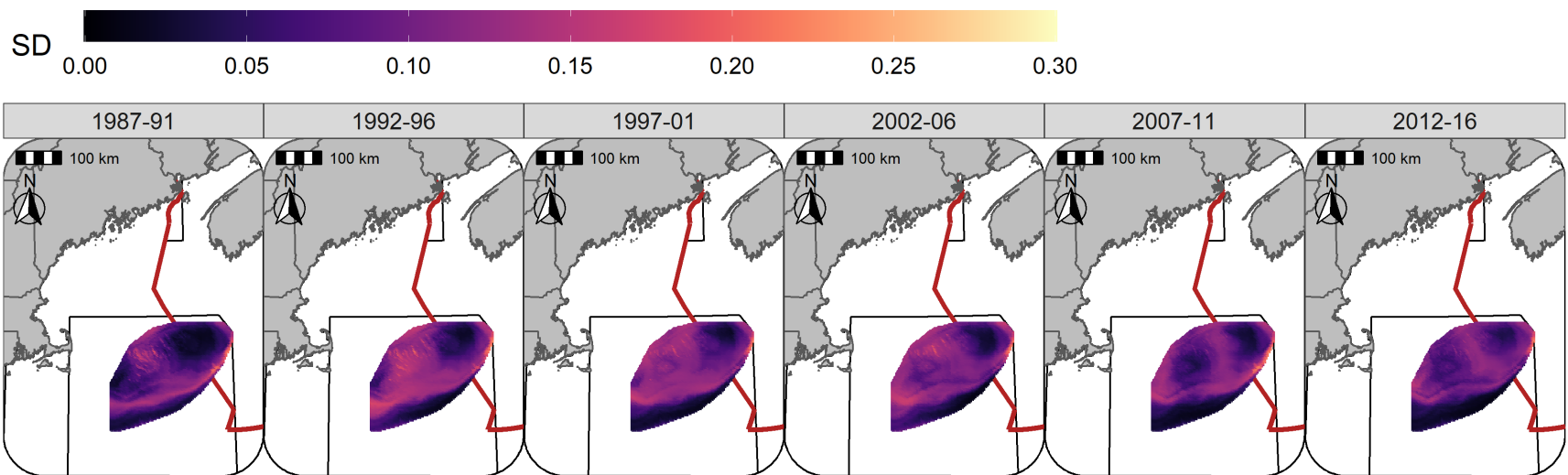


Figure S15: Standard deviation (logit scale) of predicted occurrence probability for Atlantic Cod in each era during the Winter (RV survey) using the SST + Dep model and 5-year random field.

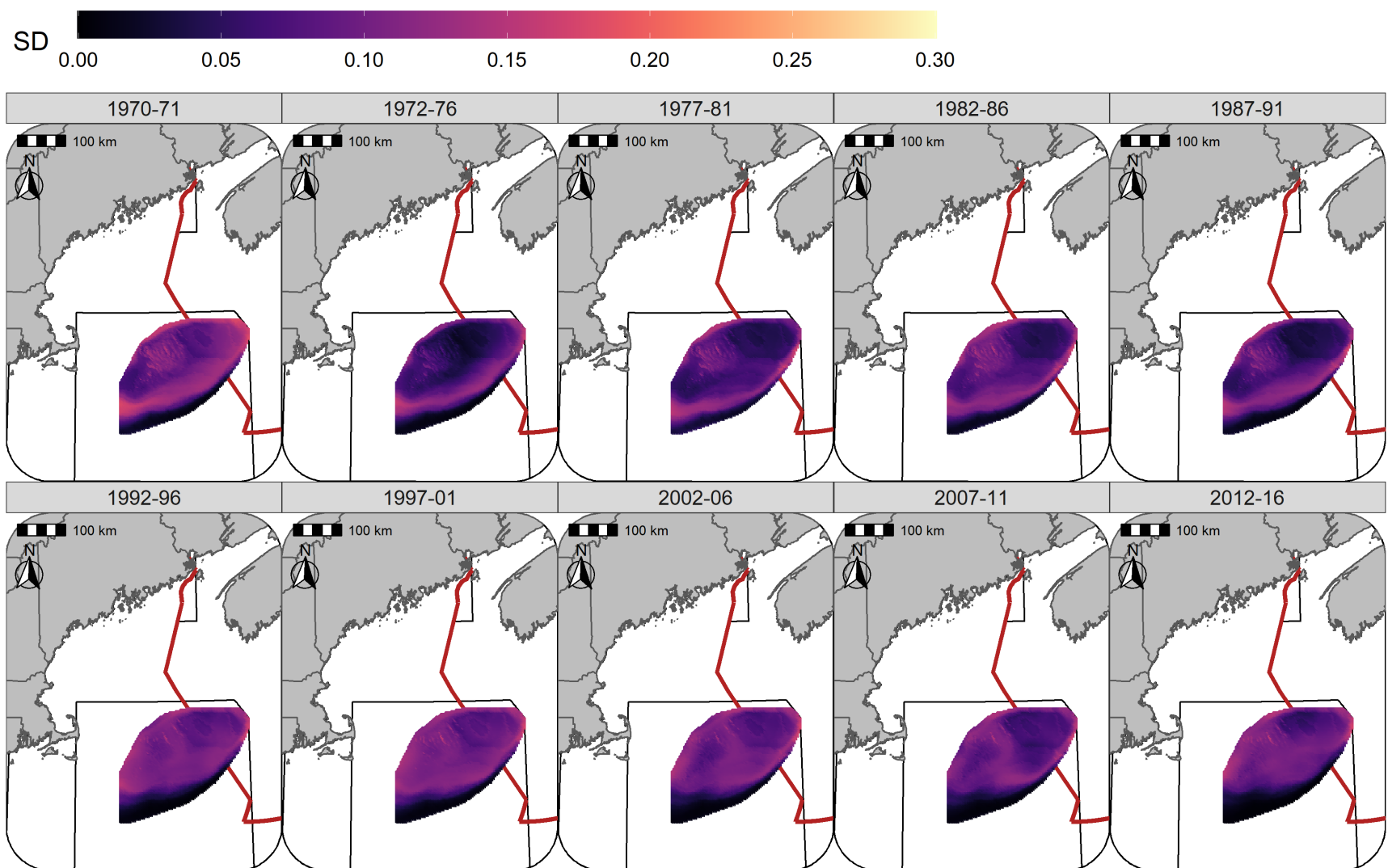


Figure S16: Standard deviation (logit scale) of predicted occurrence probability for Atlantic Cod in each era during the Spring (NMFS-spring survey) using the SST + Dep model and 5-year random field.

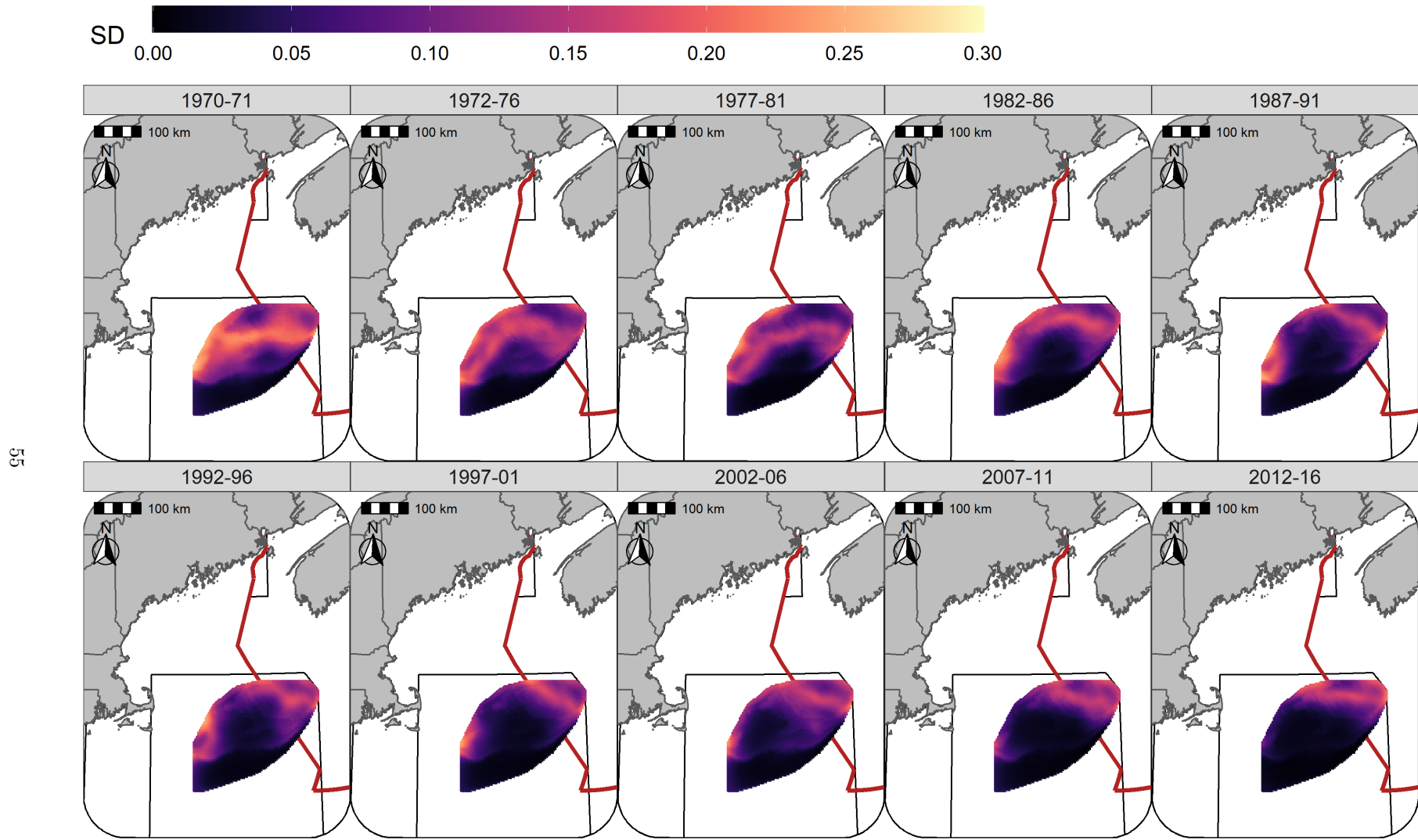


Figure S17: Standard deviation (logit scale) of predicted occurrence probability for Atlantic Cod in each era during the Fall (NMFS-fall survey) using the SST + Dep model and 5-year random field.

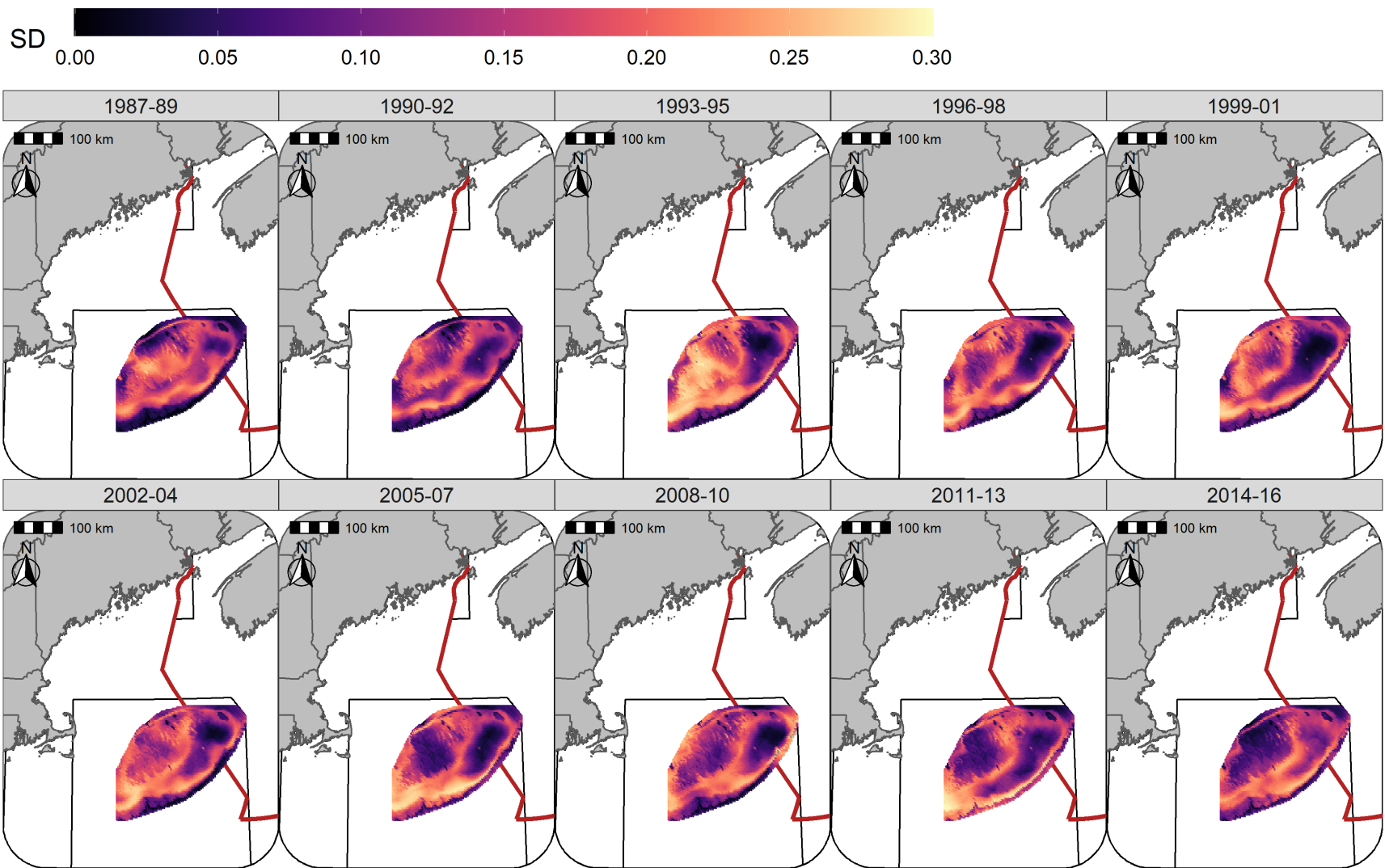


Figure S18: Standard deviation (logit scale) of predicted occurrence probability for Yellowtail Flounder in each era during the Winter (RV survey) using the SST + Dep + Sed model and 3-year random field.

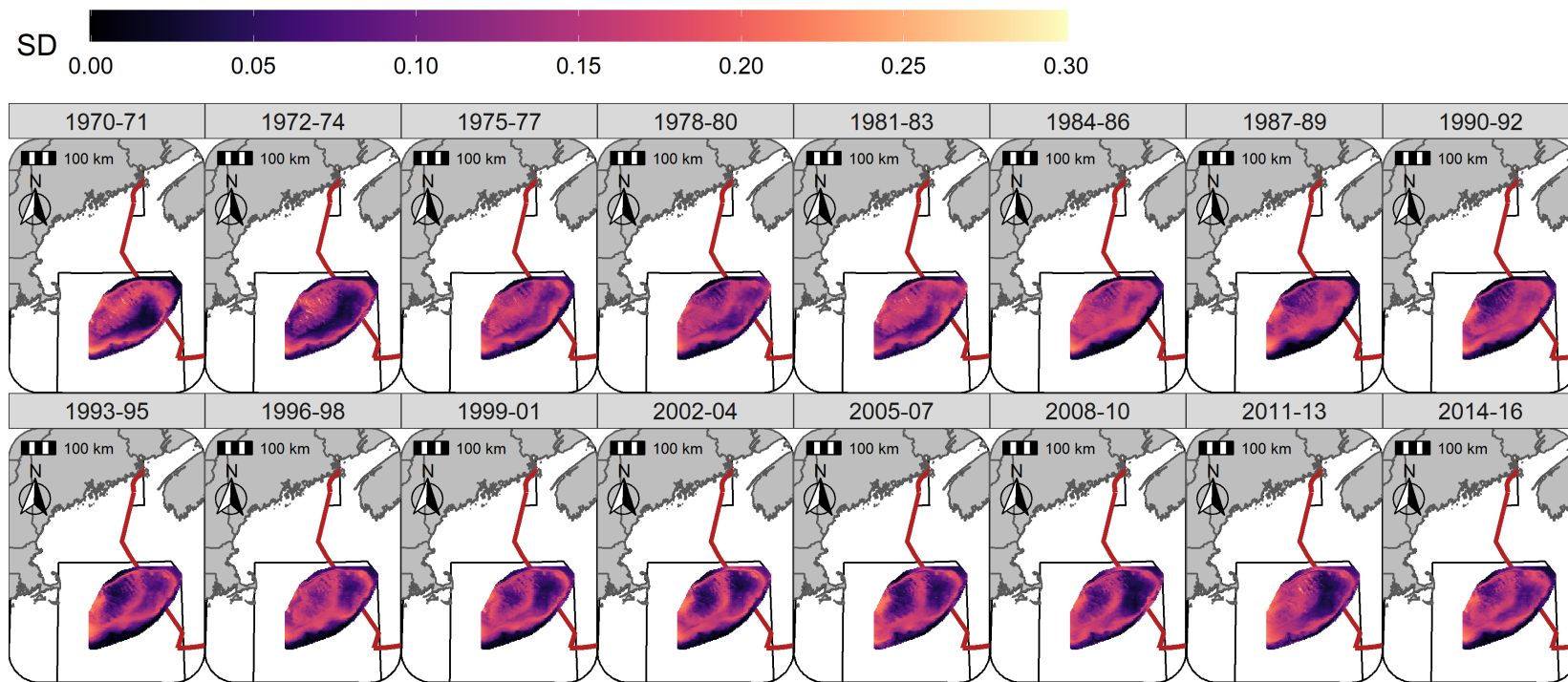


Figure S19: Standard deviation (logit scale) of predicted occurrence probability for Yellowtail Flounder in each era during the Spring (NMFS-spring survey) using the SST + Dep + Sed model and 3-year random field.

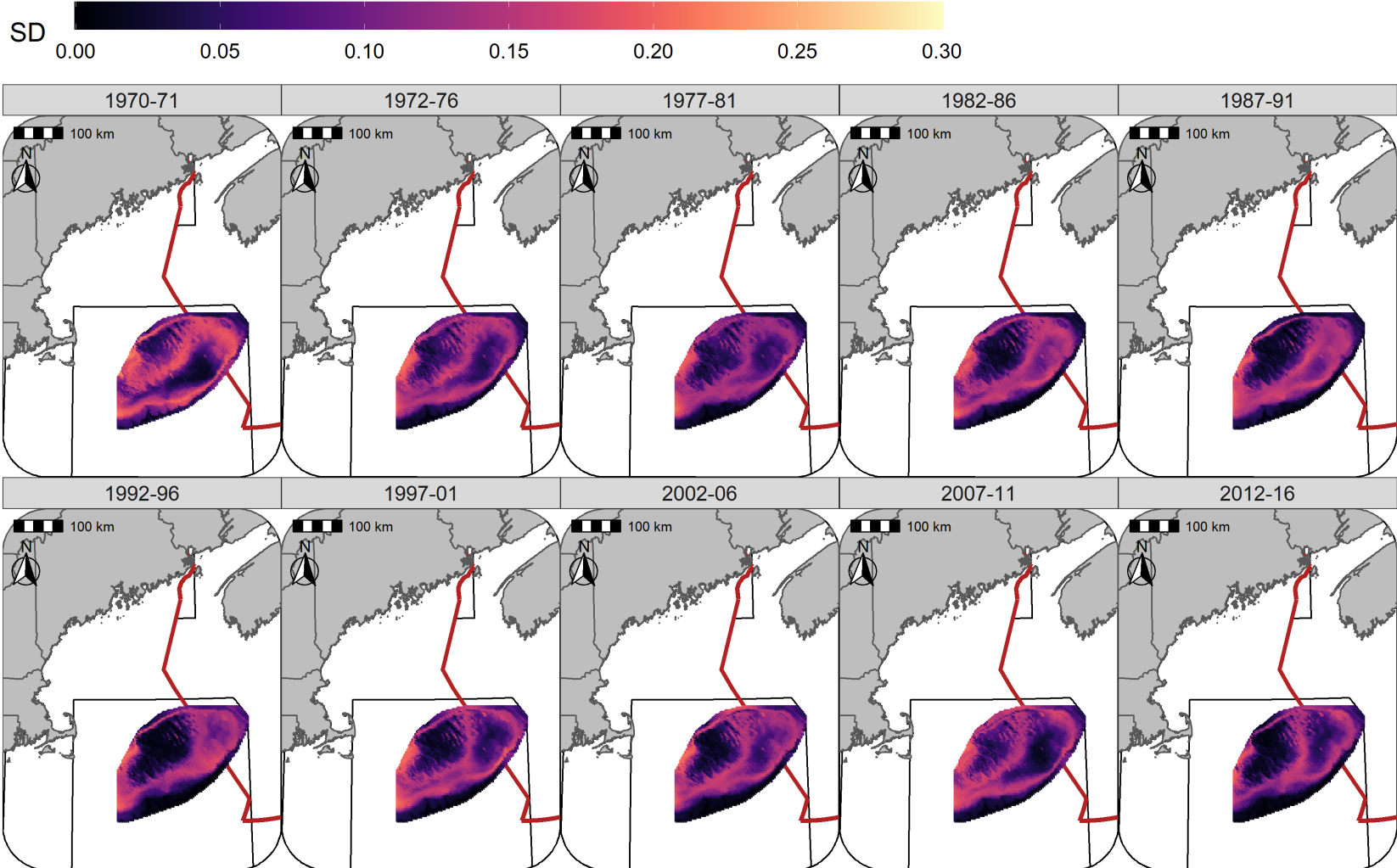


Figure S20: Standard deviation (logit scale) of predicted occurrence probability for Yellowtail Flounder in each era during the Fall (NMFS-fall survey) using the SST + Dep + Sed model and 5-year random field.

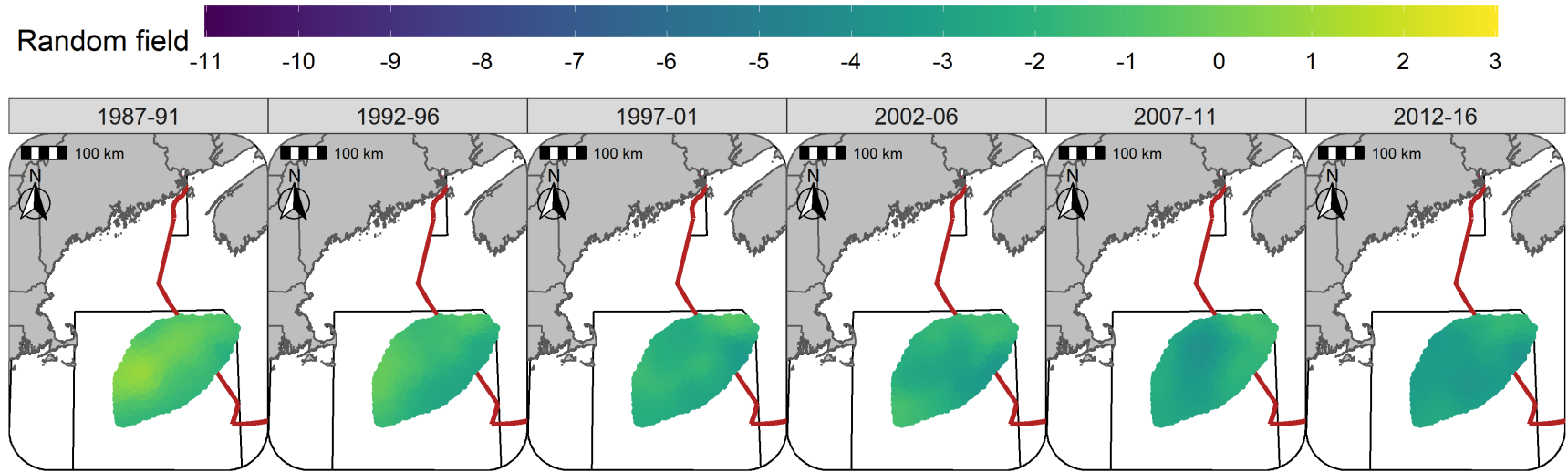
629 **Random fields**

630 The 5-year random fields for Atlantic Cod in the Winter and Spring are seasonally consistent through time,
631 with lower effect sizes observed in both seasons starting in 1992 and the largest declines in the effect size
632 observed in the southern and western portions of GB (Figures S21 - S22). In the Fall the higher effect sizes
633 were generally observed towards the north and in Canadian waters, with larger declines in the random field
634 effect size towards the west over the study period (Figure S23).

635 The Yellowtail Flounder random field patterns were similar in the Winter and Spring while the random field
636 effect sizes were somewhat smaller during the Fall (Figures S24 - S26). The effect size of the random fields,
637 in all seasons, were lower throughout the latter half of the 1980s and the early 1990s. The highest effect size
638 of the random fields were observed in the 1970s and in the 2000s. Since the mid-1970s an area straddling the
639 Canadian-U.S. border has been consistently identified as an area where the Yellowtail Flounder effect size of
640 the random field is elevated (Figures S24 - S26).

641 The standard deviation (SD) of the random fields for Atlantic Cod were also similar between seasons with
642 the lowest SD generally observed in the north and east and highest approaching the southern flank of GB.

643 The SD was somewhat higher in the Fall throughout the central portion of GB (Figures S27 - S29). For
644 Yellowtail Flounder, the SD was higher towards the southern portions of the bank with localized regions
645 having elevated SD scattered throughout the bank in the Winter, Spring, and Fall. (Figures S30 - S32).



60

Figure S21: Random fields (logit scale) for Atlantic Cod in each era during the Winter (RV survey) using the SST + Dep model and 5-year random field.

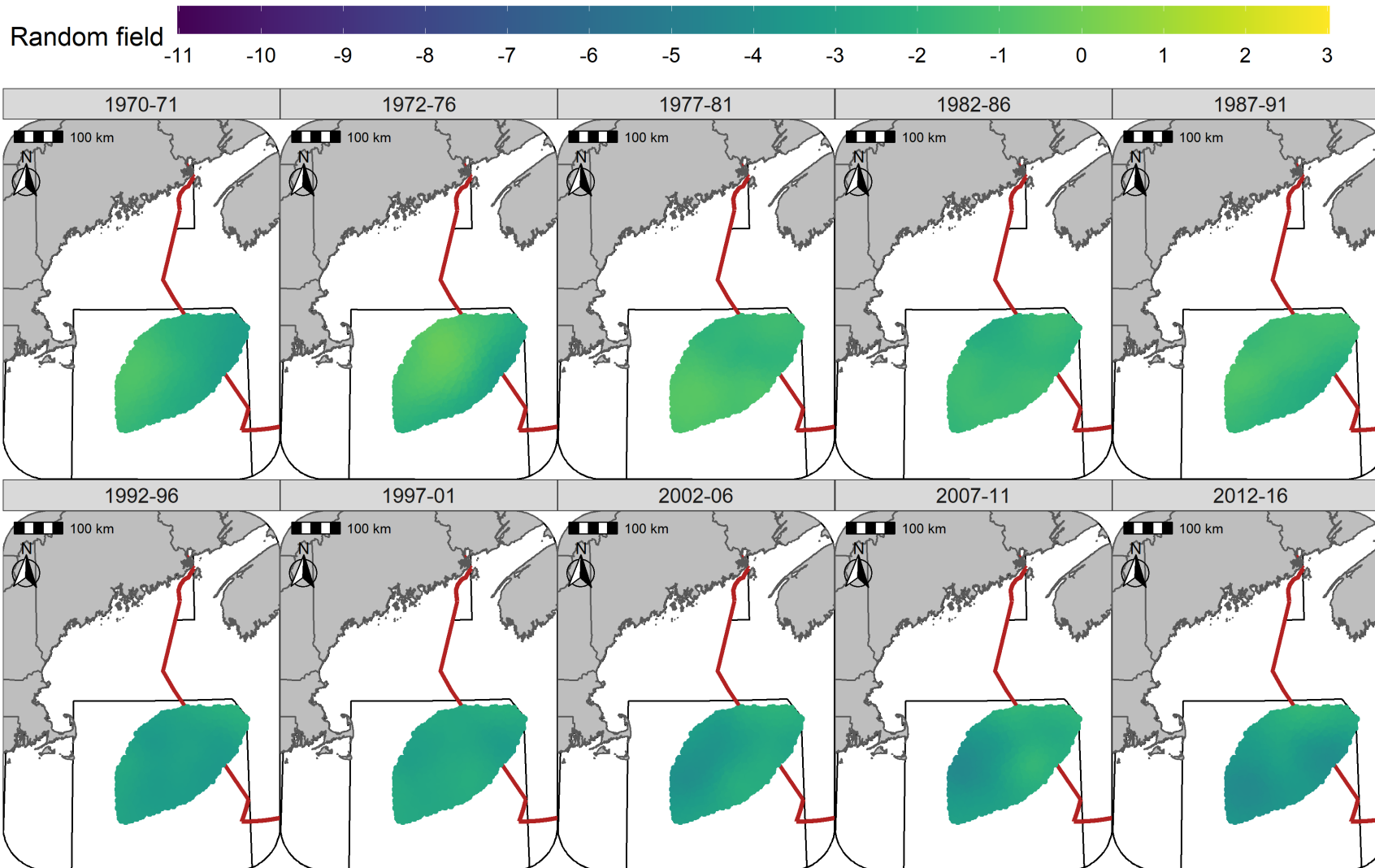


Figure S22: Random fields (logit scale) for Atlantic Cod in each era during the Spring (NMFS-spring survey) using the SST + Dep model and 5-year random field.

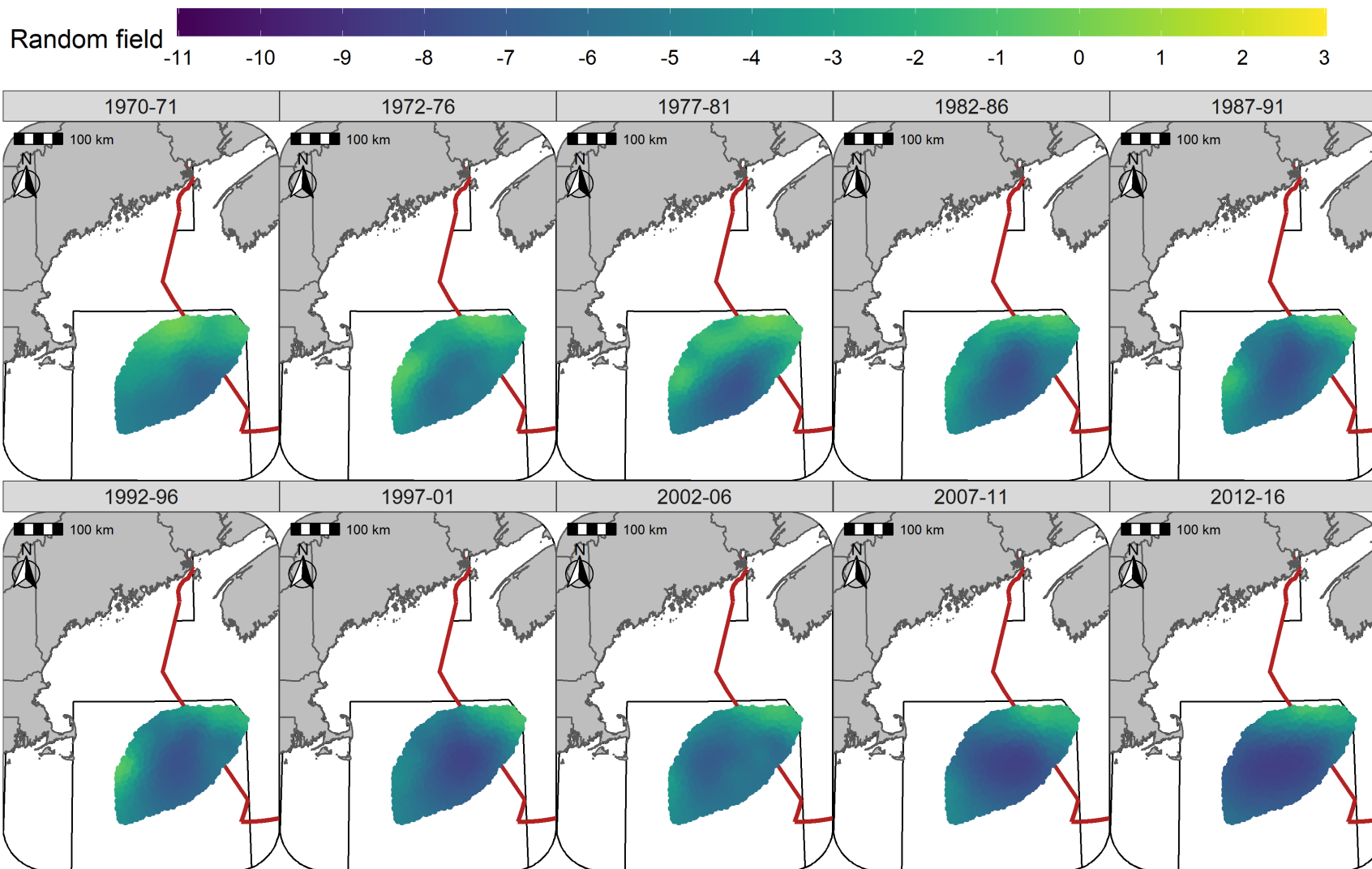


Figure S23: Random fields (logit scale) for Atlantic Cod in each era during the Fall (NMFS-fall survey) using the SST + Dep model and 5-year random field.

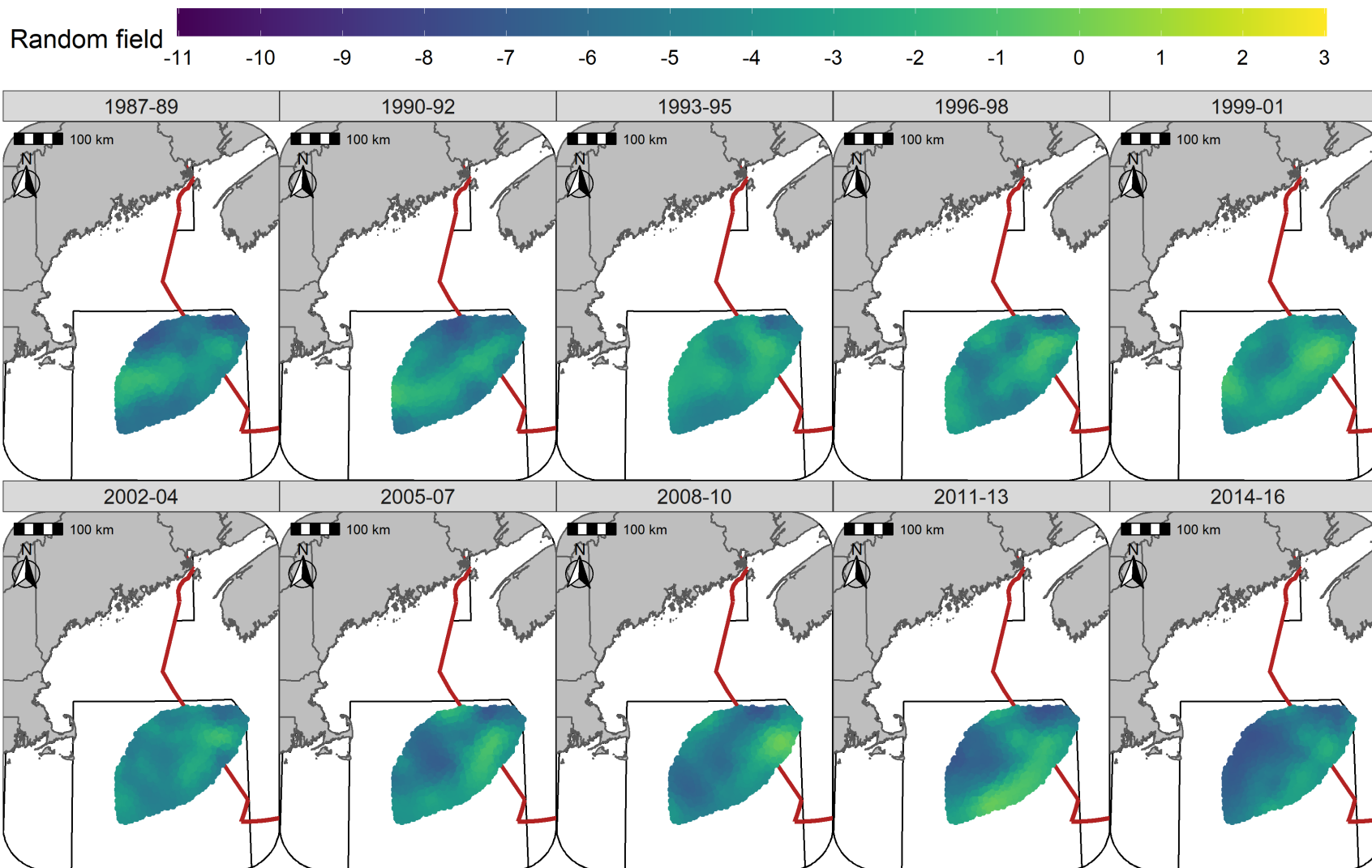


Figure S24: Random fields (logit scale) for Yellowtail Flounder in each era during the Winter (RV survey) using the SST + Dep + Sed model and 3-year random field.

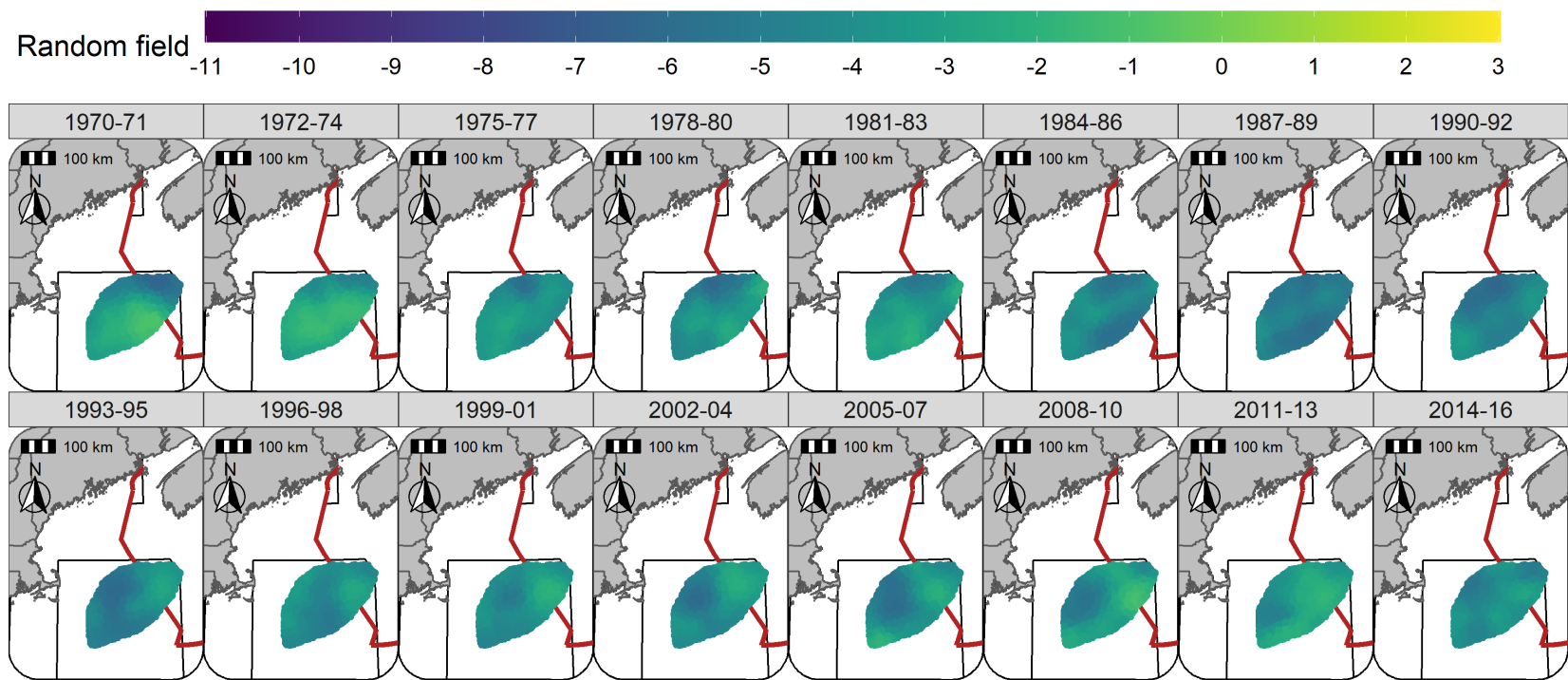


Figure S25: Random fields (logit scale) for Yellowtail Flounder in each era during the Spring (NMFS-spring survey) using the SST + Dep + Sed model and 3-year random field.

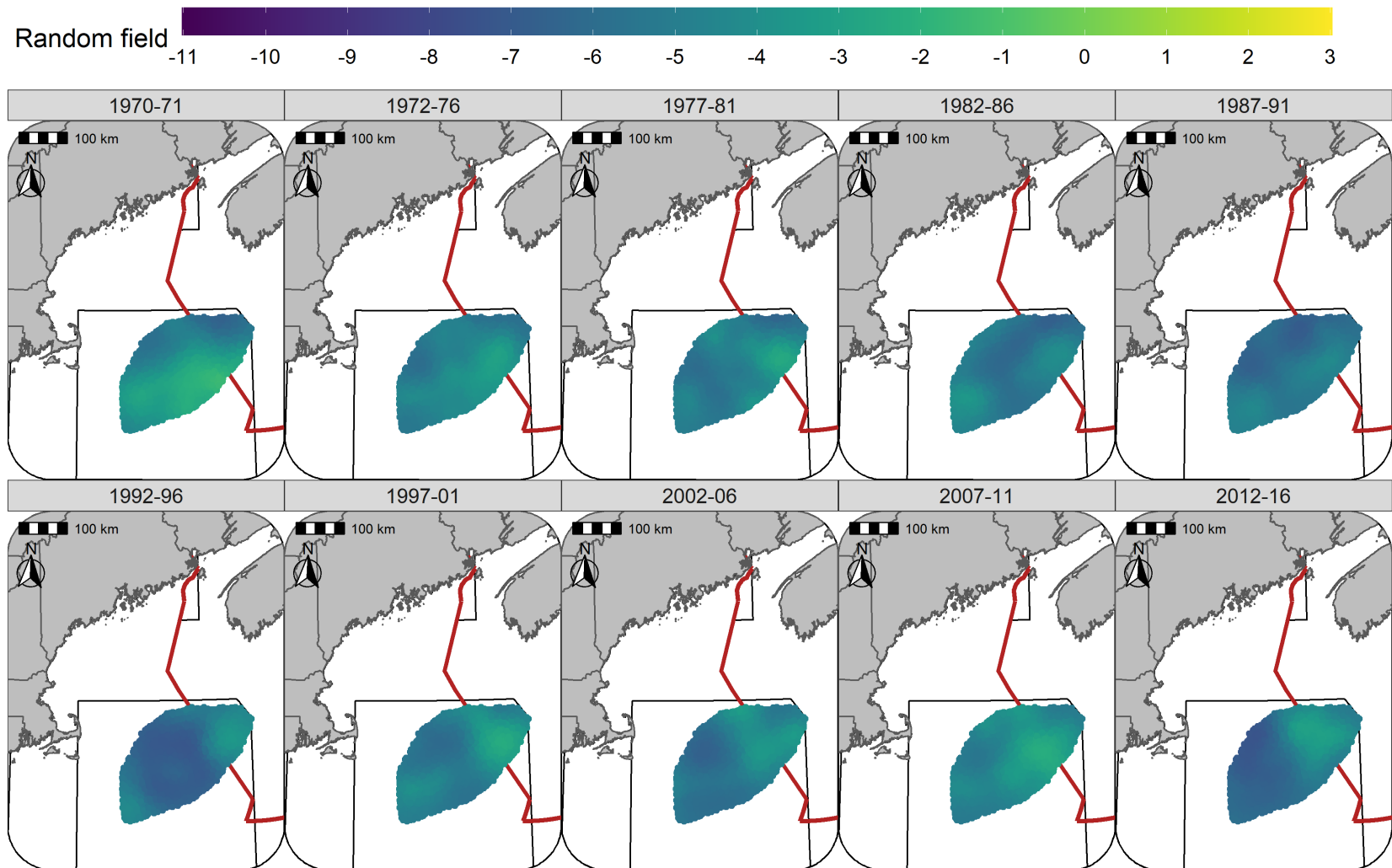


Figure S26: Random fields (logit scale) for Yellowtail Flounder in each era during the Fall (NMFS-fall survey) using the SST + Dep + Sed model and 5-year random field.

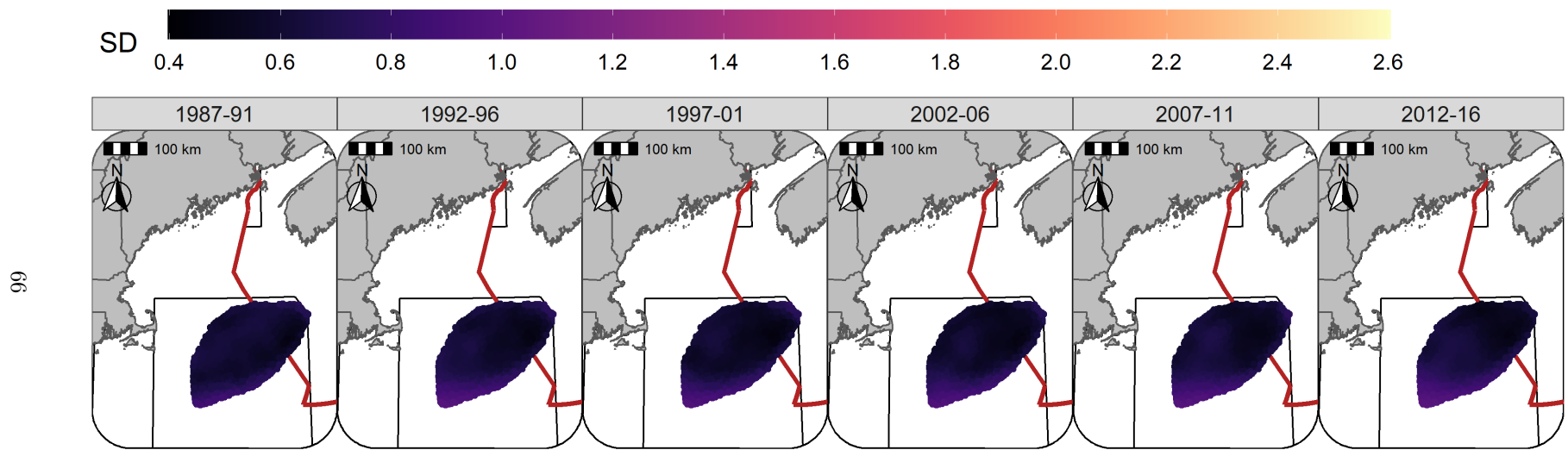


Figure S27: Standard deviation of random fields (logit scale) for Atlantic Cod in each era during the Winter (RV survey) using the SST + Dep model and 5-year random field.

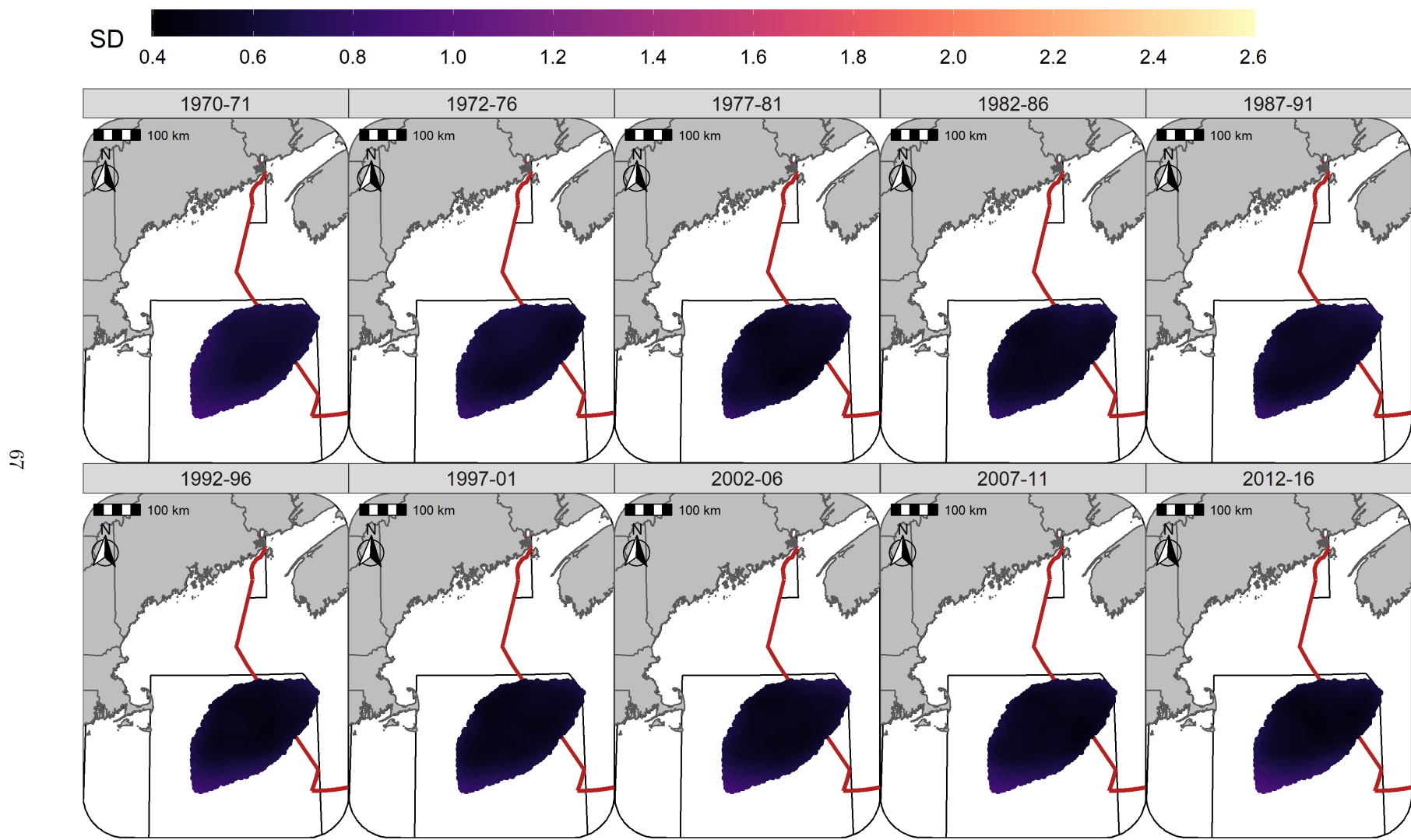


Figure S28: Standard deviation of random fields (logit scale) for Atlantic Cod in each era during the Spring (NMFS-spring survey) using the SST + Dep model and 5-year random field.

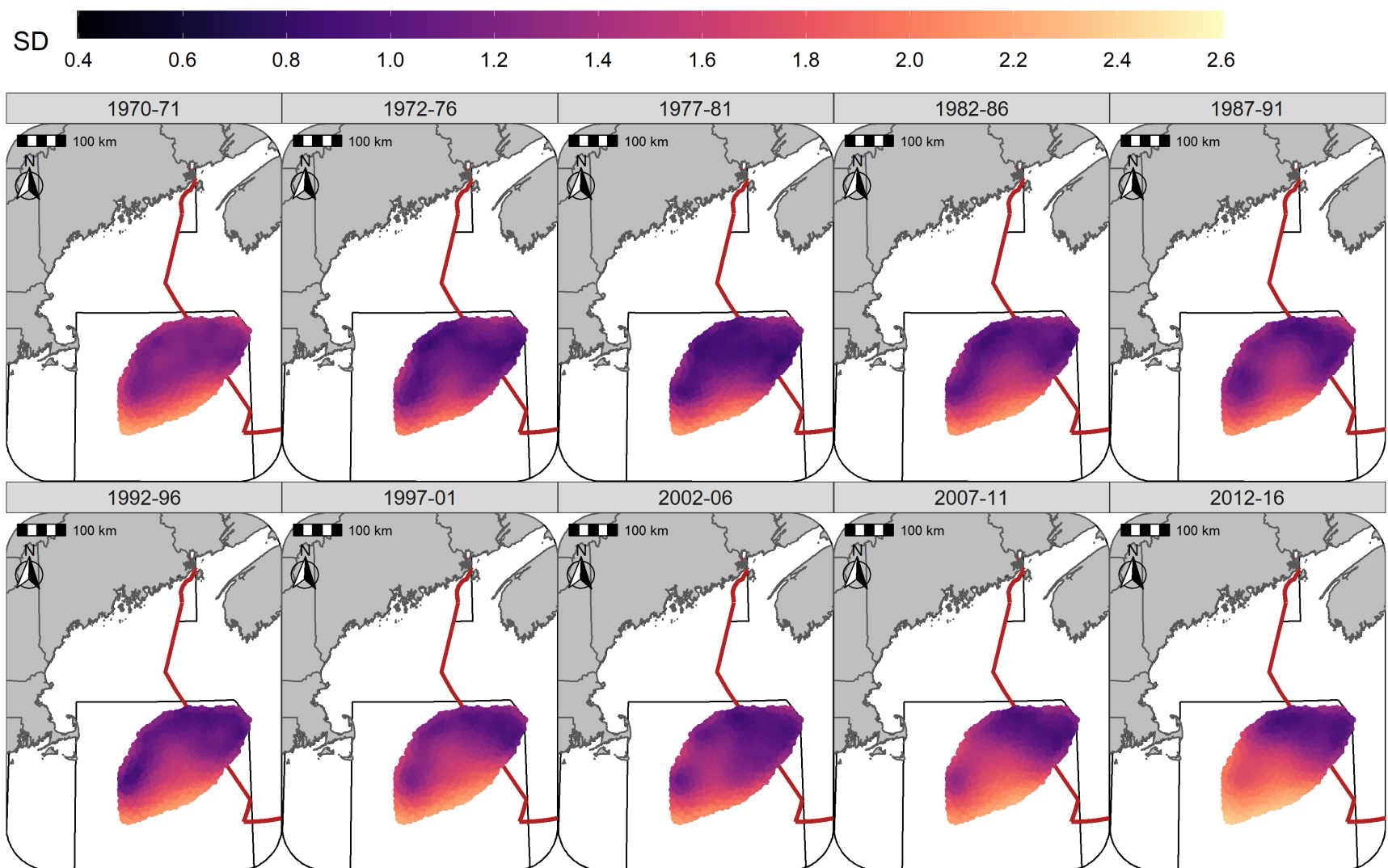
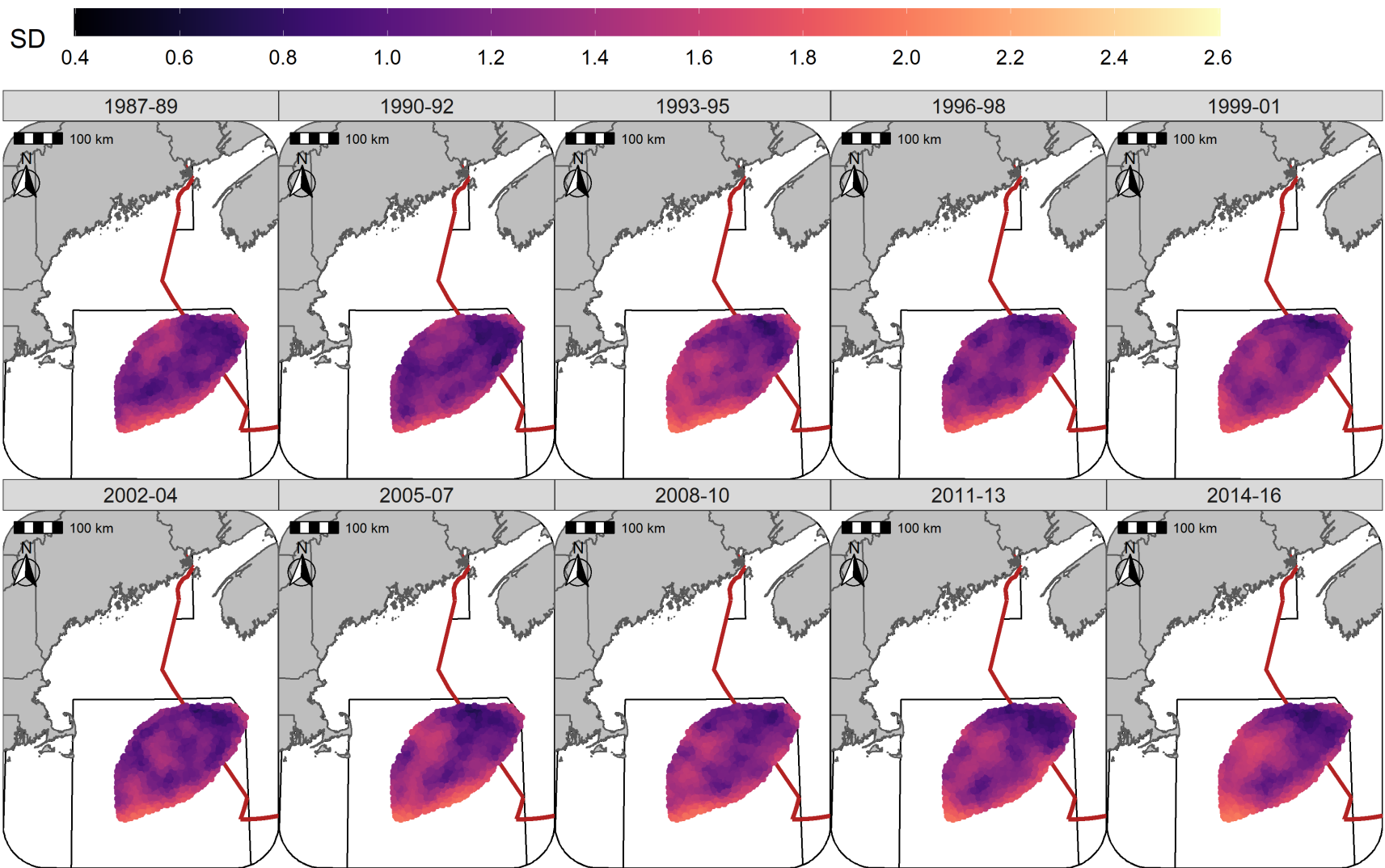


Figure S29: Standard deviation of random fields (logit scale) for Atlantic Cod in each era during the Fall (NMFS-fall survey) using the SST + Dep model and 5-year random field.



69

Figure S30: Standard deviation of random fields (logit scale) for Yellowtail Flounder in each era during the Winter (RV survey) using the SST + Dep + Sed model and 3-year random field.

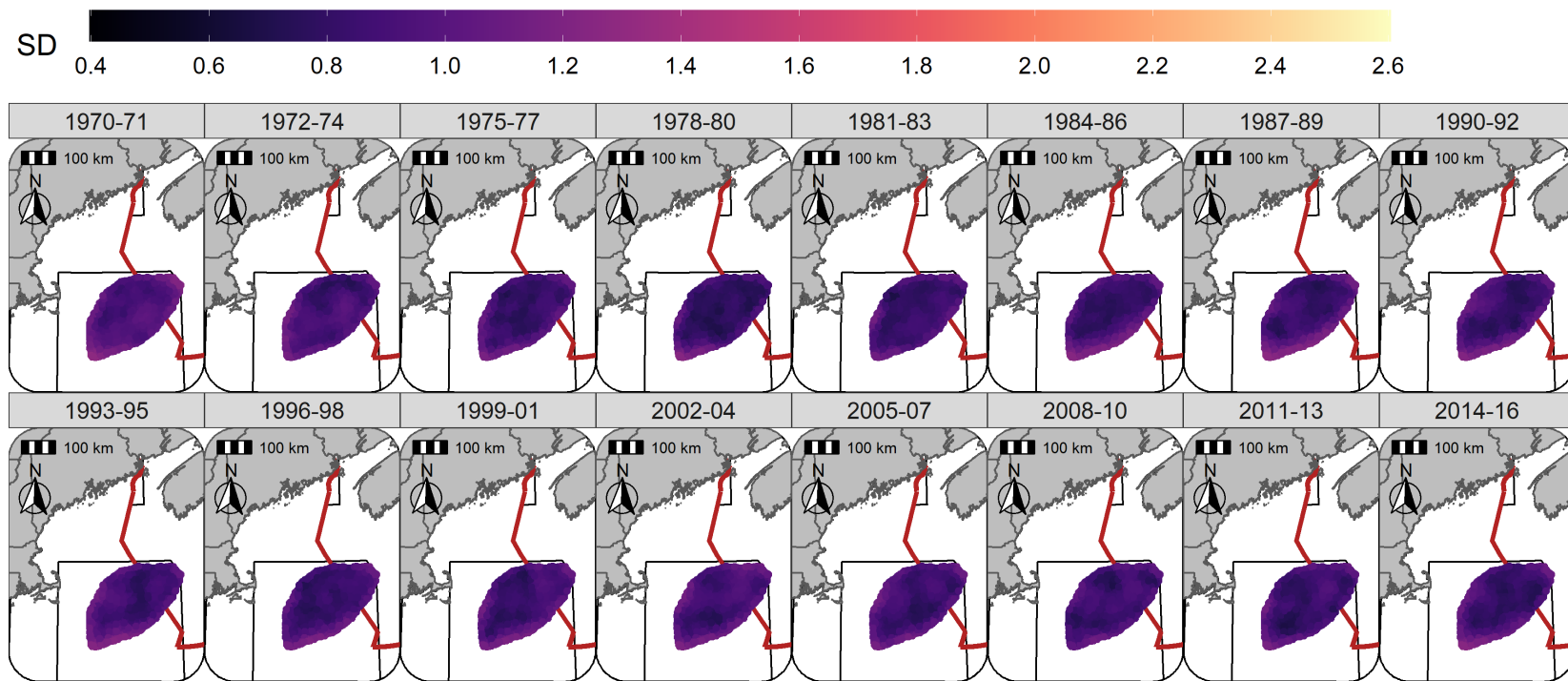


Figure S31: Standard deviation of random fields (logit scale) for Yellowtail Flounder in each era during the Spring (NMFS-spring survey) using the SST + Dep + Sed model and 3-year random field.

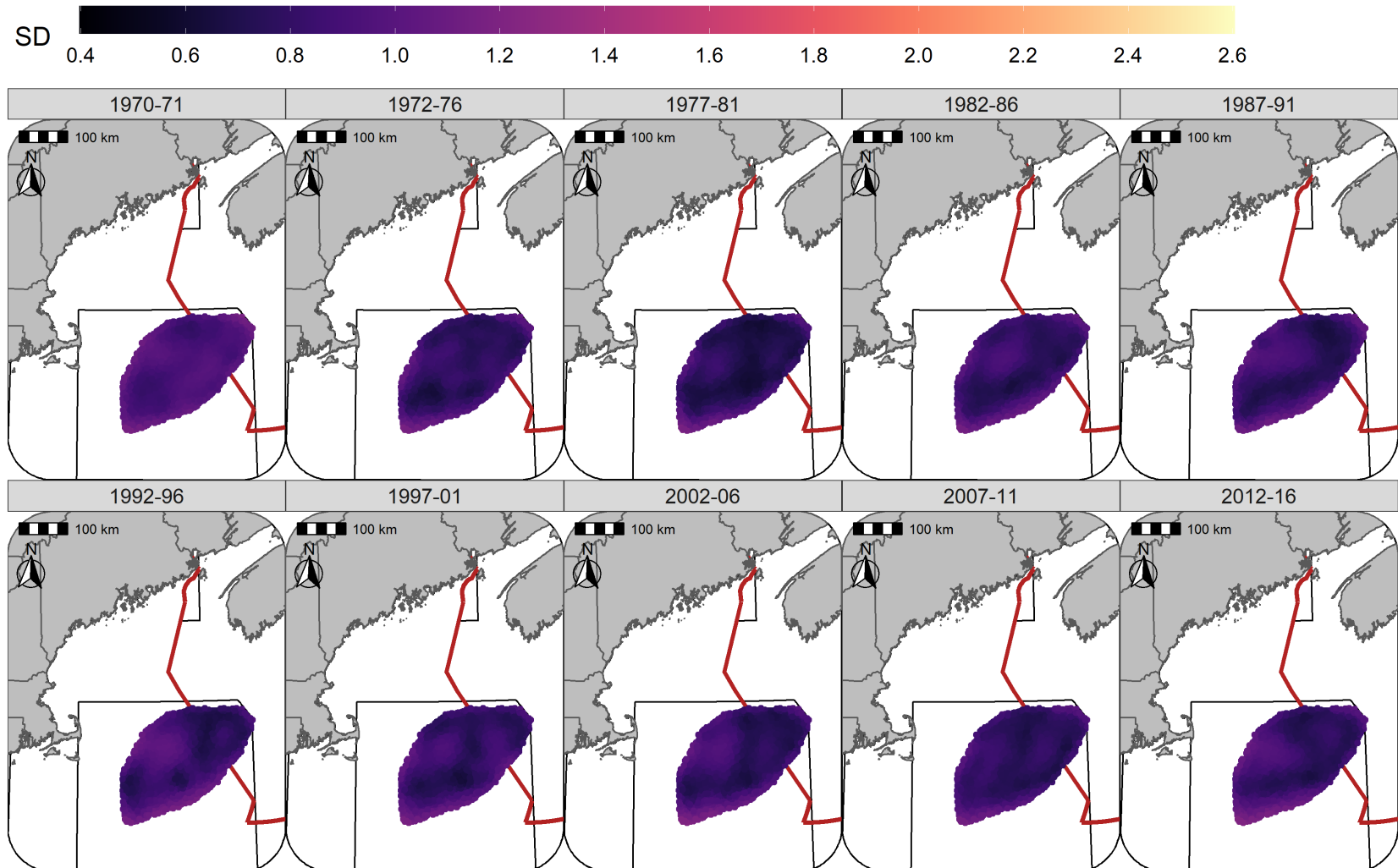


Figure S32: Standard deviation of random fields (logit scale) for Yellowtail Flounder in each era during the Fall (NMFS-fall survey) using the SST + Dep + Sed model and 5-year random field.

646 **Hyperparameters**

647 For Atlantic Cod, the estimate for the variance of the Dep variance hyperparameter was highest in Winter
648 and declined through to the Fall, reflecting the decline in the influence of this covariate in the Fall (Figure
649 S33). For Yellowtail Flounder, the variance of the Dep hyperparameter was higher than observed for Atlantic
650 Cod throughout the year and reflected the relative stability in the effect size of this covariate throughout
651 the year (Figure S33). The SST variance hyperparameter for Atlantic Cod was relatively stable throughout
652 the year and reflects the consistent influence of the SST covariate on the distribution of cod. For Yellowtail
653 Flounder, the SST variance hyperparameter was relatively low throughout the year and aligns with the
654 consistent small effect of the SST covariate on the distribution of Yellowtail Flounder (Figure S34). The
655 uncertainty of these estimates precludes any statistical differences being observed between the seasons.

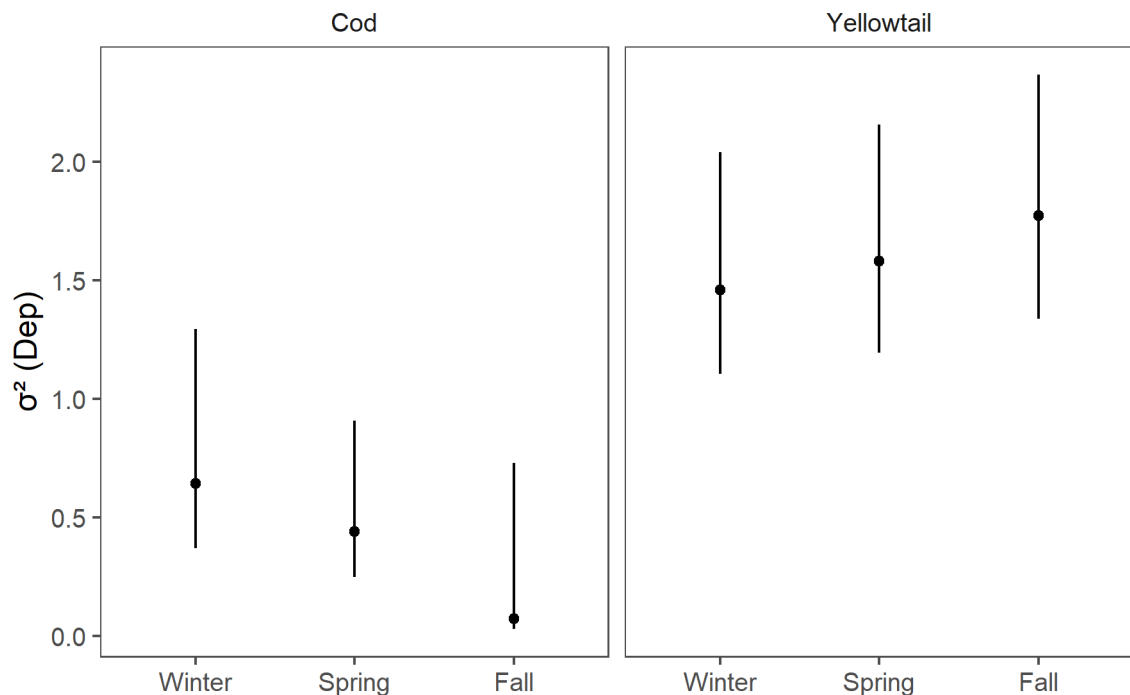


Figure S33: Dep variance hyperparameter estimate with 95% credible intervals for each stock in each season.

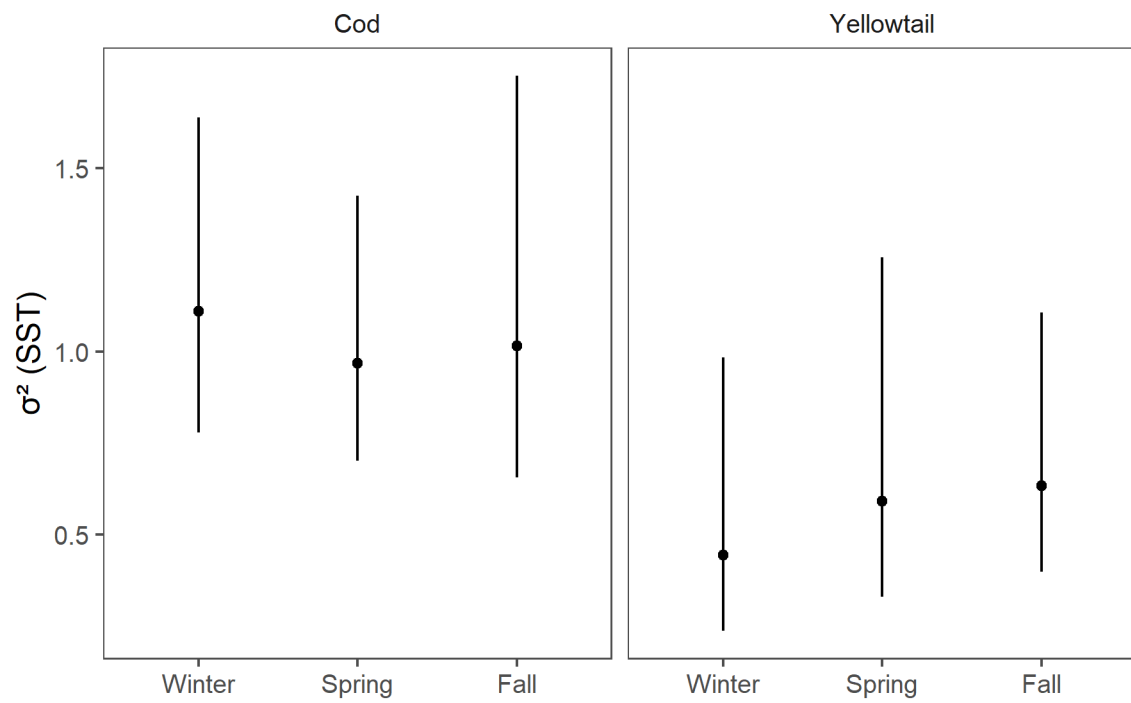


Figure S34: SST variance hyperparameter estimate with 95% credible intervals for each stock in each season.

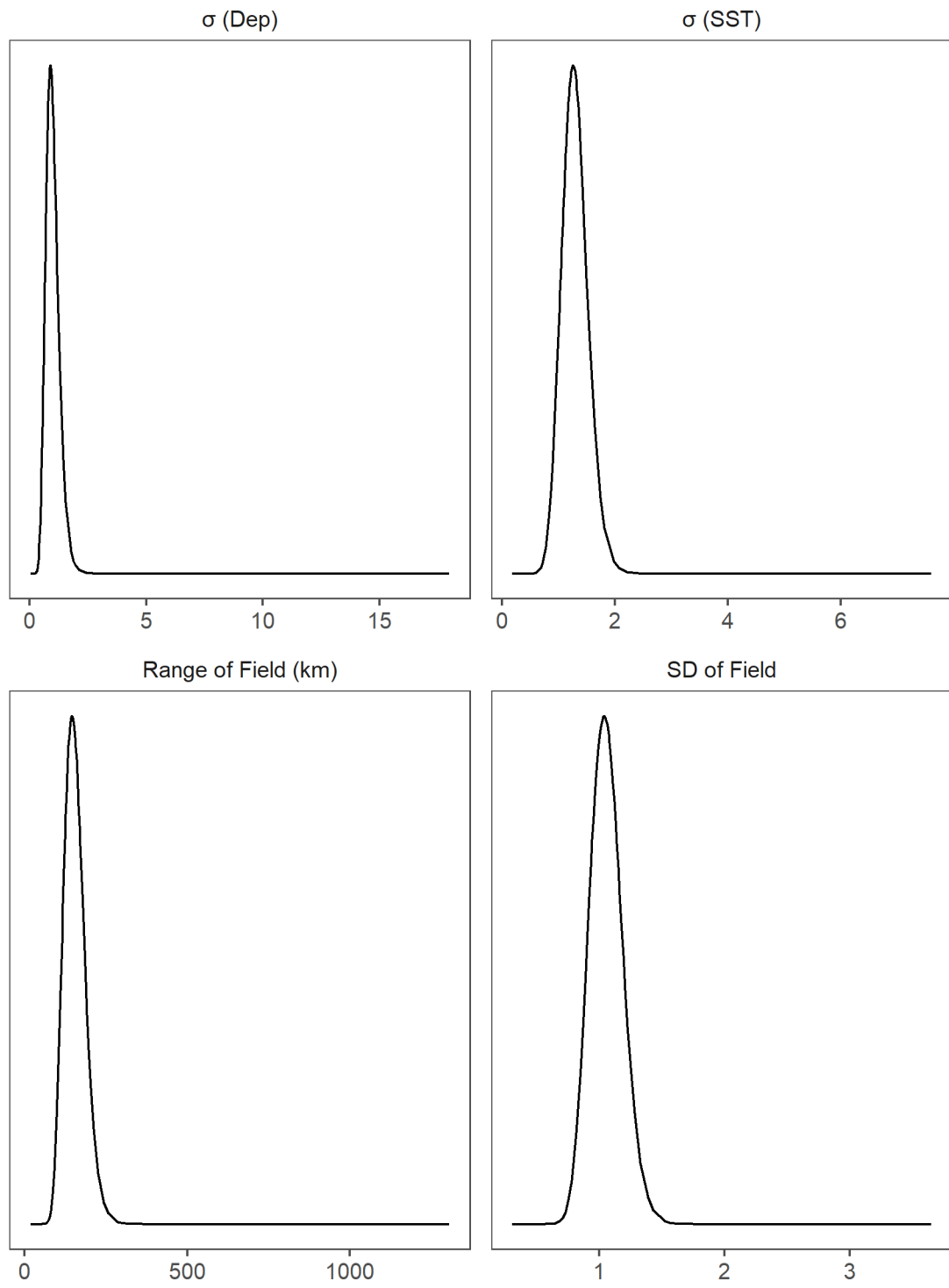


Figure S35: Posteriors distributions of the four model hyperparameters for Atlantic Cod in the Winter.

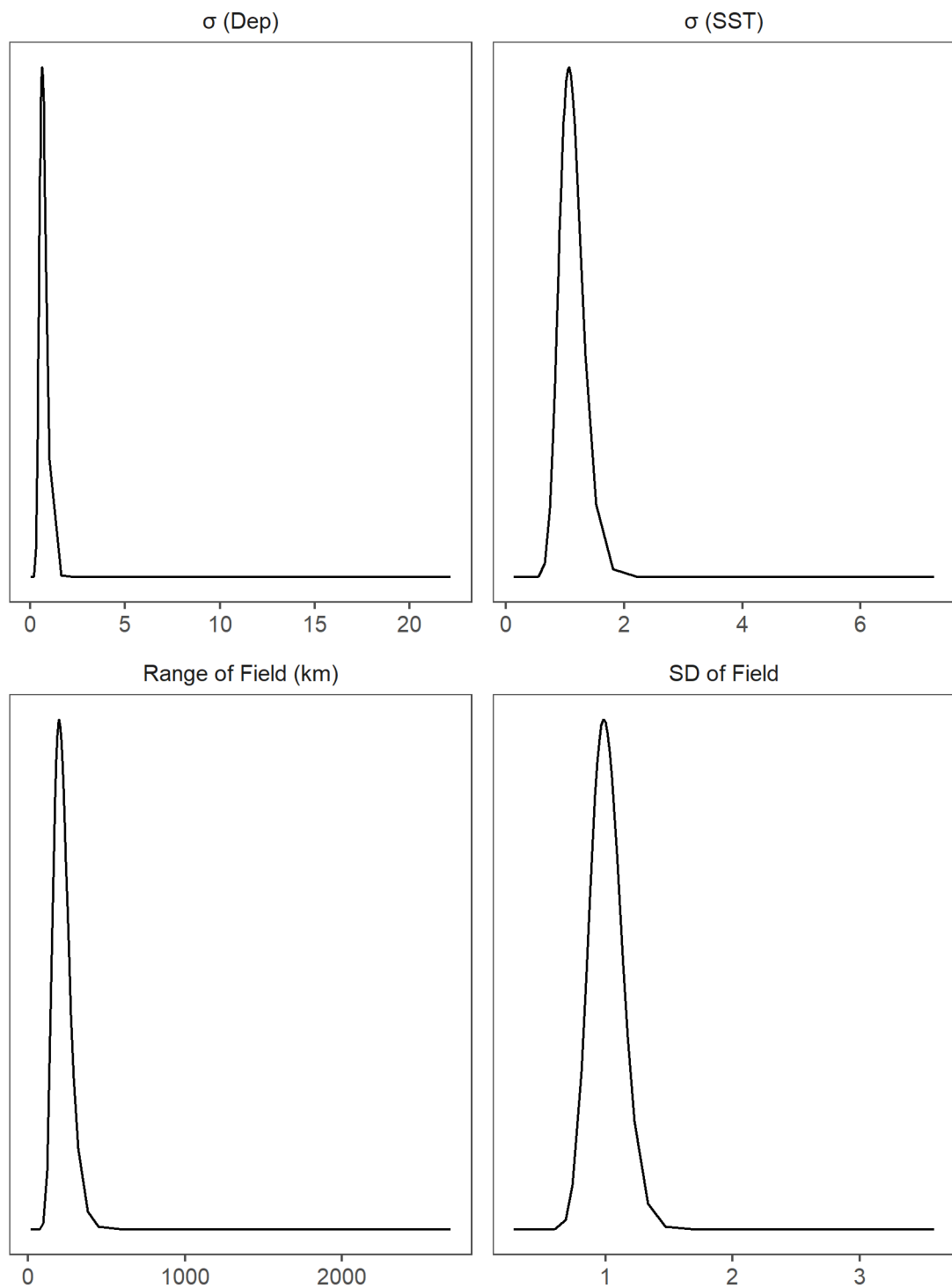


Figure S36: Posteriors distributions of the four model hyperparameters for Atlantic Cod in the Spring.

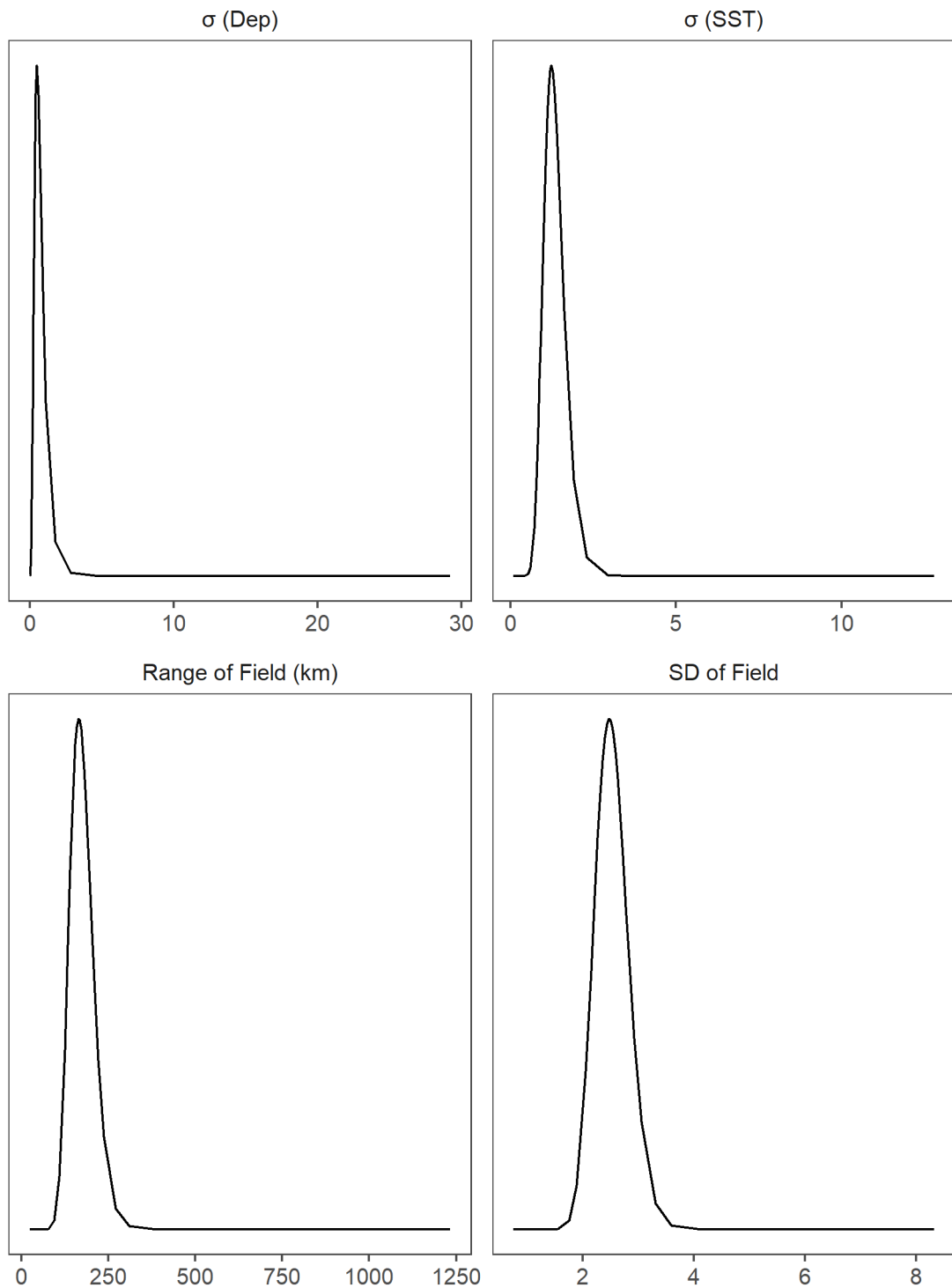


Figure S37: Posteriors distributions of the four model hyperparameters for Atlantic Cod in the Fall.

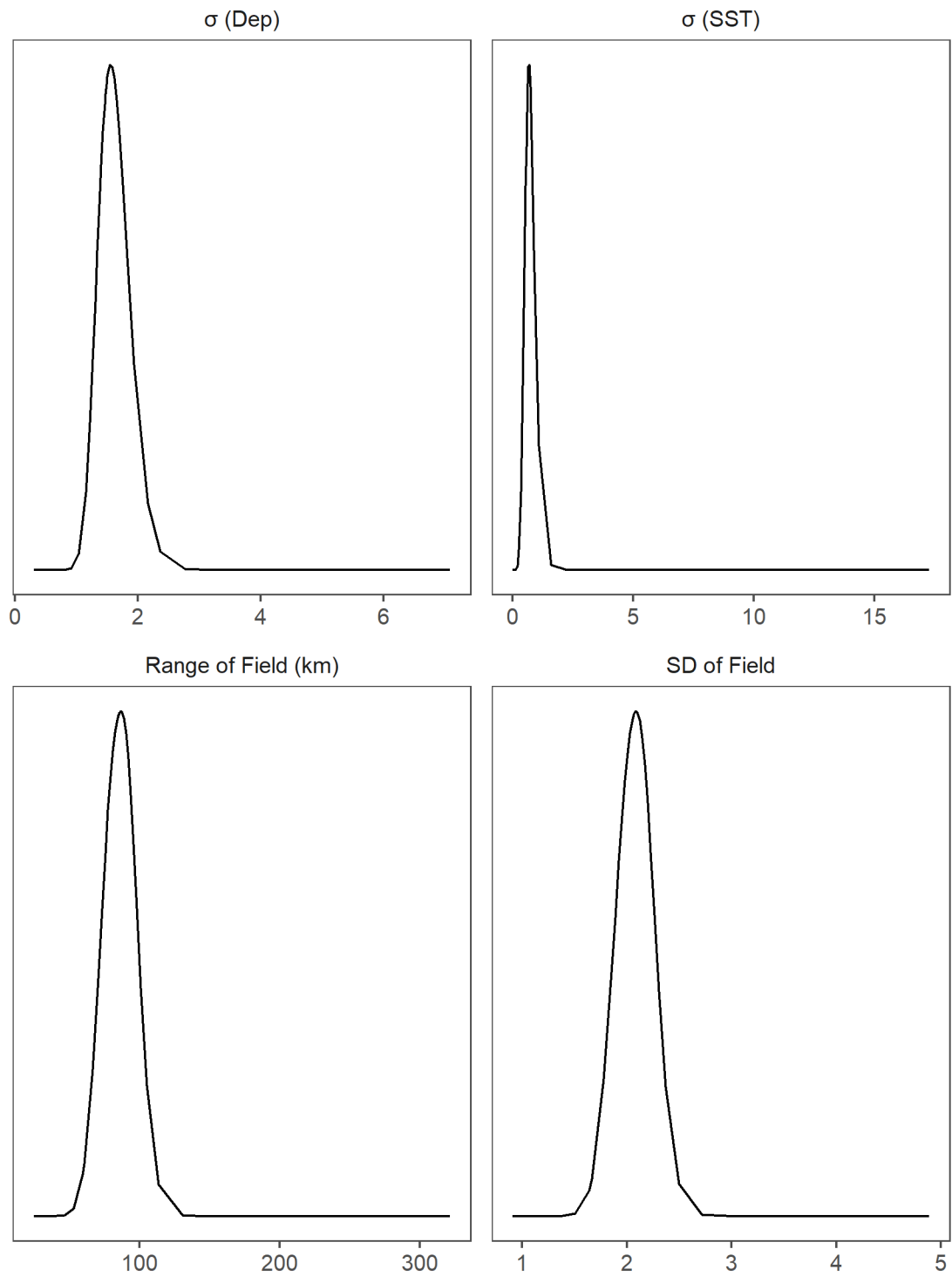


Figure S38: Posteriors distributions of the four model hyperparameters for Yellowtail Flounder in the Winter.

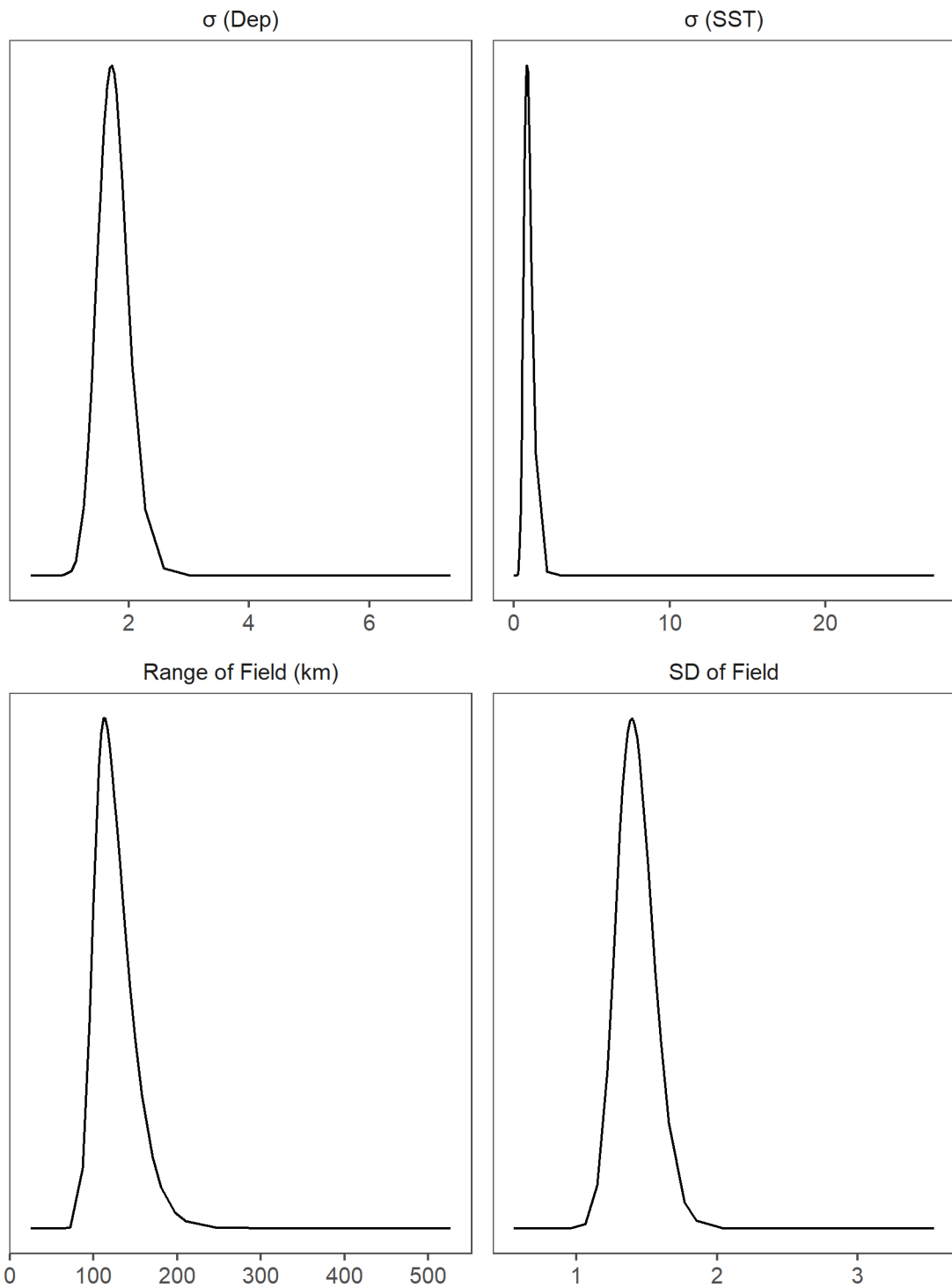


Figure S39: Posteriors distributions of the four model hyperparameters for Yellowtail Flounder in the Spring.

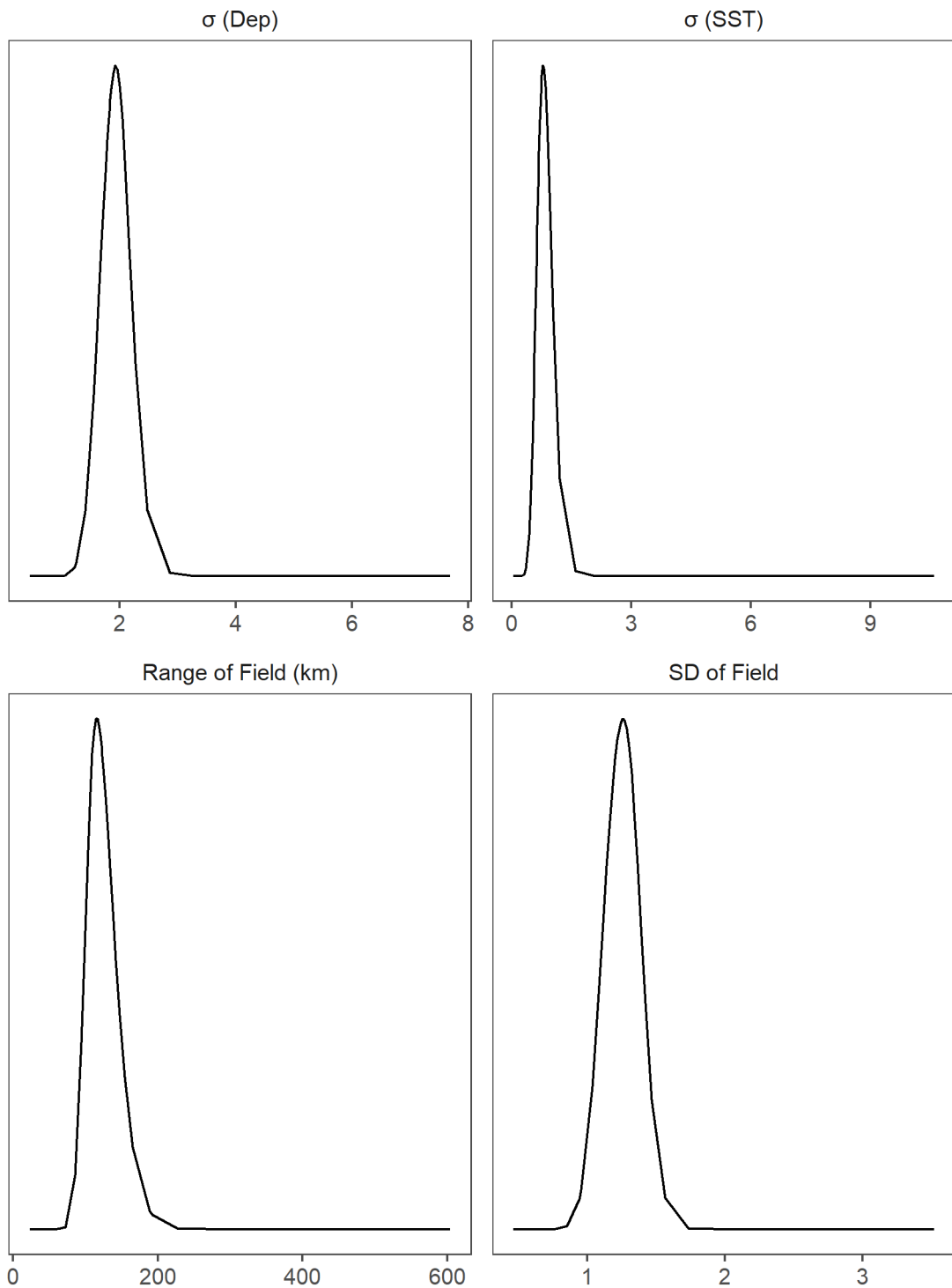


Figure S40: Posteriors distributions of the four model hyperparameters for Yellowtail Flounder in the Fall.